AD-A033 618 CALSPAN CORP BUFFALO N Y F/G 1/3
A STUDY TO DETERMINE THE FEASIBILITY OF SIMULATING THE AV-8A HA--ETC(U)
JUL 76 J V LEBACQZ, E W AIKEN N00019-76-C-0225
UNCLASSIFIED CALSPAN-AK-5876-F-1 NL

1 OF 2
AD
A033618



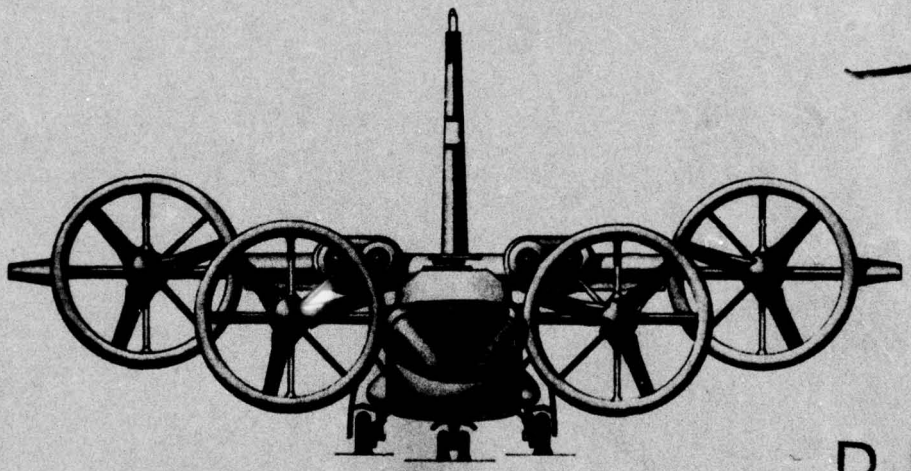
ADA033618

AK-5876-F-1

A STUDY TO DETERMINE THE FEASIBILITY OF SIMULATING THE AV-8A HARRIER WITH THE X-22A VARIABLE STABILITY AIRCRAFT

Final Report
July 1976

By
J. V. Lebacqz
E. W. Aiken



DDC
DEC 16 1976

Prepared Under Contract N00019-76-C-0225
For
Naval Air Systems Command
Department of the Navy
By
Calspan Corporation
Buffalo, New York

Approved for Public Release: Distribution Unlimited

A STUDY TO DETERMINE THE FEASIBILITY OF SIMULATING THE AV-8A HARRIER WITH THE X=22A VARIABLE STABILITY AIRCRAFT

J. V. Lebacqz
E. W. Aiken

CALSPAN REPORT NO. AK-5876-F-1

July 1976

DDC
RECEIVED
DEC 16 1976
F

Contract No. N00019-76-C-0225

Prepared For:
Naval Air Systems Command
Department of the Navy

ACCESSION for
NTIS White Section
DDC Buff Section
UNANNOUNCED
JUSTIFICATION
BY
DISTRIBUTION/AVAILABILITY CODES
Dist. AVAIL. and/or SPECIAL
A

DISTRIBUTION STATEMENT A
Approved for public release;
Distribution Unlimited

FOREWORD

This report was prepared for the United States Naval Air Systems Command under Contract Number N00019-76-C-0225 by Calspan Corporation (formerly Cornell Aeronautical Laboratory, Inc.), Buffalo, New York, and documents the research conducted under that contract from November 1975 through June 1976.

The analyses reported herein relate to the feasibility of using the X-22A aircraft to simulate an advanced jet-lift VTOL fighter, and were performed by the Flight Research and Facilities Department of Calspan. Mr. J. L. Beilman was the Program Manager. Mr. J. V. Lebacqz was the Project Engineer, and Mr. E. W. Aiken was the Assistant Project Engineer; Mr. R. D. Till, who is project engineer for electronic systems on X-22A programs, assisted in the preparation of the ground simulator. Technical monitoring was performed by both the Naval Air Systems Command and the Naval Air Development Center. The authors wish expressly to acknowledge the assistance and support of Mr. John W. Clark, Jr., Navy X-22A Program Manager at NADC; in addition, the authors acknowledge their appreciation to Mr. C. Mazza at NADC and Messrs. D. Hutchins and R. Siewert at NAVAIR.

Messrs. J. Lyons and C. Mesiah at Calspan performed the digital programming for the analyses discussed in this report. The authors are also grateful to Messrs. R. C. Radford and R. E. Smith who assisted in the generation of the AV-8A mathematical model. Finally, special thanks are given to Mses. F. Scribner and D. Kantorski for their efforts in the preparation of this report.

PRECEDING PAGE BLANK-NOT FILMED

ABSTRACT

A study program was undertaken to investigate the feasibility of conducting ground- and in-flight simulations of a jet-lift VTOL aircraft performing terminal area operations using the U. S. Navy X-22A V/STOL Research Facility. The objectives of the program were:

- to develop a generic mathematical model of the AV-8A aircraft during a decelerating approach to hover;
- to develop the methodology for computing the variable stability gains required to simulate the AV-8A model with the X-22A, and
- to develop the procedures for implementing the simulation in the X-22A ground simulator.

The general conclusion for this study is that it is feasible to simulate in the X-22A aircraft an AV-8A class VTOL aircraft during terminal area operations. The methodology for performing such a simulation is developed and the techniques for mechanization on the X-22A ground simulator for further experimental investigation are described. Excellent simulation fidelity is possible during low-speed flight (≤60 kts). Areas which require further investigation include the discrepancies in response to throttle inputs at higher speeds and the necessity for matching lateral acceleration responses at the pilot's station to control inputs.

EQUAL TO OR LESS THAN

TABLE OF CONTENTS

Section		Page
1	INTRODUCTION	1
2	DEVELOPMENT OF AV-8A MATHEMATICAL MODEL	3
	2.1 REQUIRED MATH MODEL AND EXISTING DATA FORM	3
	2.2 AV-8A MATH MODEL GENERATION	5
3	SIMULATION FIDELITY	17
	3.1 INTRODUCTION	17
	3.2 OBJECTIVES OF THE SIMULATION	18
	3.3 QUALITY OF THE AV-8A MATHEMATICAL MODEL	19
	3.4 SIMULATOR CAPABILITIES AND LIMITATIONS	20
	3.5 SIMULATION GUIDELINES	21
4	SIMULATION METHODOLOGY	23
	4.1 LATERAL-DIRECTIONAL	23
	4.2 LONGITUDINAL	27
	4.2.1 Summary of the Problem	27
	4.2.2 Development of Feedback Laws	35
	4.2.3 Feedback Gain Computations	43
	4.2.4 Control Effectiveness Computations	47
	4.2.5 Resulting Longitudinal Simulation	50
	4.3 SUMMARY OF SIMULATION FIDELITY	57
5	IMPLEMENTATION IN GROUND SIMULATOR	58
	5.1 SIMULATOR PREPARATION	58
	5.2 AV-8A MODEL MECHANIZATION	60
	5.3 SIMULATOR CHECKOUT	66
6	CONCLUSIONS AND RECOMMENDATIONS	67

TABLE OF CONTENTS, CONT'D

Section	Page
REFERENCES.	71
GLOSSARY OF SYMBOLS	74
APPENDIX I BASIC AV-8A MODEL STABILITY/CONTROL DERIVATIVES	79
APPENDIX II AV-8A SAS CHARACTERISTICS	92

LIST OF TABLES

Table No.		Page
2-1	AV-8A MODEL STABILITY DERIVATIVES	7
2-2	AV-8A MODEL MOMENT CONTROL DERIVATIVES	9
2-3	AV-8A MODEL THRUST CONTROL DERIVATIVES	11
2-4	COMPARISON OF ASSUMED M_{δ_T} (θ_i = 81°) WITH APPROXIMATE VALUE DERIVED FROM PITCH STICK TRIM	16
2-5	TRANSFER FUNCTIONS OF AV-8A MODEL IN FORM $K(1/\tau)[\zeta;\omega_n]$	16
4-1	CALCULATED LATERAL/DIRECTIONAL VSS GAINS (BASIC AV-8A)	25
4-2	COMPARISON OF STABILITY/CONTROL PARAMETERS	26
4-3	LATERAL-DIRECTIONAL CHARACTERISTIC ROOTS AND TRANSFER FUNCTIONS	28
4-4	WEIGHTING MATRICES AND MODEL MODIFICATIONS FOR LONGITUDINAL GAIN COMPUTATIONS	44
4-5a	LONGITUDINAL FEEDBACK GAINS: EXACT COMPUTATIONS IN COMPUTER UNITS	44
4-5b	LONGITUDINAL GAINS FOR IMPLEMENTATION IN GROUND SIMULATOR	45
4-6	COMPARISON OF MODEL AND SIMULATION CHARACTERISTIC ROOTS IN FORM $K(1/\tau)[\zeta;\omega_n]$	45
4-7	COMPARISON OF MODEL AND SIMULATED CHARACTERISTIC MATRICES	46
4-8	LONGITUDINAL GEARING GAINS	49
5-1	BASIC X-22A SIMULATOR MODEL	59
5-2	COLLECTIVE ELEVON EFFECTIVENESS DERIVATIVES	65

LIST OF FIGURES

Figure No.		Page
2-1	COMPARISON OF CHARACTERISTIC ROOTS	8
2-2	LONGITUDINAL STICK TRIM POSITIONS	12
2-3	THRUST VECTOR TRIM CONDITIONS	14
2-4	THROTTLE TRIM POSITION	15
4-1	LATERAL-DIRECTIONAL TIME HISTORIES (a) V = 0 kt; δ_{as} STEP	29
4-1	LATERAL-DIRECTIONAL TIME HISTORIES (b) V = 0 kt: δ_{rp} DOUBLET	30
4-1	LATERAL-DIRECTIONAL TIME HISTORIES (c) V = 60 kt; δ_{as} STEP	31
4-1	LATERAL-DIRECTIONAL TIME HISTORIES (d) V = 60 kt; δ_{rp} DOUBLET	32
4-1	LATERAL-DIRECTIONAL TIME HISTORIES (e) V = 120 kt; δ_{as} STEP	33
4-1	LATERAL-DIRECTIONAL TIME HISTORIES (f) V = 120 kt; δ_{rp} DOUBLET	34
4-2	OPTIMAL CONTROL EXAMPLES IN S-PLANE	40
4-3	EXAMPLE OF TRANSFORMED OPTIMAL CONTROL SOLUTION	42
4-4	LONGITUDINAL TIME HISTORIES (a) V = 0 kt; δ_{es} PULSE ($\theta_j = 81^o$)	51
4-4	LONGITUDINAL TIME HISTORIES (b) V = 0 kt; δ_r PULSE ($\theta_j = 81^o$)	52
4-4	LONGITUDINAL TIME HISTORIES (c) V = 60 kt; δ_{es} PULSE ($\theta_j = 81^o$)	53
4-4	LONGITUDINAL TIME HISTORIES (d) V = 60 kt; δ_r PULSE ($\theta_j = 81^o$)	54
4-4	LONGITUDINAL TIME HISTORIES (e) V = 120 kt; δ_{es} PULSE ($\theta_j = 50^o$)	55

LIST OF FIGURES, CONT'D

Figure No.		Page
4-4	LONGITUDINAL TIME HISTORIES (f) V = 120 kt; δ_T PULSE (θ_j = 50°)	56
5-1	AV-8A MODEL MECHANIZATION	61
5-2	X-22A PITCH AND COLLECTIVE STICK TRIM POSITIONS	63
5-3	REFERENCE VELOCITIES	64
5-4	AV-8 LONGITUDINAL STICK AND THROTTLE TRIM POSITIONS	64

Section 1

INTRODUCTION

This report documents the results of a study directed at the in-flight simulation of a jet-lift VTOL aircraft performing terminal area operations. In particular, the feasibility of conducting such a simulation with the variable stability X-22A V/STOL aircraft was addressed and the requisite methodologies were developed. The study underwent several changes in emphasis and concomitant modification of the original objectives during its performance period. In this section, therefore, a brief summary of the program's evolution will be presented followed by a statement of the resulting study objectives; an outline of this report, which documents the accomplishment of these objectives, concludes the section.

As originally planned, the study was to concentrate primarily on angular augmentation control system designs for a "generic" jet-lift aircraft; this generic model was intended to include only representative values of major stability derivatives in the moment equations, and hence would require a minimal effort to formulate. Shortly after the commencement of the contract, however, the effort was redirected by NAVAIR toward simulating a specific jet-lift VTOL -- the AV-8A Harrier -- in order that the flight experiment to be performed subsequent to this study would provide results directly applicable to the Harrier.

As a result of this redirection, considerably more effort than originally planned was required to (1) formulate a suitable Harrier mathematical model from available data, and (2) develop the simulation methodology. The objectives of the study therefore were modified: a major emphasis was to be placed on developing an accurate model of the AV-8A so that one would be available at the onset of the flight program. Accordingly, for the first half of the program, attention was focussed on acquiring and analyzing available AV-8A data toward this end.

The development of an accurate and suitable mathematical model was hampered by delays in acquiring data and significant discrepancies among those data that were obtained; further, some required information could not be extracted from the data available. In the same time period that the modelling inadequacies were becoming clear, the objectives of the follow-on flight program were again altered: rather than a simulation of the AV-8A, the flight experiment was to be tied into the development of the McDonnell-Douglas AV-8B aircraft, and the in-flight simulation will be of the design characteristics of this machine when they become available. This change eliminated the necessity to develop a precise AV-8A model during this study program, and thereby permitted increased attention to be paid to simulation methodology and implementation mechanization.

As can be seen, the evolution of the goals for the follow-on flight program led to concomitant modifications in the objectives of this study from those given at its onset. The final objectives were:

- Develop a model of the AV-8A which contains representative stability and control parameters but may not be exactly correct.

- Develop the methodology for computing the variable stability gains required to simulate the AV-8A model with the X-22A. Assess simulation fidelity to the extent possible.

- Develop the procedures for implementing the simulation in the X-22A ground simulator, and check out resulting mechanization.

The remainder of this summary report documents the procedures and analyses conducted to accomplish these objectives. Section 2 discusses the development of the AV-8A mathematical model, including a review of the requisite model form and the form in which the available data appeared, a summary of necessary assumptions and procedures, and a documentation of the resulting model characteristics. A general discussion of means for investigating and assessing simulation fidelity is presented in Section 3. In Section 4, detailed descriptions of the development and application of various methods for determining the variable stability system gains for this problem are given, both for the lateral-directional simulation (4.1) and for the longitudinal computations (4.2). The modifications made to the ground simulator and the implementation of the AV-8A model simulation are described in Section 5, including the checkout results. Finally, Section 6 summarizes the conclusions of this study and the implications of the results for the follow-on AV-8B in-flight simulation.

Section 2

DEVELOPMENT OF AV-8A MATHEMATICAL MODEL

2.1 REQUIRED MATH MODEL AND EXISTING DATA FORM

The variable stability system of the X-22A is of the response feedback type. As implemented in the X-22A, the characteristics of such a system imply certain constraints on the model of the aircraft to be simulated. In particular, the system commands designated control motions linearly proportional to measured signals less "reference" values (which may be constant or a function of flight condition) to alter the basic stability/control derivatives of the X-22A directly; the proportionality between a measurement and a control motion may be varied as a function of flight condition but it is linear (e.g., the control cannot move as the square of the measurement). As a result, the model of the AV-8A must be developed in terms of reference conditions which explicitly depend on a defined evaluation task, and "linearized" (though non-constant) stability and control derivatives around these references.

As an example, consider the longitudinal equations of motion which, with some simplifications, may be written:

$$\dot{u} + g \sin\theta + \dot{\theta} w = X(u, w, q, \delta_T, \delta_E, \theta_j)$$

$$\dot{w} - g \cos\theta - \dot{\theta} u = Z(u, w, q, \delta_T, \delta_E, \theta_j)$$

$$\ddot{\theta} = M(u, w, q, \delta_T, \delta_E, \theta_j)$$

$$\gamma = \theta - \alpha$$

$$\alpha = \tan^{-1}(w/u)$$

By requiring that $\ddot{\theta} = \dot{\theta} = q = \dot{\gamma} = \dot{\alpha} = 0$ be included as reference conditions, this set of equations may be reduced to three equations in seven unknowns: $\dot{u}$, γ, u, w, δ_T, δ_E, θ_j. By specifying four of the unknowns through a selection of the evaluation task, the remaining three may be uniquely determined. For example, the reference conditions at various points along the AV-8A reference trajectory may be computed by specifying γ, α, u and θ_j and calculating the required values of $\dot{u}$, δ_T, and δ_E from the complete "global" representation of the aerodynamic/propulsive forces and moments acting on the aircraft. If the deceleration schedule is defined for the task, then $\dot{u}$, γ, u and θ_j (or w) may be specified and the reference values of δ_T, δ_E and w (or θ_j) may be calculated. These reference conditions, either specified or calculated, are denoted by the subscript R for convenience.

The coefficients for a Taylor series representation of the aerodynamic/ propulsive forces and moments may now be obtained in a manner similar to the technique described in Reference 1. The general approach used to calculate the longitudinal dimensional derivatives is to:

- calculate the values of X , Z , and M which correspond to the reference conditions $[u_R , \omega_R , q_R , \delta_{T_R} , \delta_{\epsilon_R} , \theta_{j_R}]$ at selected points on the reference trajectory
- perturb one of the variables in suitable increments from the reference value and determine the corresponding values of X , Z and M.
- calculate and plot the change in X , Z and M versus the change in the variable being perturbed
- fit an nth order polynomial to the data on a least-square error basis (e.g. n = 3)
- differentiate the polynomial successively to determine first, second, and third-order derivatives.

The cross derivatives such as $X_{u_{\delta_T}}$ may be obtained by repeating the above procedure for a series of throttle positions at positive and negative increments from the reference value, cross-plotting the resultant values of X_u vs. δ_T , and calculating the slope of the curve.

It is clear, then, that the development of an AV-8A model in the appropriate form is an involved process unless data in a similar form are available The data reports investigated for this study are listed below (References 2 through 21, respectively):

MCAIR A1410: AV-8A Aerodynamics (Wind Tunnel Data Summary)
MCAIR A1411: AV-8A Estimated Flying Qualities
Rockwell NR72H-268: AV-8A Hover Simulation
MCAIR A3278: AV-8A Landing Approach Simulation
MCAIR A3618: AV-8A Landing Approach Simulation
MCAIR A3580: AV-8A Stability Augmentation Design
NRC 10257: XV-6A Landing Approach Simulation
NASA TND-6791: XV-6A Landing Approach
AFFTC TR No. 69-26: USAF Harrier Evaluation
NATC FT-98R-66: XV-6A Carrier Suitability
AFFTC TR No. 68-10: XV-6A Handling Qualities
NATC FT-52R-71: Harrier Flying Qualities
NATC FT-59R-71: AV-8A Carrier Suitability
NASA TND-7296: XV-6A Aerodynamic Parameters from Flight Data
NASA TND-6826: XV-6A Wind Tunnel Study
MCAIR A3091: AV-8A Control System Analysis
NATC FT-72R-72: AV-8A Shipboard Suitability
NATC FT-05R-69: Navy MPE of Harrier
NATC FT-27R-71: AV-8A Flying Qualities
NAVAIR 01-AV8A-1: AV-8A Flight Manual

References 4 - 8 contain scattered documentation on stability and control derivatives in the desired dimensional form (e.g., X_u etc.) as a function of velocity; these data do not include trim information and are generally inconsistent with each other. The flight test reports (References 9 - 14, 18 - 20) are useful for qualitative understanding of trim requirements and transition capabilities, although again inconsistencies appear in the limited quantitative information that exists. Reference 2 is a compilation of AV-8A wind tunnel data in non-dimensional form, generally for speeds above 50 kts; it is the most complete of the data sets available, although considerable "massaging" is required to obtain the desired form, and it gives a qualitative understanding of the global characteristics of the AV-8A. Reference 3 presents characteristic roots computed on the basis of the Reference 2 data; although incomplete, some comparisons of the stability characteristics of a developed model can be made.

A general summary of the quality and deficiencies of the available data is therefore:

- Stability derivatives. Fairly complete information from Reference 2 above 50 kts. Comparison of selected derivatives possible with References 7, 8; comparison of selected modal characteristics possible with Reference 3.

- Control derivatives. Information about the three moment controller effectivenesses available in Reference 2. Essentially no quantitative information on throttle sensitivities for the longitudinal force equations or on nozzle angle effectiveness; no information on moment sensitivities for thrust and nozzle.

- Reference values. No direct information. References 5 and 6 discuss landing approach evaluation tasks from which some reference information may be inferred; limited quantitative data from flight test are in References 10, 12, 18 - 20.

- Trims. No direct information for throttle. Longitudinal stick trim estimates may be inferred from Reference 3.

2.2 AV-8A MATH MODEL GENERATION

As the preceding discussion indicates, significant gaps exist in the data base available for formulating an AV-8A mathematical model in an appropriate form. In view of the redirection to the AV-8B aircraft for the follow-on flight program, it was decided to formulate the AV-8A model for this study by extrapolating from these data where possible and estimating undocumented characteristics by "engineering judgment" (e.g., geometries). A summary of the resulting assumptions and procedures is given in this subsection.

The initial assumptions involve the definition of an evaluation task, since the reference conditions depend upon it. Following the general guidelines provided by previous MCAIR simulations (References 5, 6), the following task

characteristics were selected:

- constant glide slope: γ = -5 deg
- constant angle of attack: α = 8 deg
- two possible initial velocities: V_o = 80 kt, 120 kt
- one-step deceleration: nozzle angle $\Rightarrow$ 81 deg "instantaneously" at appropriate range

The choice of 8 degrees constant angle of attack rather than pitch attitude was selected by MCAIR because the AV-8A runs out of longitudinal control authority at approximately 15 degrees for low speeds; the two approach speeds are those investigated by MCAIR in Reference 5.

Longitudinal and lateral-directional stability derivatives were then calculated from the non-dimensional wind tunnel data of Reference 2 for six trim (unaccelerated) flight conditions, all at γ = -5 deg, α = +8 deg: V_o = 0, 30, 60, 80, 100, 120 kt. The resulting dimensional stability derivatives are given in Appendix I; also shown are available data from References 4, 6, 7, and 8 when applicable. It is emphasized that the V_o = 0, 30 kt data are extrapolations: the wind tunnel data in Reference 2 are generally valid only for $V \geq 60$ kt. In general, consistent trends are exhibited, and the agreement among data sets is fair (with the exception of some Reference 4 data incorrect signs). Unfortunately, the major uncertainties are for the derivatives M_u, M_w, L'_v, and N'_v, which have a major effect on the aircraft dynamics; the selected values of M_w and M_u are a reasonable average of the Reference 2 and Reference 8 values, while the L'_v and N'_v values of Reference 7 were weighted most highly in the selection of these derivatives.

Table 2-1 summarizes the stability derivatives of the resulting AV-8A model used in this study. Figure 2-1 compares the characteristic roots of this model at the six trim velocities with available documentation from Reference 3; considering the assumptions and extrapolations made in the model development, the correlation is outstanding for both the longitudinal and the lateral-directional degrees of freedom. It appears that this part of the developed AV-8A model is representative of the MCAIR estimate of the actual aircraft.

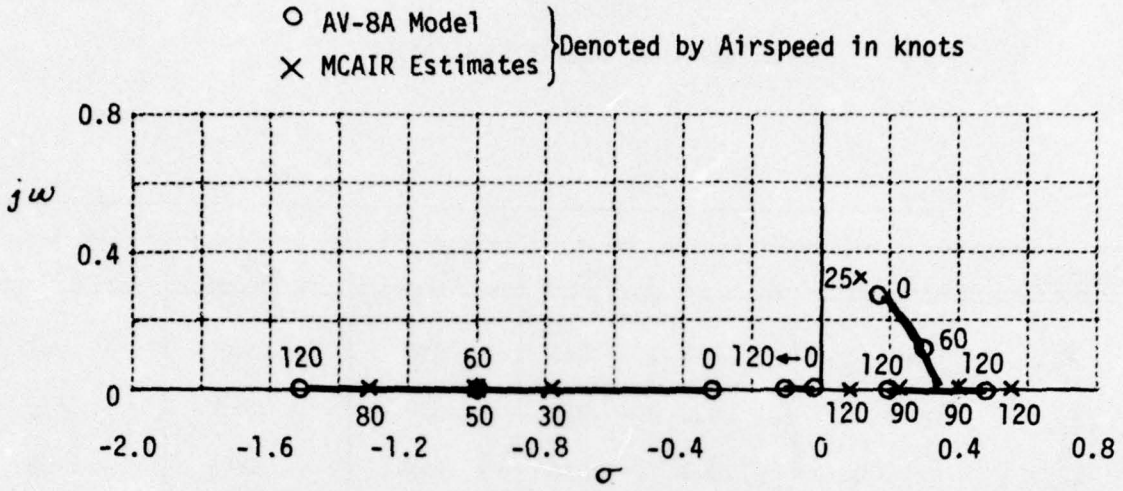
The moment control derivatives were also estimated from the data presented in Reference 2. Both aerodynamic and reaction control data are required: the reaction control derivatives were selected for maximum thrust and singular demand (no effect of simultaneous control usage on available bleed air is included). Appendix I presents the data; Table 2-2 summarizes the estimated control effectivenesses. The values are somewhat smaller than those given in Reference 7, and hence may be considered to reflect some effects of simultaneous control usage.

Quantitative throttle control effectiveness data are very limited in the available references. The value of Z_{δ_T} for the nozzles at 90 degrees was

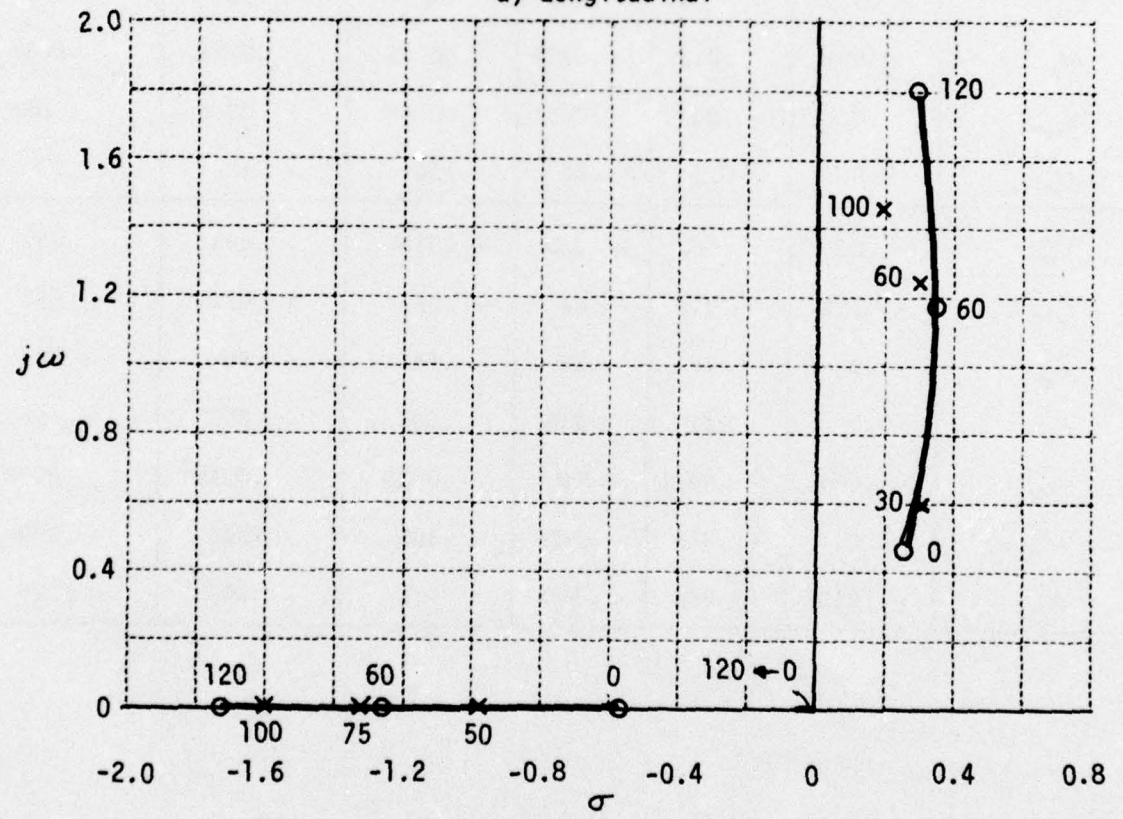
TABLE 2-1

AV-8A MODEL STABILITY DERIVATIVES

	V					
Derivative	0	30	60	80	100	120
X_u	- .026	- .035	- .043	- .049	- .055	- .061
X_w	0.0	- .020	- .027	- .029	- .030	- .030
Z_u	0.0	- .011	- .036	- .060	- .083	- .108
Z_w	- .020	- .105	- .190	- .250	- .310	- .370
M_u	.001	.0017	.0022	.0025	.0026	.0026
M_w	.0009	.0042	.0054	.0059	.0060	.0058
M_q	0.0	- .13	- .26	- .34	- .43	- .52
Y_v	- .025	- .042	- .059	- .070	- .081	- .092
L'_v	- .005	- .012	- .04	- .053	- .059	- .058
L'_p	- .04	- .26	- .48	- .64	- .80	- .94
L'_r	0.0	.110	.215	.285	.360	.430
N'_v	- .0045	- .0021	0.00	.0013	.0019	.0020
N'_p	0.0	- .075	- .145	- .195	- .240	- .290
N'_r	- .015	- .060	- .100	- .130	- .160	- .190



a) Longitudinal



b) Lateral-Directional

Figure 2-1 COMPARISON OF CHARACTERISTIC ROOTS

TABLE 2-2

AV-8A MODEL MOMENT CONTROL DERIVATIVES

	V_o					
Derivative*	0	30	60	80	100	120
X_{δ_E}	0.0	0.0	0.0	0.0	0.0	0.0
Z_{δ_E}	.41	.53	.67	.77	.88	1.00
M_{δ_E}	.15	.20	.25	.28	.31	.34
L'_{δ_A}	.45	.45	.45	.45	.45	.45
N'_{δ_A}	.014	.014	.014	.014	.014	.014
Y'_{δ_R}	- .61	- .69	- .78	- .84	- .90	- .96
L'_{δ_R}	- .080	- .085	- .095	- .100	- .105	- .110
N'_{δ_R}	.185	.215	.240	.260	.280	.295

*per inch control deflection

selected to be 0.1 g/in. = 3.2 ft/sec^2/in. This value is higher than that used in Reference 4 (2.58), Reference 8 (2.7), and an estimate based on data from Reference 9 (2.6), but is lower than estimates made from information given in Reference 14 (4.9) and Reference 21 (5.6); no direct information on the thrust derivatives is given in the MCAIR simulation reports (References 5, 6, 7). With this value selected, the values of Z_{δ_T} and X_{δ_T} at other nozzle angles were estimated by simple geometric arguments:

$$Z_{\delta_T} = -3.2\left[\cos\left(90 - \theta_j'\right)\right]$$
$$X_{\delta_T} = 3.2\left[\sin\left(90 - \theta_j'\right)\right]$$

where $\theta_j' = \theta_j + 2^\circ$ (engine angle in fuselage)

Essentially no information on pitching moment caused by thrust was available in the literature. Although a value of M_{δ_T} = -0.03 rad/sec^2/in. could be computed from Reference 2 for one flight condition, the sign of this estimate was inconsistent with qualitative information from flight test. It was therefore assumed arbitrarily that M_{δ_T} was positive, increased with speed, and decreased with increasing nozzle angle. The resulting values of X_{δ_T}, Z_{δ_T}, and M_{δ_T} are listed in Table 2-3.

The remaining formulation required is the trim information -- the reference values for the controls. No antisymmetric characteristics of the aircraft are included in the model, and so the trim lateral stick and rudder pedal control positions are zero. Longitudinal stick trim data were available in Reference 3, and are reproduced in Figure 2-2. Also shown is an approximate variation labelled $M_{\delta_T} = 0$ calculated on a piece-wise linear basis using the formulated stability and control derivatives and reference conditions from the equation:

$$\Delta\delta_\epsilon = \frac{-M_u \Delta u - M_w \Delta w}{M_{\delta_\epsilon}}$$

where $\Delta u = u_{trim_1} - u_{trim_2}$, etc.

As can be seen, the correct trim trend is reproduced although somewhat larger changes are predicted; the differences between the curves can be used as a qualitative check on the values of M_{δ_T} assumed earlier once the trim throttle positions are computed.

The trim throttle positions and nozzle angles were estimated on the basis of geometric arguments since again no data were available in the references. On a piece-wise linear basis, the following approximate expressions were used to compute the required X and Z forces supplied by the propulsion system:

TABLE 2-3

AV-8A MODEL THRUST CONTROL DERIVATIVES

		V_o					
	Derivative*	0	30	60	80	100	120
$\theta_j = 81^o$	X_{δ_T}	.38	.38	.38	.38	.38	.38
	Z_{δ_T}	-3.18	-3.18	-3.18	-3.18	-3.18	-3.18
	M_{δ_T}	0.0	.005	.010	.015	.020	.020
$\theta_j = 70^o$	X_{δ_T}	---	---	---	.99	---	---
	Z_{δ_T}	---	---	---	-3.04	---	---
	M_{δ_T}	---	---	---	.020	---	---
$\theta_j = 50^o$	X_{δ_T}	---	---	---	---	---	1.97
	Z_{δ_T}	---	---	---	---	---	-2.52
	M_{δ_T}	---	---	---	---	---	.025

*per inch throttle
θ_j is nozzle angle w.r.t. engine

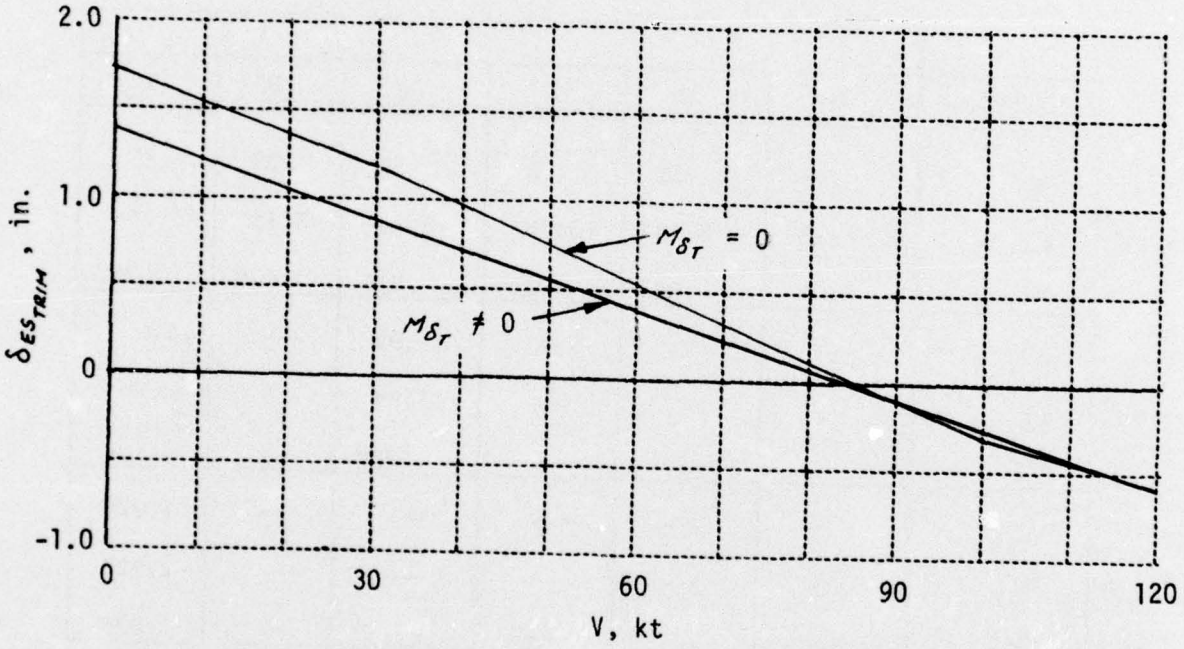


Figure 2-2 LONGITUDINAL STICK TRIM POSITIONS

$$\Delta X = X_u \Delta u + X_w \Delta w - \Delta(\dot{u}_o + g \sin \theta_o)$$

$$\Delta Z = Z_u \Delta u + Z_w \Delta w + Z_{\delta_{es}} \Delta \delta_e - \Delta(\dot{w}_o - g \cos \theta_o)$$

where $$\Delta(\ ) = (\ )_{TRIM_1} - (\ )_{TRIM_2}$$

Approximate values for the kinematic terms were obtained by using the reference condition α_o = 8 degrees, γ = -5 degrees and assuming an average deceleration of approximately 0.05 g on the glide slope. From these computations, a plot of X vs. Z propulsive force is shown in Figure 2-3. Using θ_j = 81 degrees as the hover nozzle angle, approximate trim nozzle angles for the velocities of interest can be found. With these values, trim throttle positions may be computed using the relationships for X_{δ_T} or Z_{δ_T} given earlier; the approximate trim throttle positions are plotted in Figure 2-4.

As was noted earlier, it is possible to check qualitatively the assumed values of M_{δ_T} by using the developed trim throttle and longitudinal stick positions along with the estimate of longitudinal control sensitivity:

$$M_{\delta_T} \cong \frac{M_{\delta_E} \Delta \delta_{E_{TRIM}}}{\delta_{T_{TRIM}}}$$

Table 2-4 presents the comparison of these values with the assumed values of M_{δ_T}, and indicates qualitative agreement in magnitude and sign. Hence, the assumed values are at least reasonable, and were therefore retained in the model.

The formulation of a generic AV-8A model is thus complete. Table 2-5 summarizes the transfer functions of the model at three flight conditions for reference. The simulation of this model with the X-22A is discussed in Sections 4 and 5 of this report.

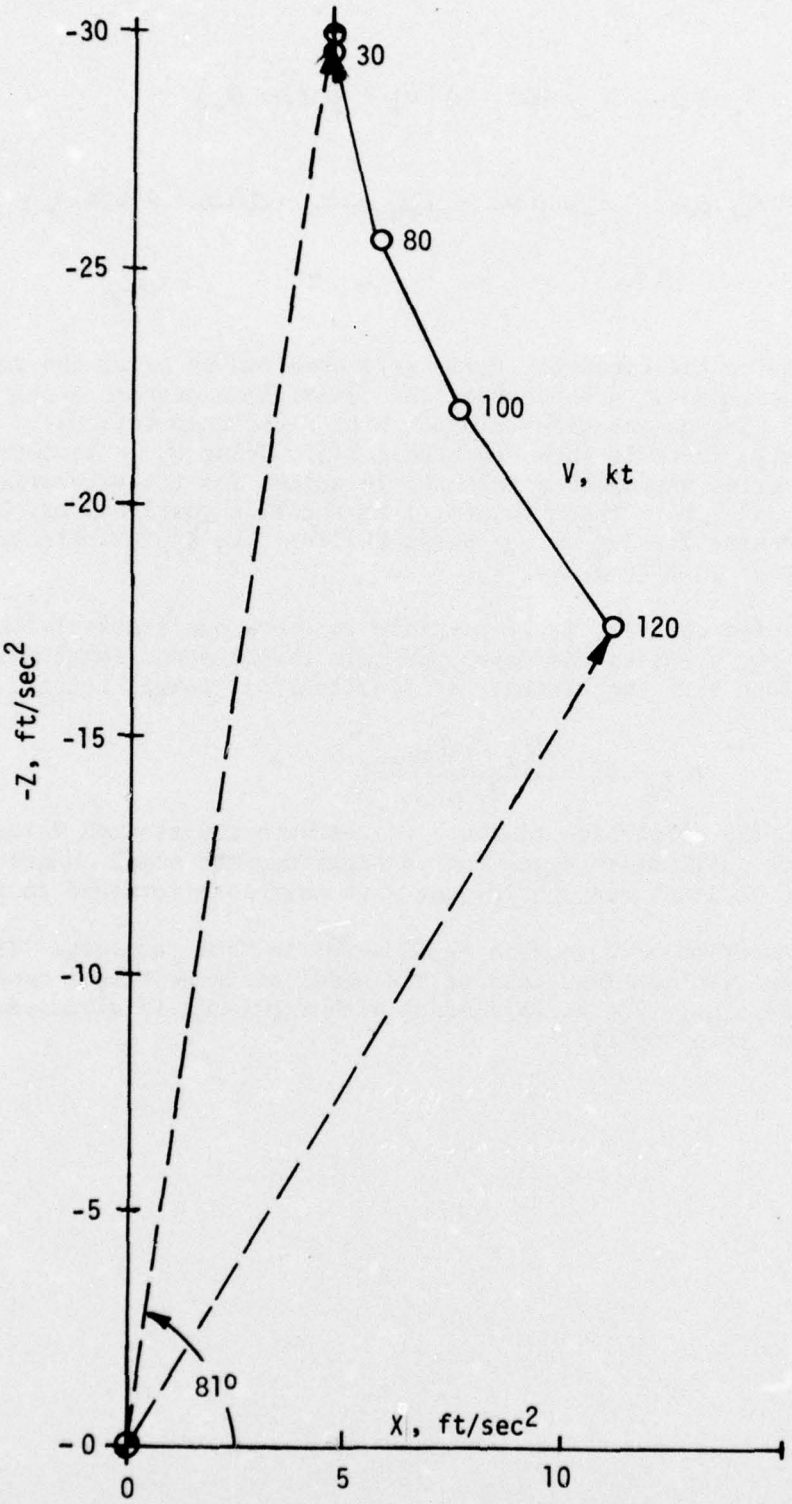


Figure 2-3 THRUST VECTOR TRIM CONDITIONS

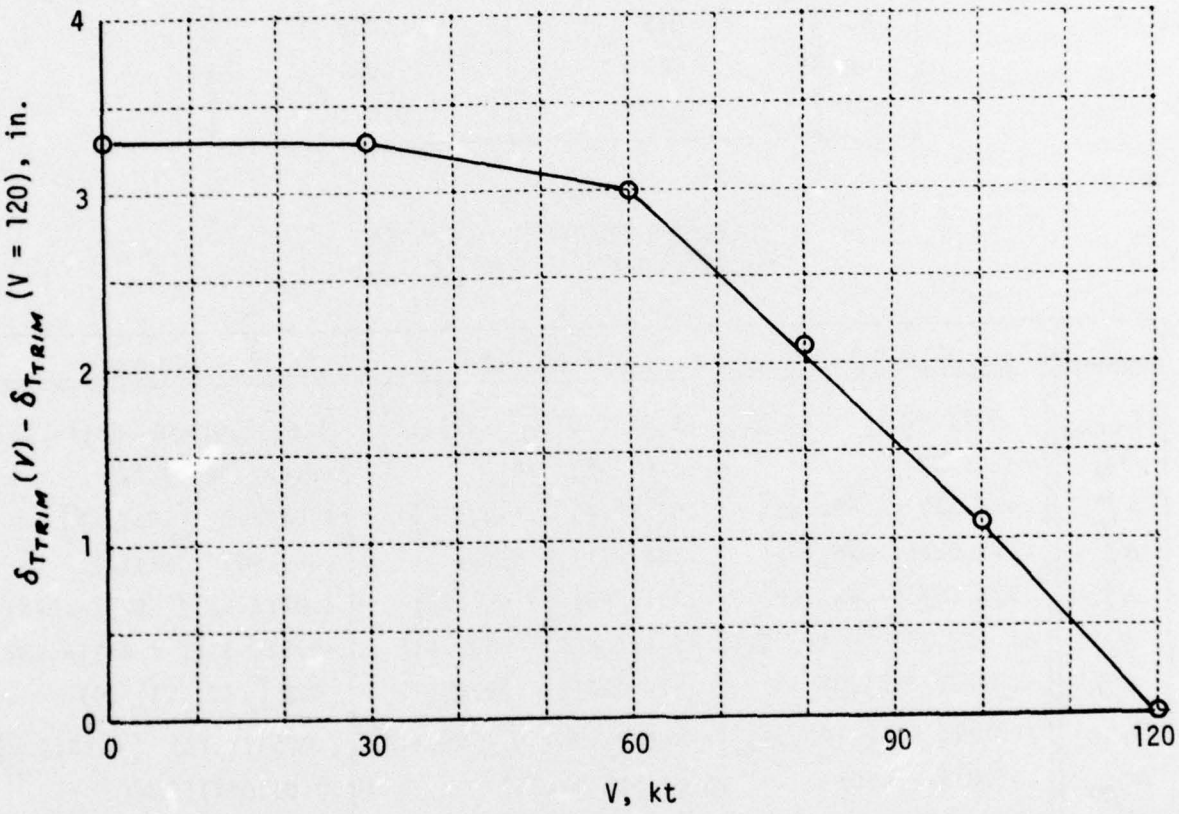


Figure 2-4 THROTTLE TRIM POSITION

TABLE 2-4

COMPARISON OF ASSUMED M_{δ_T} (θ_j = 81°)
WITH APPROXIMATE VALUE DERIVED FROM PITCH STICK TRIM

V	Assumed	Derived
0	0.0	0.0
30	.005	.006
60	.010	.014
80	.015	.025
100	.020	.020
120	.020	0.0

TABLE 2-5

TRANSFER FUNCTIONS OF AV-8A
MODEL IN FORM $K\,(1/\tau)\,[\zeta;\omega_n]$

	V = 0 kt*	V = 60 kt*	V = 120 kt**
Δ_{LONG}	(.33)(.02) [-.48;.31]	(1.00)(.073) [-.91;.32]	(1.53)(.084)(-.46)(-.187)
$N^u_{\delta_e}$	-4.8(.022)	-3.6(2.5)(.19)	-9.69(.31)(1.42)
$N^w_{\delta_e}$	.41(.33) [-.48;.31]	.67(37.9) [.14;.11]	1.0(68.5) [.26;.13]
$N^q_{\delta_e}$	.15(.022)(.026)(0)	.25(.21)(.036)(0)	.34(.40)(.051)(0)
$N^u_{\delta_T}$	.38(.63) [-.49;.62]	.38(1.45) [-.61;.95]	1.97(1.51)(-.87)(-.075)
$N^w_{\delta_T}$	-3.18(.33) [-.48;.31]	-3.18(.40) [-.50;.41]	-2.52(.33)(-1.55)(-.10)
$N^q_{\delta_T}$	-.0025(.027)(0)	.01(.027)(-1.43)(0)	.025 [.19;.13] (0)
Δ_{LID}	(.015)(.58)[-.50;.52]	(.068)(1.26) [-.28;1.2]	(.056)(1.73) [-.15;1.8]
$N^v_{\delta_{as}}$	.4(.015)(34.3)	5.0(.075)(4.15)	10.0(.074)(3.99)
$N^p_{\delta_{as}}$	.45(-.17)(.21)	.45 [.23;.36]	.45 [.17;.88]
$N^r_{\delta_{as}}$	.014[.53;1.64](-1.66)	.014(.49)(-.66)(-4.0)	.014(.53)(-.94)(-7.9)
$N^v_{\delta_{rp}}$	-.6(.015) [.67;2.07]	-.78(.08)(.69)(32.8)	-.96(-.052)(1.06)(64.8)
$N^p_{\delta_{rp}}$	-.08(.37)(-.37)	-.10(2.9)(-3.6)	-.11(4.9)(-6.3)
$N^r_{\delta_{rp}}$	.19 [-.46;.6] (.63)	.24 [-.24;1.07] (1.11)	.3 [.01;1.3] (1.12)

* θ_j = 81°

** θ_j = 50°

Section 3

SIMULATION FIDELITY

3.1 INTRODUCTION

The purpose of this section is to present a discussion of, and a rationale for, the guidelines used to establish the preliminary criteria for a valid piloted simulation of the AV-8A aircraft during a decelerating instrument landing approach. "It is trite to say that to build an exact replica of the aircraft to be simulated, and operate it in a representative environment, is a perfect simulation, and yet no simulation at all." (Reference 22). This statement contains the primary issue of the subject of simulation fidelity: since exact replication is not possible, a determination must be made of which characteristics one should attempt to duplicate, and, further, to what accuracy the duplication must be performed. The extent to which this determination can be objective rather than subjective is dictated by the exigencies of the particular simulation problem: imperfect knowledge about the effects of imperfect duplication of all simulation characteristics renders a generalized set of objective measures impossible. This inchoate situation has a direct parallel - and raison d'etre - in the continuing research efforts to devise appropriate parameters for flying qualities specifications, and fundamentally mandates a determination process that is incompletely objective and at least partly judgmental. Factors which have a major influence on the objectivity possible in assessing simulation validity include:

- Objectives of the simulation
  - training/procedures vs. research/flying qualities
  - missions, tasks
- Quality of AV-8A mathematical model
  - validity of model used
  - accuracy of individual parameters
- Simulator capabilities and limitations
  - ability to reproduce model stability/control characteristics
  - motion/visual cues
  - ergonomic considerations
  - environmental factors.

The implications of the applicable topics subsumed by each of the above three categories for the AV-8 simulation problem are briefly discussed in the following subsections; following this discussion, the resultant general guidelines from which were derived the specific techniques for implementing the AV-8A model on the X-22A simulator/aircraft are summarized.

3.2 OBJECTIVES OF THE SIMULATION

The general goal of the in-flight simulation experiment for which this program is a prerequisite is to provide information relative to the interaction of angular augmentation control systems, displayed information, and task variables during the landing approach of a jet-lift VTOL aircraft.

General guidance for the accuracy of VTOL aircraft flying qualities simulations such as the subject AV-8A simulation is implicitly contained in the military flying qualities specification, MIL-F-83300 (Reference 23), and suggested revisions (Reference 24). These documents identify key flying qualities parameters for both forward and hover flight and delineate boundaries for these parameters as a function of aircraft Class and Flight Phase Category based upon pilot rating data. This concept of flying qualities Levels may also be applied to the simulation fidelity problem; the important flying qualities parameters of the AV-8A model and the X-22A simulation of that model must be within the same flying qualities Level boundaries in order that a valid simulation can reasonably be anticipated.

A similar technique has been applied to the task of establishing dynamic response criteria for simulators used in training applications in Reference 25 for conventional aircraft and in Reference 26 for VTOL aircraft. Allowable tolerances in significant flying qualities parameters are established based upon pilot rating sensitivity analyses; the range of acceptable values for each parameter corresponds to that interval of values about the nominal for which pilot rating varies no more than one rating unit (Reference 25), or one-half a rating unit (Reference 26), about the nominal rating. Although flying qualities research programs in general require a higher degree of simulation fidelity than training simulations, the results of Reference 26 as well as MIL-F-83300 provide useful guidance for the AV-8A simulation problem in cases where a particular stability/control parameter of the AV-8A cannot be exactly reproduced by the X-22A because of system limitations.

The specific objective of the flight program is to define the dynamic characteristics required of the various stability/control augmentation systems as a function of major task elements such as breakout range/altitude for representative levels of displayed information (probably both head-up and head-down). Although the evaluation task details are currently undefined, it is reasonable to assume an approach profile of the type used in MCAIR ground simulations (Reference 6), which consist of a level deceleration to partially jet-borne flight, constant speed instrument glide slope tracking, and a final deceleration just prior to or during breakout. The purpose of the augmentation systems to be considered is to improve the "short-term" attitude response characteristics, and the evaluation procedure will emphasize tracking tasks which highlight the short-term behavior. Hence, short-term aspects of the response to control inputs (e.g. the first five seconds) should be matched as accurately as possible with less weight attached to longer-term matching.

Stability problems which are inherent in the jet-lift VTOL concept must be accurately simulated. The well-documented lateral-directional flying qualities deficiencies of the Harrier between 90 and 30 knots (Reference 21 , for example) caused by large stable values of L_β and small values of N_β (unstable below $\sim$60 knots) must be very nearly duplicated in the X-22A simulation. Longitudinally, the AV-8A exhibits an angle-of-attack instability throughout the transition speed regime which must also be reproduced in the simulation.

The foregoing considerations have all been pertinent to a fixed operating point simulation of the Harrier. However, a primary part of the evaluation task involves a decelerating transition during the landing approach; hence the important characteristics of the AV-8A during a conversion from partially jet-borne flight to jet-borne flight must also be simulated. Experience in previous X-22A programs (References 1 and 27) has shown that transitions at relatively low deceleration levels may be very adequately treated as a series of fixed operating points defined by a single variable, e.g. X-22A duct angle, and that no explicit deceleration effects need to be included in the equations of motion. Two characteristics of the Harrier in transition must, however, be included in the simulation:

- Aircraft response to nozzle rotation. The primary AV-8A deceleration control is through thrust vector rotation. The celerity with which the AV-8A nozzle angle may be varied requires a consideration of simulating not only the long-term deceleration characteristics of the vehicle, dictated primarily by the AV-8A drag damping, but also the short-term deceleration caused by the almost instantaneous rotation of the thrust vector.

- Trim changes in transition. It is desirable to reproduce the general characteristics of pitch stick and throttle trim changes with speed and nozzle setting in transition in order that the control task be similar to the AV-8A. Perfect replication is less important than for the constant speed characteristics, however, as long as the general sense of the motion required is correct, because the transitions are non-constant maneuvers.

3.3 QUALITY OF THE AV-8A MATHEMATICAL MODEL

The concept of using a simulation technique based upon linearized, small perturbation equations of motion for a VTOL aircraft in transition provides an adequate ground simulation of the X-22A (Reference 27). However, a valid simulation of the Harrier in transition may need to include some important higher-order effects; for example:

- The effect of thrust level on control authority/sensitivity. As indicated in Appendix I, RCS control power is dependent upon thrust level. Maximum thrust has been assumed in the calculation of the model control derivatives; the effect on control power of any large deviation from maximum thrust may have to be accounted for in the simulation.

- The effect of multi-control usage on individual control authorities/sensitivities. Appendix I also demonstrates the reduction in individual control power/sensitivity which results from a simultaneous usage of one or both of the remaining RCS controls. The inclusion of this effect may be required in order to ensure simulation fidelity in the event of large deviations from "trim" control positions.

- The effect of large perturbations of the state variables. The sensitivity of any of the stability/control parameters of the AV-8A presented in Section 2 to perturbations from the established reference conditions is currently unknown. Conversations with MCAIR personnel have indicated that, for example, the value of L'_β is heavily dependent upon angle-of-attack and power setting. These effects cannot currently be quantified and evaluated; hence they are not included in the simulation. However, future simulations of the AV-8B will require an investigation of these effects.

In addition to the exclusion of the above higher-order effects, a further potential limitation to the fidelity of the simulation is the accuracy of the AV-8A model stability/control parameter values. As discussed in Section 2, these values are the result of a fairly extensive data search, analyses, and the application of engineering judgment; the object is to provide the best possible simulation of the resulting AV-8A model characteristics rather than to be concerned about the detailed validity of the model.

3.4 SIMULATOR CAPABILITIES AND LIMITATIONS

The X-22A aircraft, hence simulator, does not have independent control over all six degrees of freedom. This fundamental limitation has implications for both the longitudinal and lateral-directional simulation of the AV-8A. Longitudinally, the X- and Z-force characteristics of the AV-8A cannot be independently matched by the X-22A since collective blade pitch is currently the only longitudinal force control available, and its effect is dictated primarily by thrust vector (duct) angle. The ability to incorporate the collective use of the elevons as a third longitudinal controller will serve to ameliorate this potential problem area; however, no means exists for a similar alleviation in the lateral-directional degrees of freedom. The higher value of side-force-due-to-sideslip of the X-22A, which is not variable, means that matching both sideslip and lateral acceleration time histories perfectly is not possible if bank angle responses are matched. The effect of a lateral acceleration mismatch will not be revealed in a fixed-base ground simulator experiment; in flight, lateral acceleration may be an important proprioceptive and vestibular sideslip cue, and continuous control of sideslip is important in the AV-8A at low speeds because of the high dihedral effect and reduced roll control power. As a result, a compromise between matching lateral acceleration and sideslip response may be required for a valid in-flight simulation.

The effect of the discrepancy between the rotation rates of X-22A duct angle and AV-8A nozzle angle has been discussed as it applies to the simulation of the initial deceleration due to an instantaneous nozzle rotation.

In addition, the existence of a variable mismatch between AV-8A nozzle angle (θ_j) and X-22A duct angle (λ) through a transition may require that the simulator throttle gearings be made functions of the difference between θ_j and λ rather than simply functions of λ.

In addition to the well-documented capabilities of the X-22A VSS and the additional flexibility afforded by the airborne analog computer, the simulator and aircraft are both equipped with a variable feel system which adds an important dimension to the potential fidelity of the AV-8A simulation. A faithful reproduction of the AV-8A control system force-feel characteristics in pitch, roll, and yaw is possible, given sufficient information about them. Moreover, the capability to vary the control trim rates, especially in pitch, yields the ability to duplicate the Harrier trim control characteristics during the transition.

3.5 SIMULATION GUIDELINES

Based upon the above considerations of which AV-8A characteristics should be reproduced for a valid simulation and which of these desiderata can reasonably be accomplished within the current limitations of the X-22A research facility, the following guidelines for simulation fidelity are proposed:

- Fixed operating point simulation (V_o = 0, 30, 60, 80, 100, 120 kts)

    1. Match control system force-displacement relationships. Match control authorities.

    2. Match short-term (~5 seconds) pitch, roll, and yaw attitude reponses of the simulator and the AV-8A mathematical model to specified control inputs.

    3. Match major modal characteristics (short term frequency, damping; Dutch roll frequency, damping; roll mode time constant; roll-due-to-sideslip).

    4. Attempt to reproduce specific derivatives judged to be important, e.g. M_w, L'_v, N'_v.

    5. Attempt to match short-term vertical and longitudinal velocity responses to throttle inputs, i.e., time constants and relative magnitudes.

    6. Attempt to match short-term lateral velocity response to control inputs. Further study of the lateral acceleration/sideslip mismatch is warranted.

- Transition Simulation

    1. Treat transition as series of fixed operating points where dynamic response characteristics are functions of duct angle, hence trimmed velocity. Consider treating throttle gearings as functions of (θ_j - λ).

2. Match trends of trim changes (pitch, power) in transition.

3. Attempt to match both short-term and long-term deceleration characteristics in response to nozzle rotation.

The effects of these guidelines on generating a simulation methodology and on determining the techniques for the actual mechanization of the AV-8A simulation are described in the following two sections.

Section 4

SIMULATION METHODOLOGY

4.1 LATERAL-DIRECTIONAL

As a result of its current lack of a mechanism for direct side force control, the X-22A aircraft is not in general capable of simulating the lateral-directional stability and control characteristics of another VTOL aircraft in toto. However, as will be demonstrated in this subsection, the important lateral-directional flying qualities parameters of the basic AV-8A may be very adequately simulated by the X-22A using only the existing VSS roll and yaw channels.

The lateral-directional rigid-body equations of motion of the AV-8A may be described by a three-degree-of-freedom, fourth-order system (Section 2):

$$\dot{x} = Fx + Gu$$

x = state vector of aircraft (4 elements)

F = aircraft system matrix (3 x 4)

G = aircraft control matrix (3 x 2)

u = aircraft control vector (2 elements - roll and yaw control)

Thus, twelve state coefficients and six control coefficients are, in general, required to describe fully the lateral-directional dynamics of the aircraft. With two independent lateral-directional controls, roll and yaw, available in the X-22A, only two of the three degrees of freedom may be independently controlled. Thus, eight state coefficients-controllable degrees of freedom (2) X order of system (4) - and four control coefficients-controllable degrees of freedom (2) X number of controls (2) - may be specified. Therefore, the X-22A, using only roll and yaw controls, is capable of reproducing twelve of the eighteen parameters which describe the lateral-directional dynamics of the basic AV-8A; the six independent coefficients which cannot be directly controlled are the side force derivatives, of which the side-force-due-to-sideslip (Y_β) has the dominant effect on the AV-8A's lateral-directional flying qualities. Accordingly, the process whose end product is an acceptable in-flight simulation of the basic AV-8A's lateral-directional characteristics initially involves the selection of the twelve flying qualities parameters to be specified for the simulation.

A Calspan-developed digital computer program utilized primarily for lateral-directional simulations involving the USAF/Calspan T-33 (Reference 28) was used to calculate the appropriate X-22A VSS gains for the Harrier lateral-directional simulation. The input requirements for this program include: 1) the X-22A dimensional stability/control derivatives in primed form, airspeed, and angle of attack at the flight conditions of interest and 2) the twelve

specified AV-8A stability/control parameters at each flight condition expressed in terms of modal characteristics and stability/control derivatives. Included in the program output for each flight condition are:

- the VSS gains required to achieve the specified parameters
- the stability/control derivatives of the simulated aircraft, i.e., X-22A with VSS in operation with calculated gains
- equations of motion and modal characteristics of simulated aircraft
- roots and transfer functions of simulated aircraft
- time histories of simulated aircraft response to control inputs.

The simulation methodology, dictated in part by the structure of the computer program, was to specify the values of the following parameters at each flight condition:

ζ_d	$\lvert\phi/\beta\rvert_d$	$L'_{\delta_{as}}$
ω_d	$L'_{\dot{\beta}}$ (= 0)	$N'_{\delta_{as}}$
τ_R	$N'_{\dot{\beta}}$ (= 0)	$L'_{\delta_{rp}}$
τ_s		$N'_{\delta_{rp}}$

The remaining parameter to be specified, $\angle(\phi/\beta)_d$, was iterated about its nominal value in an effort to achieve the best match of the derivatives L'_β and N'_β and the flying qualities parameter ω_ϕ/ω_d.

Using the above criteria, the VSS roll and yaw channel gains were calculated as a function of flight condition, specifically λ . These gains are presented in Table 4-1.

As discussed above, certain stability and control parameters of the basic AV-8A model were not specifically matched by the VSS gain calculation techniques. Table 4-2 presents the values of the parameters for the X-22A model with the VSS in operation at the calculated gain levels and compares them to the corresponding value for the basic AV-8A model described in Section II. In addition to the differences in Y_β mentioned previously, inspection of Table 4-2 reveals that discrepancies between the characteristics of the basic AV-8A model and those of the X-22A simulation of the model exist in the following areas:

TABLE 4-1

CALCULATED LATERAL/DIRECTIONAL VSS GAINS (BASIC AV-8A)

λ Deg.	$\Delta a/\beta$ ($\Delta a/v$) In./Deg (In./Ft/Sec)	$\Delta a/p$ In./Deg/Sec	$\Delta a/r$ In./Deg/Sec	$\Delta a/\delta_{as}$ In./In.	$\Delta a/\delta_{rp}$ In./In.
0	-.092 (-.026)	.006	-.070	0.96	0.65
15	-.062 (-.021)	.012	-.069	0.95	0.78
30	-.041 (-.017)	.018	-.052	1.02	0.51
45	-.002 (-.001)	.020	-.039	1.06	0.36
65	.033 (.037)	.010	-.016	1.13	0.09
90	.005 (.033)	.006	-.003	1.23	-0.43

(a) Roll Channel

λ Deg.	$\Delta r/\beta$ ($\Delta r/v$) In./Deg (In./Ft/Sec)	$\Delta r/p$ In./Deg/Sec	$\Delta r/r$ In./Deg/Sec	$\Delta r/\delta_{as}$ In./In.	$\Delta r/\delta_{rp}$ In./In.
0	.349 (.098)	-.042	.065	-1.08	4.46
15	.244 (.083)	-.039	.064	-0.87	3.92
30	.060 (.025)	-.024	.036	-0.47	2.29
45	-.010 (-.006)	-.015	.027	-0.31	1.59
65	-.024 (-.027)	-.011	.019	-0.19	1.08
90	-.004 (-.027)	-.025	.012	-0.17	0.86

(b) Yaw Channel

TABLE 4-2

COMPARISON OF STABILITY/CONTROL PARAMETERS

V Kts.	λ Deg	L'_β (Rad/Sec^2/Rad)	(L'_v) (Rad/Sec^2/Ft/Sec)	L'_p (Rad/Sec^2/Rad/Sec)	L'_r (Rad/Sec^2/Rad/Sec)	N'_β (Rad/Sec^2/Rad)	(N'_v) (Rad/Sec^2/Ft/Sec)	N'_p (Rad/Sec^2/Rad/Sec)	N'_r (Rad/Sec^2/Rad/Sec)	$(\phi/\beta)_s$ Deg	$[\zeta_{\phi_{OR}}; \omega_\phi]$ $(\frac{1}{T_{\phi_1}})(\frac{1}{T_{\phi_2}})$
120	0 (1)	-11.3	(-.056)	-0.76	0.16	0.42	(.0021)	-0.30	-0.18	39	[.26; .91]
	(2)	-11.8	(-.058)	-0.94	0.43	0.41	(.0020)	-0.29	-0.19	45	[.17; .88]
100	15 (1)	- 9.6	(-.057)	-0.58	-.015	0.37	(.0022)	-0.26	-0.15	38	[.27; .84]
	(2)	-10.0	(-.059)	-0.80	0.36	0.32	(.0019)	-0.24	-0.16	45	[.16; .81]
80	30 (1)	- 6.7	(-.049)	-0.39	0.25	0.18	(.0013)	-0.23	-0.14	40	[.34; .65]
	(2)	- 7.2	(-.053)	-0.64	0.29	0.18	(.0013)	-0.20	-0.13	47	[.16; .64]
60	45 (1)	- 3.7	(-.036)	-0.24	0.29	0.0	(0.0)	-0.18	-0.11	44	[.52; .38]
	(2)	- 4.1	(-.040)	-0.48	0.22	0.0	(0.0)	-0.15	-0.10	52	[.23; .36]
30	65 (1)	-0.51	(-.010)	-0.11	0.22	-0.129	(-.0025)	-0.16	-0.04	56	(-.22) (.47)
	(2)	-0.61	(-.012)	-0.26	0.11	-0.107	(-.0021)	-0.08	-0.06	64	(-.24) (.35)
0	90 (1)	-0.04	(-.005)	0.06	0.0	-0.032	(-.0038)	-0.31	-0.015	54	(-.12) (.25)
	(2)	-0.04	(-.005)	-0.04	0.0	-0.039	(-.0045)	0.0	-0.015	63	(-.17) (.21)

(1) X-22A/VSS Simulation of AV-8A

(2) Basic AV-8A Model

- roll damping (L'_p)
- coupling derivatives (L'_r and N'_p)
- $(\pm \phi/\beta)_d$
- ζ_ϕ

A brief evaluation of the effects of these discrepancies was conducted in the frequency domain by a comparison of the transfer function numerators of the two models (Table 4-3) and in the time domain by a comparison of time histories of state variable responses to identical roll and yaw control inputs (Figure 4-1). Both the transfer functions and the time history data indicate acceptable matches of the state variables to pilot control inputs with the possible exception of the yaw rate response to lateral stick input in hover. However the magnitude of the lateral acceleration response to control of the basic AV-8A model is significantly less than the corresponding X-22A/VSS response because of the order of magnitude difference in the Y_v derivative between the two vehicles. This same discrepancy will also result in widely different lateral acceleration responses to turbulence.

4.2 LONGITUDINAL

4.2.1 Summary of the Problem

The longitudinal simulation problem is similar to but more difficult than the lateral/directional situation. Again, three degree of freedom motion is to be simulated with two controllers, if possible; although the use of the elevons in a collective fashion would provide three controllers and hence exact simulation could be possible, the elevons would have limited authority and hence is was judged desirable to avoid using feedbacks to them. Unfortunately, the digital computer design procedure used to compute the lateral/directional feedback gains was not an appropriate tool for the longitudinal design problem because:

- The collective blade controller changes from being effective at changing vertical-force equation characteristics at low speeds to changing longitudinal-force equation characteristics at high speeds. Hence a uniform set of desirable modal characteristics cannot be simulated over the entire velocity range.

- Although the majority of important modal characteristics for lateral/directional flying qualities can be achieved through control of the yaw and roll moment equations, for the longitudinal problem the individual force equations (particularly longitudinal force) are not as effective. In addition, equivalent modal characteristics (e.g. $|\phi/\beta|_d$) are not as well defined in terms of flying qualities for the longitudinal problem, particularly in transition.

TABLE 4-3

LATERAL-DIRECTIONAL CHARACTERISTIC ROOTS AND TRANSFER FUNCTIONS

V Kts	λ Deg	Δ(s)	$N^{v}_{\delta_{as}}$	$N^{\phi}_{\delta_{as}}$	$N^{r}_{\delta_{as}}$
120	0 (1)	(.074)(1.74) [-.14; 1.8]	10.0(.086)(4.36)	0.47 [.30; .89]	.017(.60)(-.74)(-7.5)
	(2)	(.056)(1.73) [-.15; 1.8]	10.0(.074)(3.99)	0.45 [.17; .88]	.014(.53)(-.94)(-7.9)
60	45 (1)	(.056)(1.23) [-.27; 1.2]	5.1(.063)(4.11)	0.43 [.51; .36]	.009(.54)(-.38)(-7.6)
	(2)	(.068)(1.26) [-.28; 1.2]	5.0(.075)(4.15)	0.45 [.23; .36]	.014(.49)(-.66)(-4.0)
0	90 (1)	(.015)(0.59) [-.50; 0.52]	0.4(.014)(37.3)	0.45(-.12)(.25)	.014 [.14; 0.61] (-10.2)
	(2)	(.015)(0.58) [-.50; 0.52]	0.4(.015)(34.3)	0.45(-.17)(.21)	.014 [.53; 1.64] (-1.66)

V	λ	$N^{v}_{\delta_{rp}}$	$N^{\phi}_{\delta_{rp}}$	$N^{r}_{\delta_{rp}}$
120	0 (1)	-62.3(-.025)(.88)	-.09(5.9)(-6.1)	0.3 [.04; 1.3] (1.04)
	(2)	-0.96(-.052)(1.06)(64.8)	-.11(4.9)(-6.3)	0.3 [.01; 1.3] (1.12)
60	45 (1)	-25.8(-.16)(.57)	-.10(2.8)(-3.2)	0.24 [-.22; 1.05] (1.07)
	(2)	-0.78(.08)(.69)(32.8)	-.10(2.9)(-3.6)	0.24 [-.24; 1.07] (1.11)
0	90 (1)	-1.67(.010)(1.61)	-.08(.42)(-.28)	0.19 [-.40; 0.55] (0.65)
	(2)	-0.6(.015) [.67;2.07]	-.08(.37)(-.37)	0.19 [-.46; 0.60] (0.63)

(1) X-22A/VSS Simulation of AV-8A (Simplified VSS Gains of Section 5)

(2) Basic AV-8A Model

$$K\left(\frac{1}{T}\right)[\zeta;\ \omega] = K\left(s+\frac{1}{T}\right)\left(s^2+2\zeta\omega s+\omega^2\right)$$

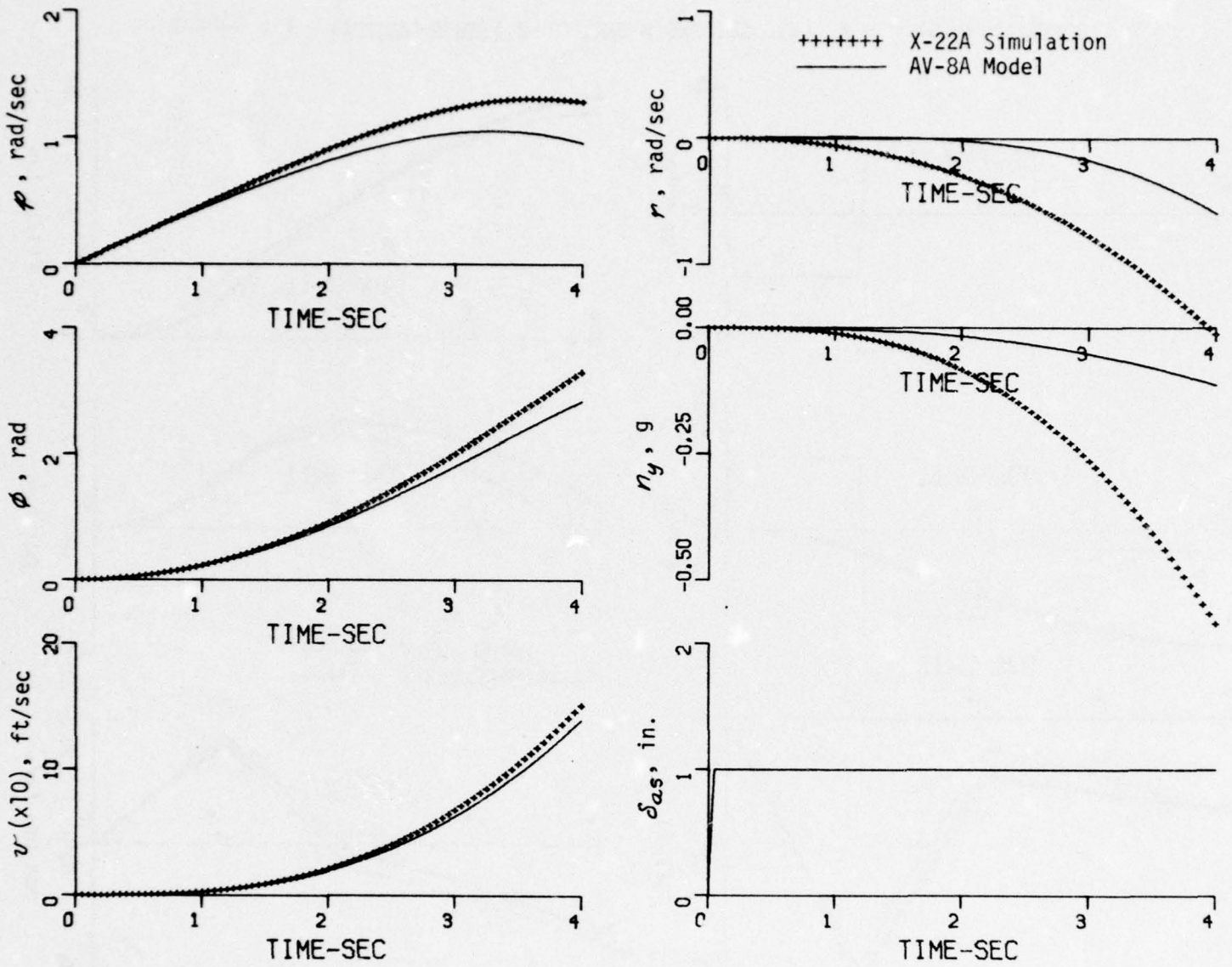


Figure 4-1 LATERAL-DIRECTIONAL TIME HISTORIES (a) V = 0 kt; δ_{as} STEP

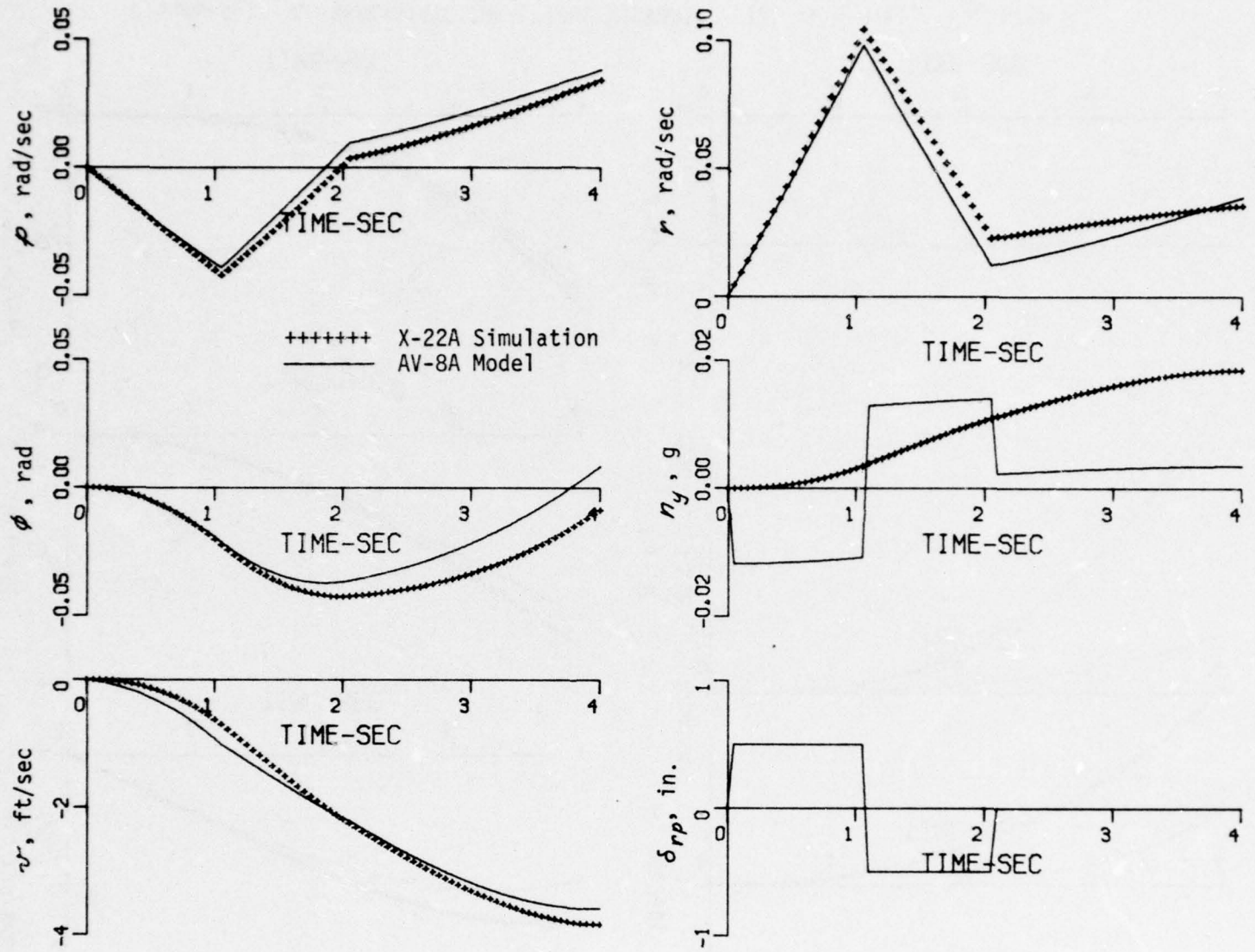


Figure 4-1 LATERAL-DIRECTIONAL TIME HISTORIES (b) V = 0 kt: δ_{rp} DOUBLET

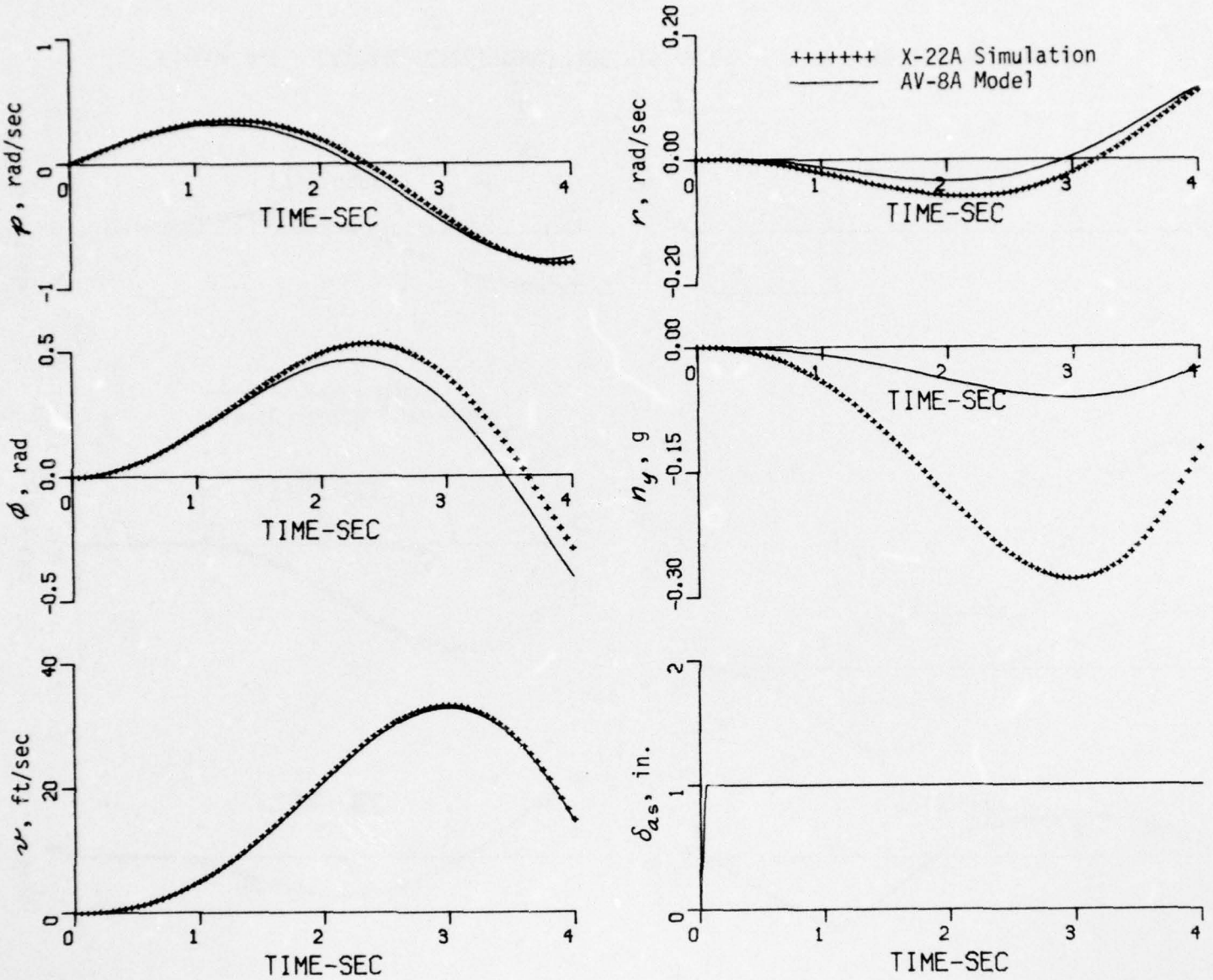


Figure 4-1 LATERAL-DIRECTIONAL TIME HISTORIES (c) V = 60 kt; δ_{as} STEP

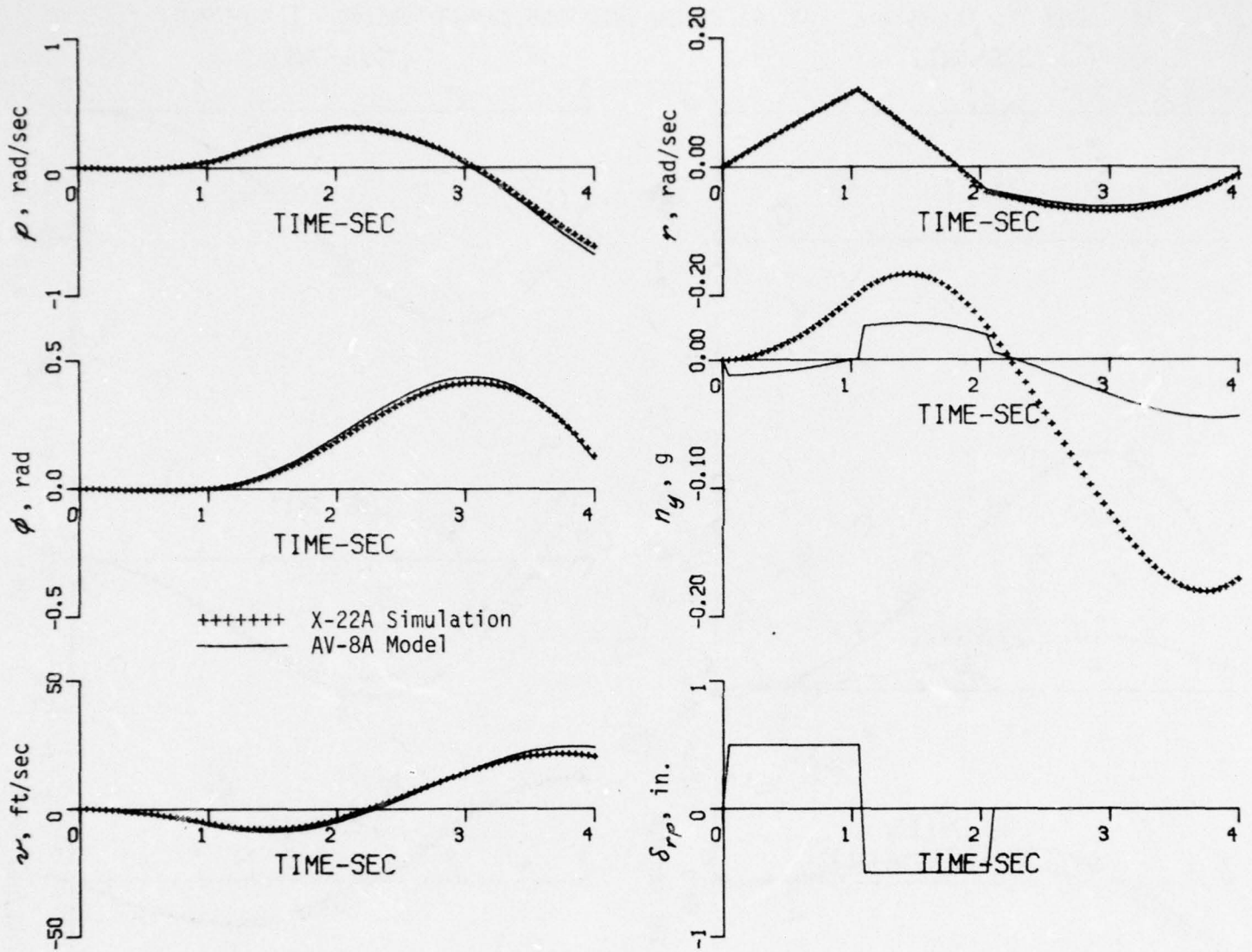


Figure 4-1 LATERAL-DIRECTIONAL TIME HISTORIES (d) V = 60 kt; δ_{rp} DOUBLET

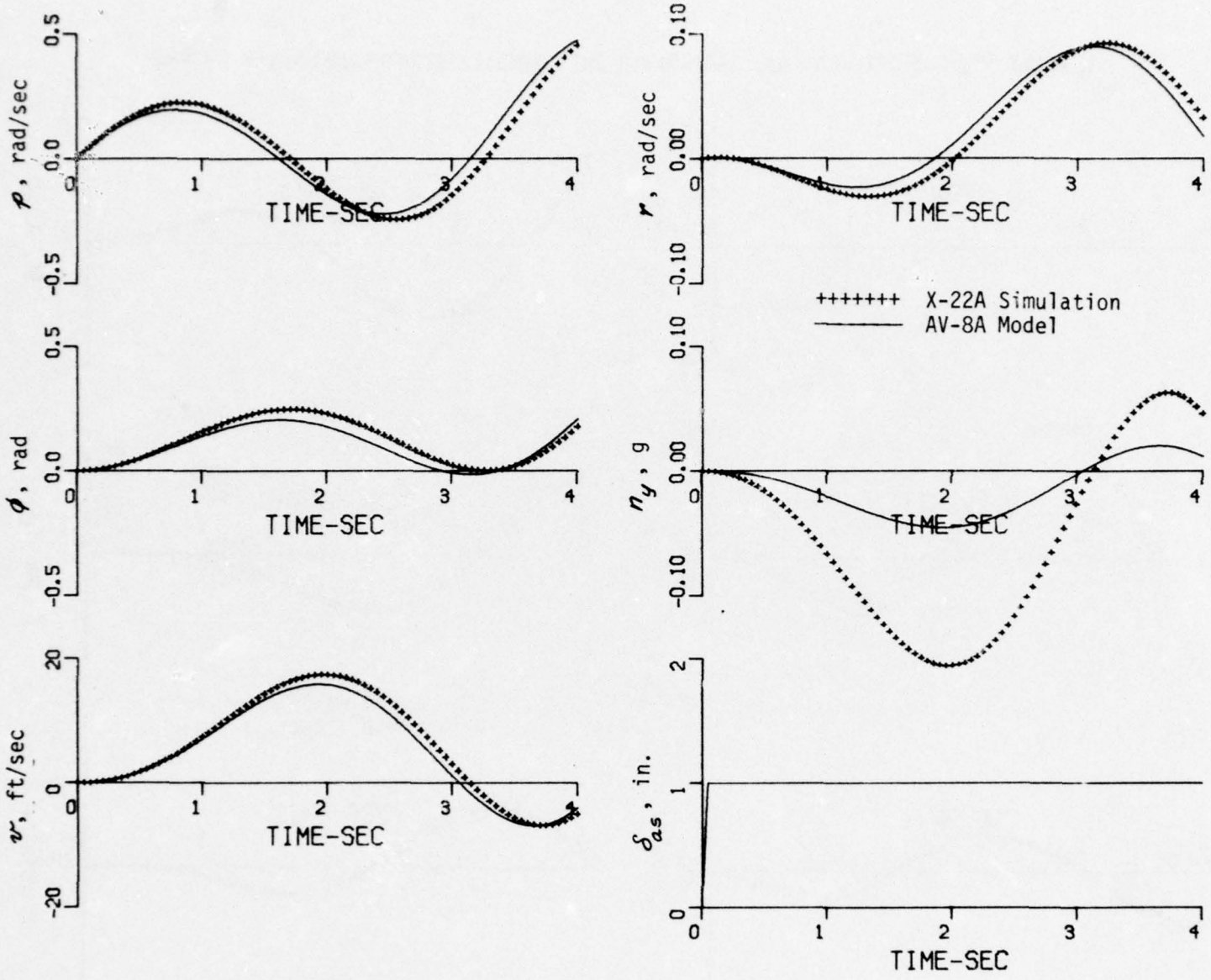


Figure 4-1 LATERAL-DIRECTIONAL TIME HISTORIES (e) V = 120 kt; δ_{as} STEP

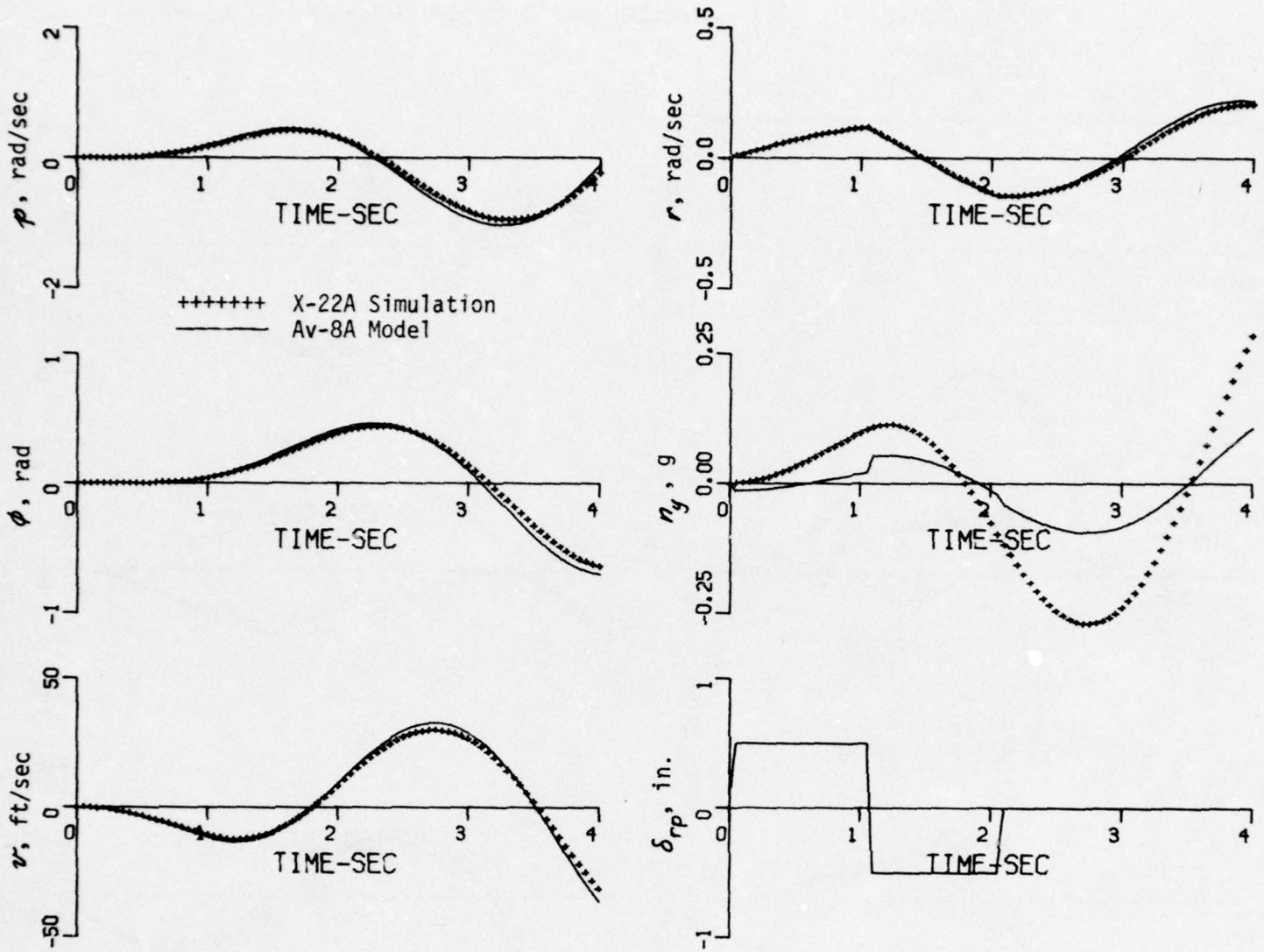


Figure 4-1 LATERAL-DIRECTIONAL TIME HISTORIES (f) V = 120 kt; δ_{rp} DOUBLET

As a result of these difficulties, alternate design procedures were investigated for the longitudinal gain calculations. In particular, "least-squares" and optimal control techniques were examined for applicability to the feedback gain computations, while least squares and modified response-error techniques were investigated for the gearing calculations. The following subsection presents a tutorial review of the feedback design procedures, indicates the reasons for selecting the optimal control procedure, and develops a theoretical extension to the optimal control methodology that is required for this application. The feedback design results are then presented and discussed in Section 4.2.3. Possible ways of computing the gearings are discussed and developed in Section 4.2.4 along with the results obtained with the selected method. Finally, time history responses of the resulting longitudinal simulation are compared with the AV-8A model responses in Section 4.2.5.

4.2.2 Development of Feedback Laws

The least-squares result is obtained by minimizing a non-integral performance index of the general form:

$$V = e^T Q e + u^T R u$$

This problem, it should be observed, is a direct minimization procedure since no integral is involved: to find the value of the control which minimizes V we set the gradient (derivative) of V with respect to u equal to zero:

$$\nabla_u V = 0, \quad \text{solve for } u.$$

Since the intent of the design is to compute feedback gains which will make one system (the "plant") match the characteristics of another system (the "model"), a convenient choice for the error term in the performance index is the equation error between the two systems. To concentrate our attention on the feedback computations, consider the following example:

$$\left.\begin{aligned} \dot{x} &= Fx + Gu \quad \text{(Plant)} \\ \dot{y} &= Ly \quad \text{(Model)} \end{aligned}\right\} \; y = Hx$$

so that $$e = \dot{x} - \dot{y} = (F - LH)x + Gu$$

Choosing $H = I$ for simplicity (i.e., the model states correspond directly to the plant states), and substituting into the equation for V, we find:

$$V = x^T (F-L)^T Q (F-L) x + 2x^T (F-L)^T Q G u + u^T \left[G^T Q G + R\right] u$$

Then:

$$\nabla_u V = 0 = 2G^T Q (F-L) x + 2\left[G^T Q G + R\right] u$$

or $$u_{LS} = -\left[G^T Q G + R\right]^{-1} G^T Q (F - L) x \qquad \text{for} \quad V = e^T Q e + u^T R u$$

In the event that control motions are not weighted, then $R = 0$ and the solution is:

$$u_{LS} = -\left[G^T Q G \quad\right]^{-1} G^T Q (F - L) x \qquad \text{for} \quad V = e^T Q e$$

The optimal control result is obtained by minimizing an integral performance index of the general form:

$$I = \int_0^\infty (e^T Q e + u^T R u)\, dt$$

The problem now is the minimization of a functional, which requires the use of somewhat more complicated mathematics, such as the calculus of variations or Pontryagin's maximum principle, to solve. The problem has been solved and discussed for many choices of the error term (see References 29, 30); although repeating the development here is not therefore strictly necessary, it may be a useful exercise to understand the result obtained. Accordingly, a brief development of this particular example follows, with some liberties taken in the cause of simplification.

For the same error expression used in the least-squares example, our problem is:

Minimize
$$I = \int_0^\infty \left[(\dot{x} - \dot{y})^T Q (\dot{x} - \dot{y}) + u^T R u\right] dt$$

$$= \int_0^\infty \left[(Fx + Gu - Lx)^T Q (Fx + Gu - Lx) + u^T R u\right] dt$$

subject to $$\dot{x} = Fx + Gu$$

Recall that, in the calculus of variations (to use the solution method most familiar), the system constraints are introduced through the use of Lagrange multipliers:

$$2V \triangleq \int_0^\infty \left[(Fx + Gu + Lx)^T Q (Fx + Gu + Lx) + u^T R u + 2\lambda \cdot (-\dot{x} + Fx + Gu)\right] dt$$

A necessary condition for the optimum to exist is then that the Euler equations plus the constraint equation be satisfied. These relationships are:

$$\left.\begin{aligned} \frac{d}{dt}\left(\frac{\partial J}{\partial \dot{x}}\right) - \frac{\partial J}{\partial x} &= 0 \\ \frac{d}{dt}\left(\frac{\partial J}{\partial \dot{u}}\right) - \frac{\partial J}{\partial u} &= 0 \end{aligned}\right\} \qquad \text{where } J \text{ is the integrand}$$

$$\dot{x} - Fx - Gu = 0$$

Considering the second equation:

$$\frac{\partial J}{\partial \dot{u}} = 0 \qquad (\dot{u} \text{ does not appear explicitly})$$

$$\frac{\partial J}{\partial u} = 2G^T Q(Fx + Gu - Lx) + 2Ru + 2G^T\lambda$$

Hence:

$$2G^T Q(F-L)x + 2(G^T QG + R)u + 2G^T\lambda = 0$$

or:

$$u_{OPT} = -\left[G^T QG + R\right]^{-1}\left\{G^T Q(F-L)x + G^T\lambda\right\}$$

Before continuing with the solution, it can be immediately noted that the form of the result for the control is different than the one obtained with the least-square computation: the Lagrange multiplier (or "adjoint variable") is added to the least-square result.

Considering now the first equation:

$$\frac{\partial J}{\partial \dot{x}} = -2\lambda, \qquad \frac{d}{dt}\left(\frac{\partial J}{\partial \dot{x}}\right) = -2\dot{\lambda}$$

$$\frac{\partial J}{\partial x} = 2(F-L)^T Q(Fx + Gu - Lx) - 2F^T\lambda$$

Hence:

$$-\dot{\lambda} - F^T\lambda - (F-L)^T Q(Fx + Gu - Lx) = 0$$

We now have three equations in the three unknowns (x , u, λ). Eliminating u by using the solution of the second equation we have:

$$-\dot{\lambda} - \left[F^T - (F-L)^T QG\left[G^TQG + R\right]^{-1}G^T\right]\lambda$$

$$-\left\{(F-L)^TQ(F-L) - (F-L)^TQG\left[G^TQG+R\right]^{-1}G^TQ(F-L)\right\}x = 0$$

$$\dot{x} - \left[F - G\left[G^TQG+R\right]^{-1}G^TQ(F-L)\right]x + G\left[G^TQG+R\right]^{-1}G^T\lambda = 0$$

These two equations constitute the necessary conditions for the optimum control to exist. It is necessary to solve them for λ in order to obtain the optimum control, as is evident in the expression for u_{OPT}. To obtain this solution, it is easiest to define first some expressions to simplify the form of the equations; although these definitions seem arbitrary at first glance, the point is to put the equations in the "canonical" form of the regulator problem ($e = x$ in the performance index), for which the solution is known.

Let:

$$\hat{F} \triangleq F - G\left[G^TQG + R\right]^{-1}G^TQ(F-L)$$

$$\hat{Q} \triangleq Q - QG\left[G^TQG + R\right]^{-1}G^TQ$$

$$\hat{R} \triangleq G^TQG + R$$

$$\hat{H} \triangleq F - L$$

Then the equations are:

$$-\dot{\lambda} = \hat{F}^T\lambda + \hat{H}^T\hat{Q}\hat{H}x$$

$$\dot{x} = \hat{F}x - G\hat{R}^{-1}G^T\lambda$$

We now assume that the adjoint variable has the form:

$$\lambda = P(t)x$$

Then:

$$\dot{\lambda} = \dot{P}x + P\dot{x} = \dot{P}x + P\hat{F}x - PG\hat{R}^{-1}G^TPx$$

Since

$$\dot{x} = \hat{F}x + G\hat{R}^{-1}G^T\lambda = \hat{F}x - G\hat{R}^{-1}G^TPx$$

Substituting into the $\dot{\lambda}$ equation:

$$\dot{P}x + P\hat{F}x - PG\hat{R}^{-1}G^TPx + \hat{F}^TPx + \hat{H}^T\hat{Q}\hat{H}x = 0$$

The assumption on the form of λ means that this expression must hold for all x ; hence:

$$\dot{P} + P\hat{F} + \hat{F}^TP - PG\hat{R}^{-1}G^TP = -\hat{H}^T\hat{Q}\hat{H}^T$$

This equation is called the Ricatti equation, and is a nonlinear differential equation in P. The use of infinity as the upper integration limit in the performance index, however, permits us to consider only the steady-state solution, which is found from the algebraic equation obtained by setting $\dot{P} = 0$. Finally, then, we have the optimal control solution as:

$$u_{OPT} = -\left[G^TQG + R\right]^{-1}G^T\left[Q(F-L)+P\right]x$$

where

$$P\hat{F} + \hat{F}^TP - PG\hat{R}^{-1}G^TP = -\hat{H}^T\hat{Q}\hat{H}$$

Comparing the optimal control and least-squares solutions, the difference in the designed feedback gains is clear. This difference is related to the following fundamental characteristics of the two procedures:

- The optimal control procedure guarantees a stable closed-loop system* regardless of whether or not the plant (or model) is unstable and regardless of the number of controllers used. No such guarantee exists for the least-squares solution.

- The least-squares result will reproduce the model characteristic roots only if three controllers are used. For one or two controllers, some of the closed-loop system roots may be unstable even if the model is stable. If the model is stable, the optimal control result can provide characteristic roots close to those of the model (depending on the relative Q and R weightings) for less than three controllers.

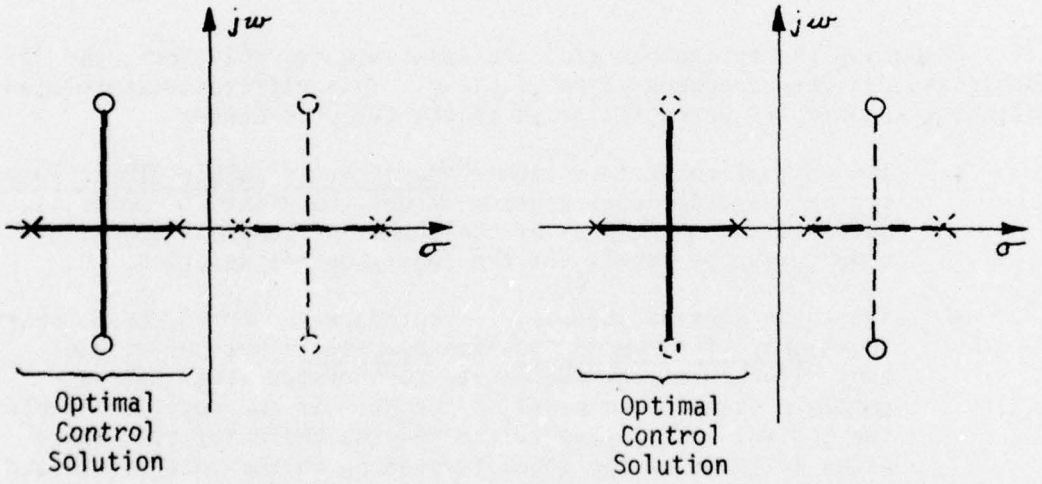
The desirability of using only two controllers makes the least-squares technique unacceptable for this application. The optimal control procedure is inherently more suitable to situations in which complete controllability (3 controllers) does not exist. However, another characteristic of the optimal control causes a different problem for this application: the closed-loop is

* Subject to R being positive definite, Q positive semi-definite

guaranteed stable, but the AV-8A model is unstable. Hence, the roots of the augmented plant using the optimal control feedback gains do not include the unstable model roots, and would therefore provide a poor simulation. It was therefore necessary to extend the plant-in-the-performance-index optimal control theory to deal with this situation.

As has been discussed by Rynaski (Reference 29), a useful visualization of the optimal control procedure is the root-square locus technique. This technique utilizes the characteristics of the Hamiltonian to show that the adjoint roots are just the reflection of the system roots about the imaginary axis, and that, with both sets of roots drawn, conventional root-locus techniques can be used to compute their migrations. When the model-in-the-performance-index procedure is used, the roots of the plant are the poles and the roots of the model are the zeroes. The loci in the left-hand plane are then the optimal control solutions for varying Q and R.

Two examples of root-square locus sketches are shown in Figure 4-2 for a second-order system: in (a), both the plant and model are stable, whereas in (b) the plant is stable but the model is unstable. The adjoint poles and zeroes are shown as dashed symbols.



a) Stable Model

b) Unstable Model

Figure 4-2 OPTIMAL CONTROL EXAMPLES IN S-PLANE

As can be seen from these sketches, what happens when the model is unstable is that the plant roots migrate to the adjoint zeroes (which are stable) to ensure a stable augmented system; in fact, for this example the optimal gains would be computed to be the same for both (a) and (b). The optimal control procedure will always use the poles and zeroes on the left-hand side in computing the gains, and will never try to "follow" an unstable model if Q and R meet positive-definite requirements.

To use the optimal control procedure for our application, therefore, it has been necessary to devise an approach to "fool" the computational technique. The basic idea is to perform the analysis in a transformed s-plane which is selected such that both plant and model are stable with respect to it; the gains which give desired transformed eigenvalues are then shown to yield following of the unstable model in the original s-plane.

The eigenvalues of the plant and model can be expressed by:

$$P^{-1}FP = \Lambda_p, \quad M^{-1}LM = \Lambda_m$$

Choose a positive number "n" such that, when it is subtracted from the most unstable eigenvalue, real or complex, the new eigenvalue is stable. Then define:

$$\Lambda'_p = \Lambda_p - nI, \quad \Lambda'_m = \Lambda_m - nI$$

It is then easy to show that:

$$P^{-1}F'P = \Lambda'_p \quad \text{if} \quad F' = F - nI$$

$$M^{-1}L'm = \Lambda'_m \quad \text{if} \quad L' = L - nI$$

We now solve the following optimal control problem:

Minimize

$$J = \int_0^\infty \left[(\dot{x} - \dot{y})^T Q (\dot{x} - \dot{y}) + u^T R u\right] dt$$

Subject to:

$$\dot{x} = F'x + Gu$$

$$\dot{y} = L'y$$

$$x = y$$

For this transformed problem, all of the system poles and zeroes are on the left-hand side of the transformed s-plane and all the adjoint roots are in the right-hand side; hence, conventional juggling of the Q and R matrices can be used to get the augmented plant roots (in the transformed plane) as close to the model roots as desired.

Calling the resulting optimal control gain matrix K' and the augmented eigenvalues in the transformed system Λ'_A, we may now write:

$$A^{-1}(F' - GK')\,A = \Lambda'_A$$

Then:

$$A^{-1}(F - GK')\,A = \Lambda'_A + nI$$

Hence, using the computed gains with the original, untransformed plant matrix yields a set of eigenvalues $\Lambda_A = \Lambda'_A + nI$; if the optimal control procedure made $\Lambda'_A \cong \Lambda'_m$, then $\Lambda_A \cong \Lambda_m$ as desired because $\Lambda_m = \Lambda'_m + nI$. Figure 4-3 sketches the result of this procedure for the unstable model example shown in Figure 4-2b.

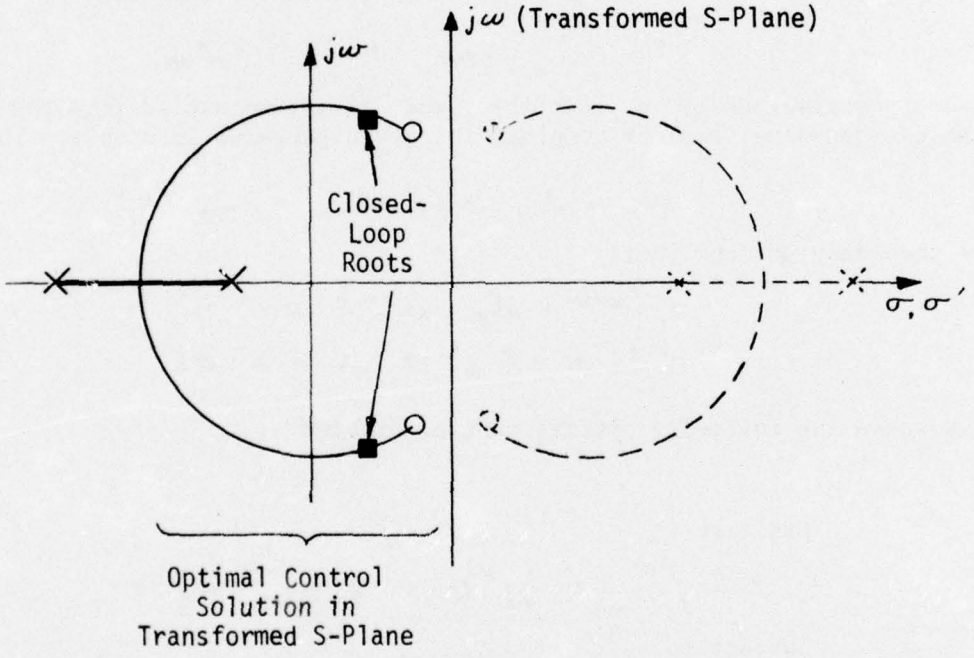


Figure 4-3 EXAMPLE OF TRANSFORMED OPTIMAL CONTROL SOLUTION

With this modified technique, it is possible to use optimal control procedures to compute feedback gains to simulate the AV-8A model in the X-22A. The following subsection presents the results of these analyses.

4.2.3 Feedback Gain Computations

Gains for the longitudinal simulation of the AV-8A were computed at the six flight conditions discussed in Section II: V_o = 0, 30, 60, 80, 100, 120 kts; γ = -5 degrees, α = +8 degrees. The model values used in the model matrix were given in Table 2-1; the plant values are the X-22A stability and control derivatives programmed on the ground simulator as listed in Table 5-1 in the next section. For the X-22A, trim velocity and duct angle are closely related; hence, the computed gains may be programmed in the variable stability system as a function of either variable. For this application, duct angle was selected since the signal is monotonic and less noisy than the velocity signal: the computed gains to be discussed here will therefore be presented for flight condition in terms of duct angle as well as trim velocity.

The gains for each flight condition were computed assuming two controllers: longitudinal stick and collective blade pitch. Since only two controllers are used, perfect matching of all the model characteristics is impossible, and hence it is necessary to decide which characteristics are most important to match. For this application, matching the characteristic roots of the model matrix was judged most important -- in particular, matching the most stable and most unstable roots was of paramount importance. The values of feedback gains selected were the ones which best achieved this desideratum.

The computational procedure consists of selecting various values of the Q and R matrices, computing the gains, and checking the resulting closed-loop eigenvalues. This iterative "art" was a fairly straightforward process for the low speed configurations, because the two controllers have major effectivenesses on the moment and vertical force equations; the higher speed cases (V_o = 80, 100, 120 kt) were more difficult because the collective pitch effectiveness is primarily on the longitudinal force equation. For these latter cases, it was necessary to assume different values of Q and/or R in the model matrix to achieve feedback gains which made the closed-loop roots as unstable as the original model roots. A summary of the values of Q and R used is given in Table 4-4.

The computed feedback gains are given in Table 4-5a, and simplified (for implementation purposes) values listed in Table 4-5b. The closed-loop roots using the simplified gains are compared with the model roots in Table 4-6. As can be seen, the correspondence is generally good for the dominant roots. Table 4-7 compares the closed-loop characteristic matrices with the model matrices; note that the M and Z equations are well matched for V_o = 0, 30, 60 kts, but that the X and Z equations are dissimilar for V_o = 80, 100, 120 kts. This dissimilarity leads to poor matching of time history responses to throttle inputs, as will be discussed shortly.

TABLE 4-4

WEIGHTING MATRICES AND MODEL MODIFICATIONS
FOR LONGITUDINAL GAIN COMPUTATIONS

V	Q	R	Modified Model
0	diag (.001, 10, .1, 100)	diag (.3, .1)	None
30	diag (.001, 10, .1, 100)	diag (.3, .1)	None
60	diag (.001, 10, .1, 100)	diag (0, 0)	None
80	diag (.001,.001,.001,100)	diag (.3, .1)	M_w = .0051, M_q = -.953
100	diag (.001,.001,.001,100)	diag (.3, .1)	M_w = .00545, M_q = -1.06
120	diag (.001,.001,.001,100)	diag (.3, .1)	M_w = .006, M_q = -1.35

TABLE 4-5a

LONGITUDINAL FEEDBACK GAINS:
EXACT COMPUTATIONS IN COMPUTER UNITS

V	Δ_E/u	Δ_E/w	Δ_E/θ	Δ_E/q	Δ_c/u	Δ_c/w	Δ_c/θ	Δ_c/q
0	.039	0	.0007	+ .633	-.0012	+.066	0	-.0672
30	-.028	-.044	-.109	+ .603	+.113	+.271	2.56	-.0491
60	-.053	-.101	-.064	+ .373	+.197	+.419	+ .841	+.020
80	-.032	-.049	-.016	- .964	-.012	-.015	.0084	-.44
100	-.028	-.032	-.013	-1.25	-.011	-.0089	- .0053	-.525
120	-.026	-.031	-.011	-1.02	-.013	-.010	- .013	-.510

TABLE 4-5b

LONGITUDINAL GAINS FOR IMPLEMENTATION
IN GROUND SIMULATOR

V	Δ_{ES}/u	Δ_{ES}/w	Δ_{ES}/θ	Δ_{ES}/q	Δ_{CS}/u	Δ_{CS}/w	Δ_{CS}/θ	Δ_{CS}/q
0	-.039	0	0	-.0111	0	-.066	0	0
30	+.028	.044	0	-.0105	- .113	-.271	-.0449	0
60	.053	.101	0	-.0065	- .197	-.419	-.0147	0
80	.032	.049	0	+.0168	+ .012	+.015	0	.0077
100	.028	.034	0	.0147	+ .011	0	0	.0066
120	.026	.031	0	.0178	0	0	0	.0089

TABLE 4-6

COMPARISON OF MODEL AND SIMULATION
CHARACTERISTIC ROOTS IN FORM $(1/\tau)[\zeta; \omega_n]$

V	AV-8A Model	X-22A Simulation of AV-8A
0	(.33)(.02) [-.48; .32]	(.40)(.02) [-.40; .33]
30	(.66)(.064) [-.70; .33]	(.61)(.10) [-.42; .28]
60	(1.00)(.073) [-.90; .32]	(1.05)(.15) [-.83; .25]
80	(1.21)(.075) (-.38)(-.26)	(1.14)(.16) (-.37)(-.12)
100	(1.39)(.079) (-.48)(-.20)	(1.37)(.16) (-.43)(-.062)
120	(1.53)(.084) (-.47)(-.19)	(1.46)(.12) (-.47)(.078)

TABLE 4-7

COMPARISON OF MODEL AND SIMULATED
CHARACTERISTIC MATRICES

V	AV-8A Model	X-22A Simulation of AV-8A
0	$\begin{bmatrix} -.026 & 0 & -32.2 & 0 \\ 0 & -.020 & 0 & 0 \\ 0 & 0 & 0 & 1.0 \\ .001 & .0009 & 0 & 0 \end{bmatrix}$	$\begin{bmatrix} -.145 & 0 & -32.2 & -2.91 \\ .0018 & -.020 & 0 & .10 \\ 0 & 0 & 0 & 1.0 \\ .00135 & .00092 & 0 & .0045 \end{bmatrix}$
30	$\begin{bmatrix} -.035 & -.020 & -32.1 & -7.1 \\ -.011 & -.105 & -1.68 & 50.7 \\ 0 & 0 & 0 & 1.0 \\ .0017 & .0042 & 0 & -.13 \end{bmatrix}$	$\begin{bmatrix} -.222 & -.156 & -33.07 & -11.81 \\ -.012 & -.107 & -1.69 & 50.75 \\ 0 & 0 & 0 & 1.0 \\ .00129 & .0030 & -.035 & -.154 \end{bmatrix}$
60	$\begin{bmatrix} -.043 & -.027 & -32.1 & -14.2 \\ -.036 & -.19 & -1.68 & 101.0 \\ 0 & 0 & 0 & 1.0 \\ .0022 & .0054 & 0 & -.26 \end{bmatrix}$	$\begin{bmatrix} -.333 & -.34 & -32.67 & -18.87 \\ -.036 & -.19 & -1.68 & 101.0 \\ 0 & 0 & 0 & 1.0 \\ .0022 & .00526 & -.020 & -.26 \end{bmatrix}$
80	$\begin{bmatrix} -.049 & -.029 & -32.1 & -18.9 \\ -.060 & -.25 & -1.68 & 135.0 \\ 0 & 0 & 0 & 1.0 \\ .0025 & .0059 & 0 & -.43 \end{bmatrix}$	$\begin{bmatrix} -.189 & .018 & -32.1 & -24.50 \\ -.251 & -.635 & -2.97 & 134.9 \\ 0 & 0 & 0 & 1.0 \\ .00196 & .00425 & 0 & .0071 \end{bmatrix}$
100	$\begin{bmatrix} -.055 & -.030 & -32.1 & -23.8 \\ -.083 & -.31 & -1.68 & 170.0 \\ 0 & 0 & 0 & 1.0 \\ .0026 & .006 & 0 & -.43 \end{bmatrix}$	$\begin{bmatrix} -.173 & .092 & -32.1 & -29.45 \\ -.258 & -.639 & -2.81 & 170.3 \\ 0 & 0 & 0 & 1.0 \\ .0022 & .0052 & 0 & -.231 \end{bmatrix}$
120	$\begin{bmatrix} -.061 & -.030 & -32.1 & -28.4 \\ -.108 & -.37 & -1.68 & 200.0 \\ 0 & 0 & 0 & 1.0 \\ .0026 & .0058 & 0 & -.52 \end{bmatrix}$	$\begin{bmatrix} -.184 & .184 & -32.1 & -34.11 \\ -.252 & -.618 & -2.77 & 200.6 \\ 0 & 0 & 0 & 1.0 \\ .00154 & .0050 & 0 & -.39 \end{bmatrix}$

4.2.4 Control Effectiveness Computations

A major difference between the AV-8A model and the X-22A is the thrust inclination as a function of velocity, both for trim conditions and particularly for the deceleration profile. This difference implies difficulty in simulating vertical and longitudinal acceleration and/or velocity responses to throttle inputs at higher speeds if only collective blade pitch and longitudinal stick controllers are used in the X-22A. For this reason, the use of the X-22A elevons in a collective fashion, which requires a minor modification to the X-22A variable stability system, appears to be required for the simulation of the AV-8A control effectiveness characteristics; this capability has been assumed in the computations.

Several methods for computing the control effectiveness gearings were investigated. The two that offered the most promise and received the most attention were least-squares equation error and weighted response-error minimization. The former is the control matrix equivalent of the least-squares feedback computational procedure; the latter is an extension of the method used for the design of the decoupled velocity control system in the Task III X-22A experiment (Reference 32).

The least squares result is obtained by minimizing:

$$J = e^T Q e, \qquad e = Gu - G_m u_m$$

Then:

$$u = (G^T Q G)^{-1} G^T Q G_m u_m$$

This method will result in the simulated control derivatives being exactly the same as the model derivatives. For all situations, therefore, the initial accelerations are properly matched. If, in addition, the characteristic matrix has been exactly matched, then a one-for-one simulation results; as can be seen, however, the simulated characteristic matrix does not enter into this computation, and if it is not well matched (such as for the V_0 = 80, 100, 120 kt cases), the time history responses after zero time may not be a good simulation of the model responses.

The method used to design the decoupled velocity control system gearings was an attempt to assure correct time history responses (in terms of steady state magnitudes) even if the characteristic matrix is not totally matched. The closed-loop equation is written as:

$$\dot{X} = F_c X + GJ u_m$$

where J are the control gearings.

For unit inputs, the steady state responses, assuming a stable system, are:

$$x = -F_c^{-1} G J \triangleq -PJ$$

Minimizing the difference between these responses and the desired steady-state responses (x_D) leads to the equation for the gearings:

$$J = -(P^T Q P)^{-1} P^T Q x_D$$

Although this procedure was found to be the most suitable for the Task III design, it was not directly applicable to the AV-8A simulation problem because the closed-loop system is not stable. Accordingly, steady-state responses do not exist and the solution $x = -PJ$ is not valid. An attempt was therefore made to extend the analysis to unstable systems as well.

The state responses at any time to unit step inputs are, regardless of whether the system is stable or unstable:

$$x = F_c^{-1}(\dot{x} - GJ)$$

Then:

$$x_D - x = x_D - F_c^{-1}(\dot{x} - GJ)$$

If we assume, in order to minimize this error term, that we desire $\dot{x} = \dot{x}_D$ also, then the expression for J becomes:

$$J = -(P^T Q P)^{-1} P^T Q \left[x_D - F_c^{-1} \dot{x}_D\right]$$

This expression was used to investigate gearing computations at the 60 kt flight condition. As can be seen from examining the equation, a major difficulty is that the results for the gearings will be different for each time selected in obtaining $\dot{x}_D$, x_D ; hence, unless a criterion exists which specifies that the responses shall be the same at one particular time, no rational method of selecting the "best" gearings on this basis is apparent.

The least-squares equation-error procedure was therefore used to compute the gearing gains; the results are listed in Table 4-8. Since three controllers are assumed, these gains reproduce the AV-8A model control matrix exactly. The initial accelerations will therefore be correct, but no guarantee about the remainder of the time history responses can be made: differences will be dependent on differences in the characteristic matrices.

TABLE 4-8

LONGITUDINAL GEARING GAINS

V	Δ_{ES}/δ_e	Δ_{ES}/δ_T	Δ_{CS}/δ_T	Δ_{CS}/δ_e	Δ_{EL}/δ_e	Δ_{EL}/δ_T
0	.43	-.0018	-.32	2.12	- .15	- .95
30	.62	-.087	-.37	2.50	- .93	1.66
60	.80	-.135	-.22	2.22	-1.54	4.20
80	.91	-.147	-.023	1.64	-1.51	5.70
100	1.06	-.060	-.174	.95	- .38	6.84
120	1.20	.023	-.178	.28	- .26	7.78
80*	.91	-.178	-.023	2.04	-1.51	4.49
120**	1.20	-.160	-.178	1.48	- .26	4.91

* $\theta_j = 70^\circ$ No asterisk: $\theta_j = 81^\circ$

** $\theta_j = 50^\circ$

4.2.5 Resulting Longitudinal Simulation

Time history responses to simulated longitudinal stick and throttle pulse inputs are given in Figure 4-4 for the V_o = 0, 60, 120 kt trim conditions. The solid lines are the AV-8A model responses, and the crosses are those of the X-22A simulation of this model. As can be seen, excellent matching of all state variable responses to pitch stick inputs is achieved for the low speed (0, 60 kt) cases; the 30 kt responses (not shown) are similar. The only real discrepancy is in the n_x reponses, which results fro the dissimilar values of X_u and X_w: these derivatives cannot be modified significantly at the low speeds (high duct angles) with the collective plade pitch controller, and matching n_x exactly would require a third controller. Hence, for example, the longitudinal velocity response (u) to throttle inputs at 60 kt (Figure 4-4d) is not a good match, but the magnitudes are still small relative to the well-matched vertical velocity responses. It is not considered that this discrepancy will have a significant flying qualities effect on the simulation.

Good matching of the state variable responses to pitch stick inputs is also apparent at the 120 kt case; similar matches were obtained at 80, 100 kt (not shown). Discrepancies exist for both n_x and n_z because neither X-force nor Z-force derivatives are replicated at the higher speeds; the inability to vary Z_u and Z_w with two controllers when the duct angle is low is reflected in the n_z differences. At 120 kt, good matches of the responses for throttle inputs were obtained also (Figure 4-4f), but the vertical velocity responses at 80 and 100 kt (not shown) were considerably different. This difference is a direct result of the inability to alter the X-22A's Z_u derivative at low duct angles without the use of a third controlier, coupled with the selection X_{δ_T} and Z_{δ_T} to be the same as for the AV-8A model. The effect of these mismatches can be seen by considering an approximate version of the transfer function numerator of vertical velocity to throttle:

$$N_{\delta_T}^{w} \cong Z_{\delta_T}\left\{S^3 - (X_u + M_q)S^2 + \left(X_u M_q - Z_u \frac{X_{\delta_T}}{Z_{\delta_T}}\right) S\right.$$

$$\left. + M_u\left(g + w_o + \frac{X_{\delta_T}}{Z_{\delta_T}} u_o\right) - Z_u M_q \frac{X_{\delta_T}}{Z_{\delta_T}}\right\}$$

for $\quad M_{\delta_T} \cong 0, \ \theta_o \cong 0.$

The situation is analogous to the placement of the zeroes in the roll-to-lateral-stick transfer function using yaw-due-to-aileron (N_{δ_a}): The $X_{\delta_T}/Z_{\delta_T}$ ratio may be changed to alter the zero locations in this transfer function at the expense of:

(1) Non-matched initial acceleration responses

(2) Variations in the longitudinal-velocity-to-throttle transfer function numerator.

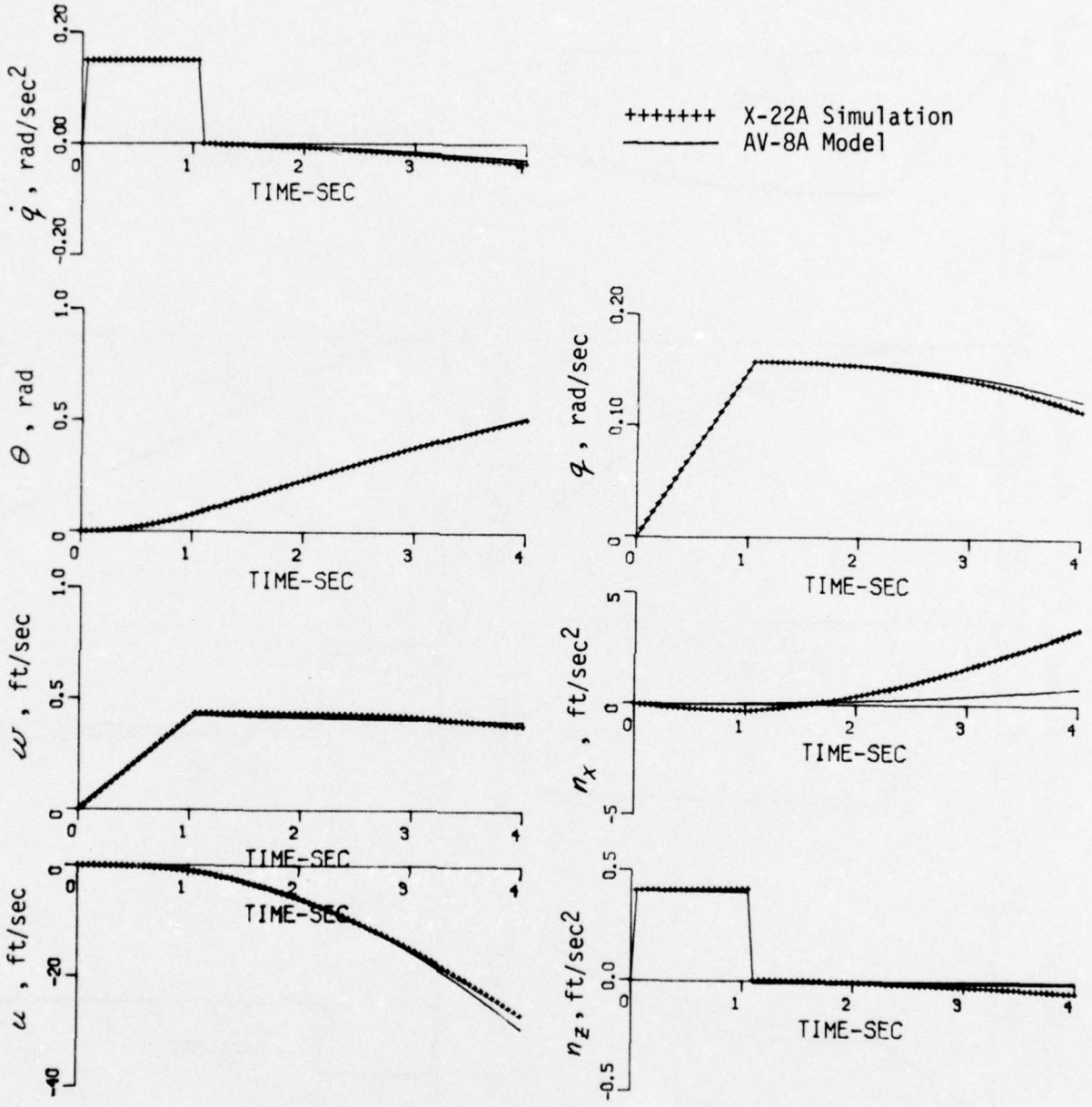


Figure 4-4 LONGITUDINAL TIME HISTORIES (a) V = 0 kt; δ_{es} PULSE (θ_j = 81°)

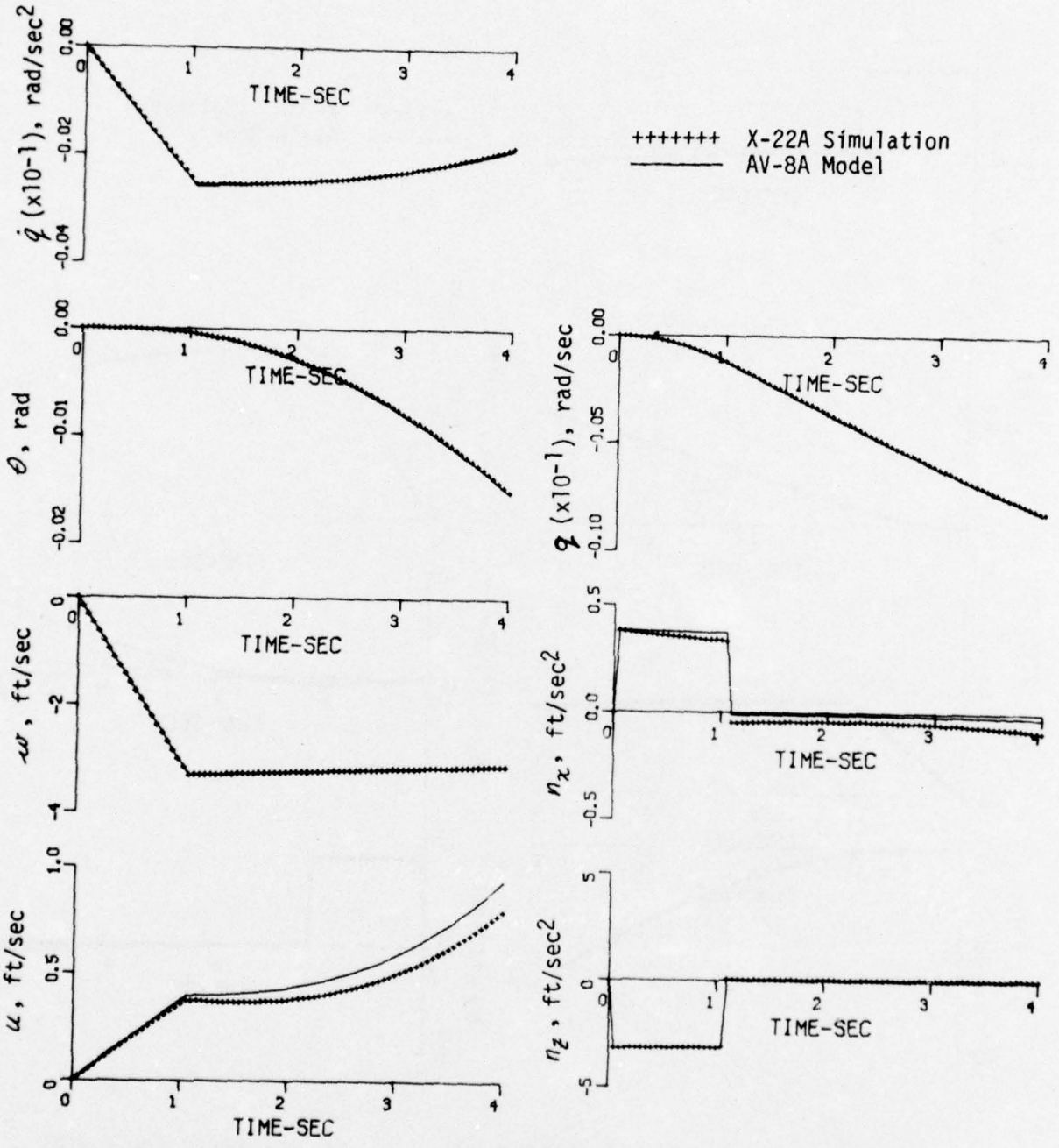


Figure 4-4 LONGITUDINAL TIME HISTORIES (b) V = 0 kt; δ_T PULSE (θ_j = 81°)

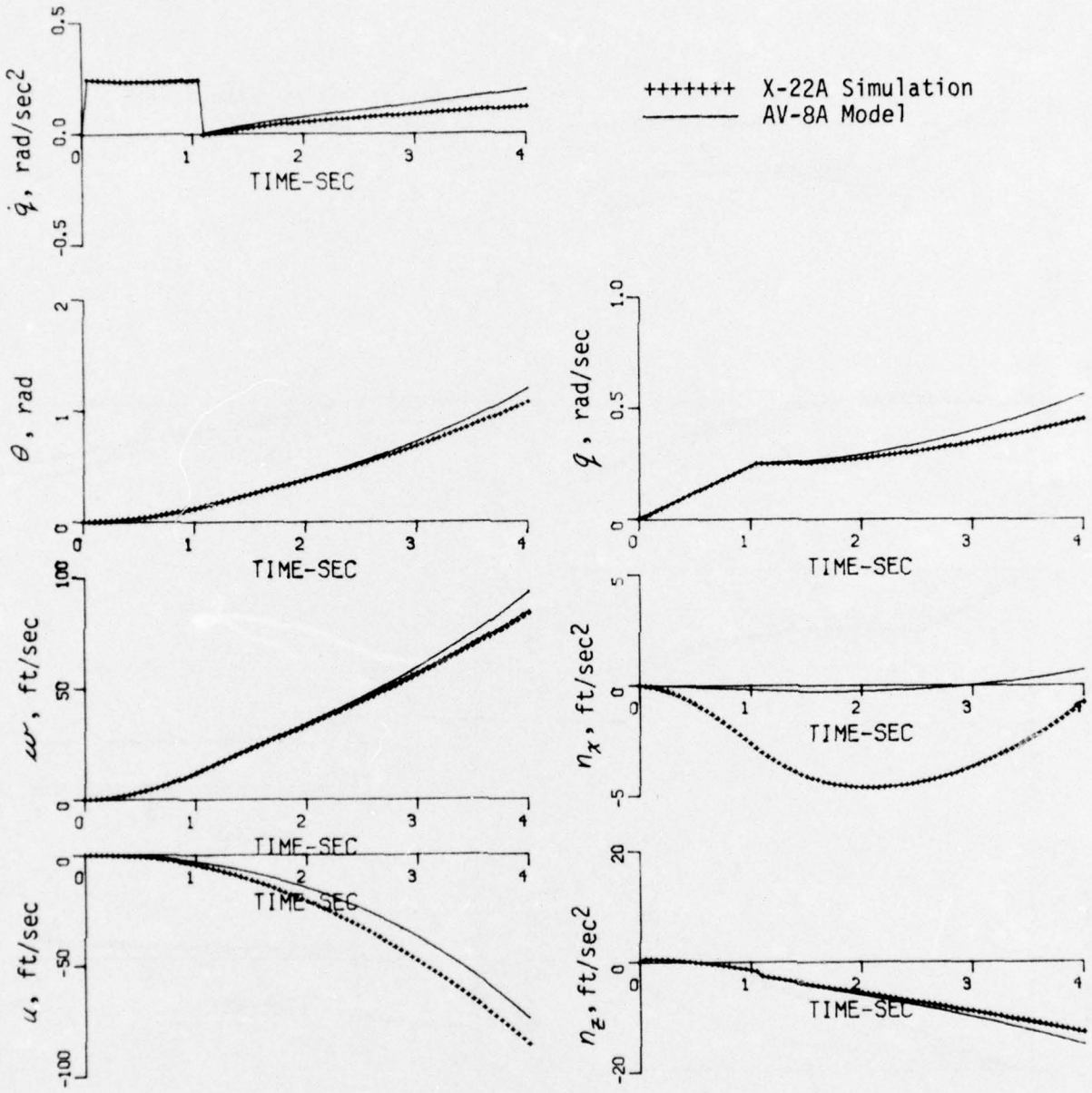


Figure 4-4 LONGITUDINAL TIME HISTORIES (c) V = 60 kt; δ_{es} PULSE (θ_j = 81°)

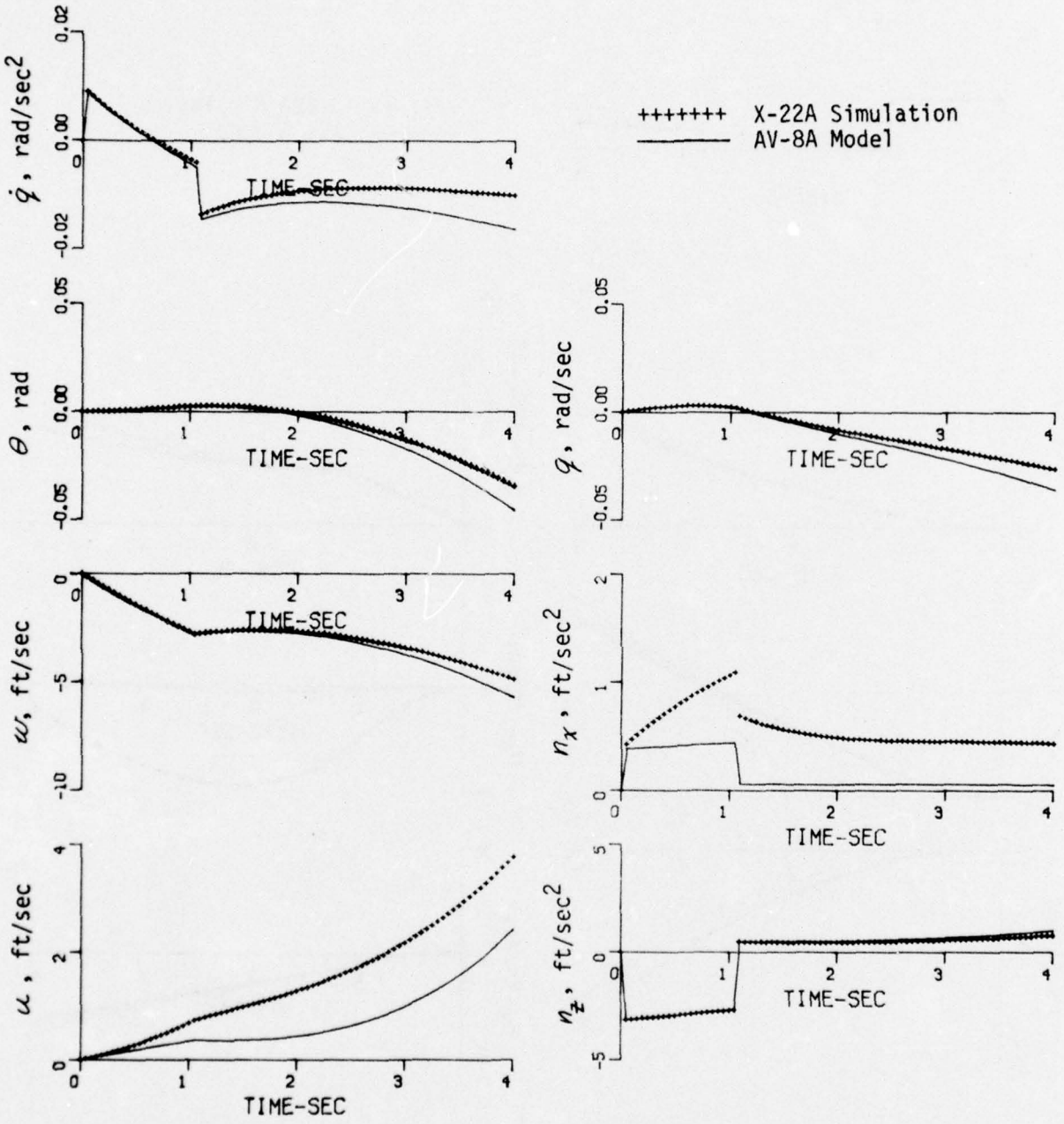


Figure 4-4 LONGITUDINAL TIME HISTORIES (d) V = 60 kt; δ_T PULSE (θ_j = 81°)

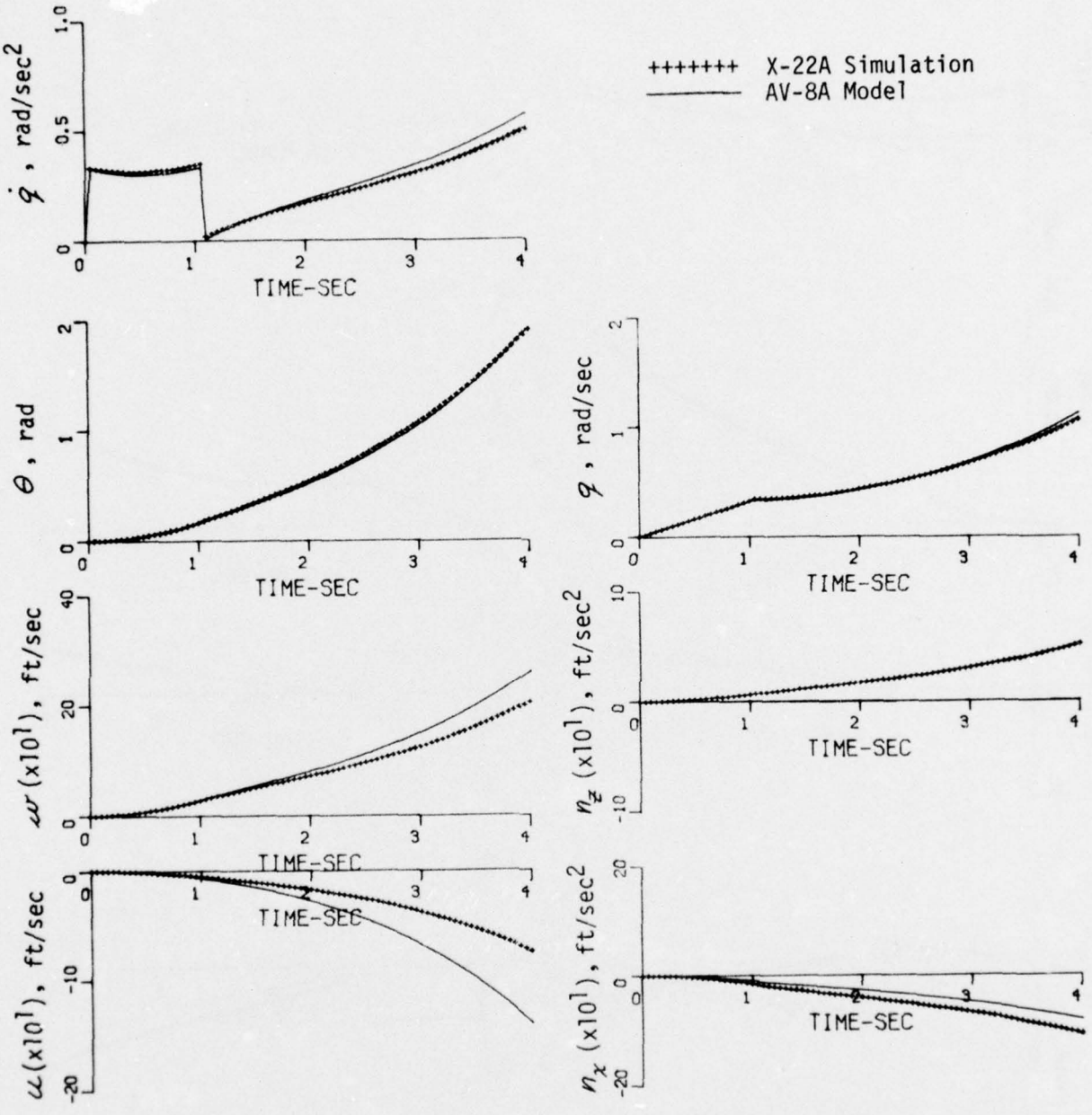


Figure 4-4 LONGITUDINAL TIME HISTORIES (e) V = 120 kt; δ_{es} PULSE (θ_j = 50°)

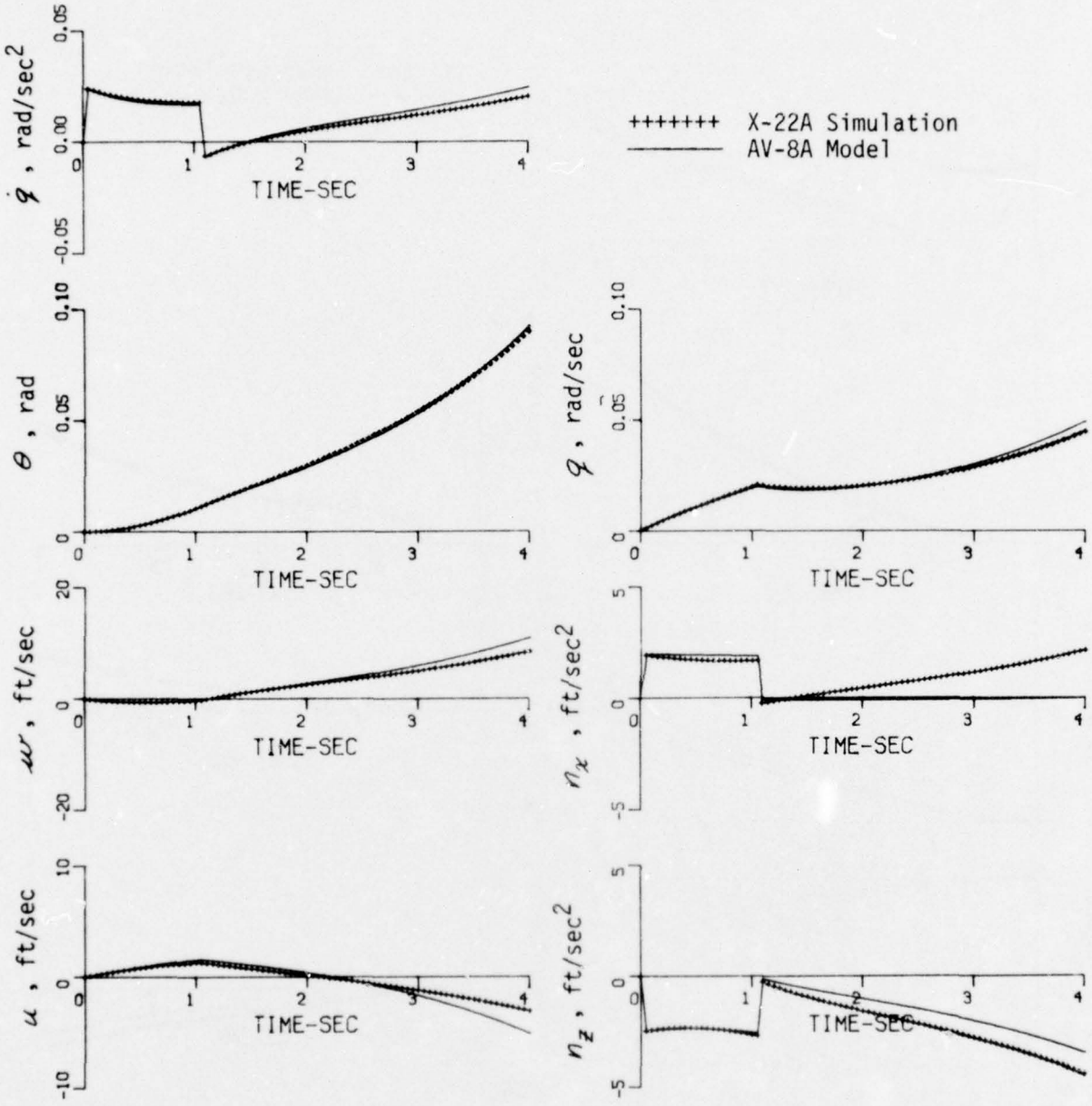


Figure 4-4 LONGITUDINAL TIME HISTORIES (f) V = 120 kt; δ_T PULSE (θ_j = 50°)

It is not clear, however, the extent to which these zeroes should be matched if the longitudinal velocity transfer function zeroes become less well matched simultaneously. This discrepancy will therefore require additional attention during the initial stages of the ground simulation experiment in the follow-on flight program.

4.3 SUMMARY OF SIMULATION FIDELITY

This section has discussed the procedures used to design the gains required to simulate the AV-8A model with the variable stability X-22A. From 0 kt to 60 kt, good duplication of the state variable responses for all control inputs was generally achieved, with some reduction in longitudinal-velocity-to-throttle fidelity at 60 kt. The only discrepancies for these flight conditions are in the longitudinal and lateral acceleration reponses. Comparison of flying qualities parameters from MIL-F-83300 for the AV-8A model and the simulation predict equivalent flying qualities. From 80 kt to 120 kt, the lateral-directional duplication remains excellent (except for n_{β}), and duplication of longitudinal responses to pitch stick inputs is good for the state variables; neither the longitudinal nor vertical acceleration responses match perfectly. Vertical velocity responses to throttle inputs are considerably different, however, at 80 kt and 100 kt; it is anticipated that, at 120 kt at least, the throttle will be primarily a speed controller and so this discrepancy will not be a major deficiency. It is recommended nonetheless that further analyses of this discrepancy be conducted and directed at:

- Alternate simulation designs: either limited use of a third controller in the feedbacks, or variation of $X_{\delta_T}/Z_{\delta_T}$ away from the AV-8A model value.
- Pilot-in-the-loop analysis: attempt to ascertain likely control techniques, assess impact of discrepancy.
- Piloted ground simulation: compare AV-8A model and the simulation with piloted evaluations.

The calculations have shown, therefore, that a generally good simulation of the AV-8A can be designed for implementation on the X-22A. The following section discusses the equally difficult task of implementing this design.

Section 5

IMPLEMENTATION IN GROUND SIMULATOR

5.1 SIMULATOR PREPARATION

In an effort to make the operation of the X-22A ground simulator more like that of the aircraft and thus to produce a more useful research tool for both ground- and in-flight simulation programs, several modifications were made to the simulator facility as part of this preliminary program. They include:

- the updating of the basic X-22A mathematical model as programmed on the simulator digital computer
- the integration of the airborne analog computer into the simulator facility
- the incorporation of the simulator VSS into the operation of the facility.

Based upon the identification results of the X-22A Task III program, documented in Reference 31, the original values of the stability and control derivatives which provide the basis for the simulator mathematical model of the basic X-22A in transition were altered to provide an updated version of that model. The current values of the X-22A stability and control derivatives are presented in Table 5-1 at the same six flight conditions for which the AV-8A model presented in Section 2 is developed.

During the Task III flight program, the airborne analog computer performed the following functions:

- guidance computations
- synthesis of control director laws and other display logic
- implementation of stability/control augmentation systems.

A portion of the preliminary program documented herein was devoted to the incorporation of the analog computer into the ground simulator facility to accomplish these same functions, originally performed by three EAI-380 computers. The current analog computer program for the simulator is similar to that documented in Reference 31.

The requirement to simulate a specific VTOL aircraft in transition for the upcoming program made mandatory the use of the simulator VSS with its capability of feedback gain variation as a function of airspeed or duct angle. Hence the system was made fully operational during the course of the preliminary program.

TABLE 5-1

BASIC X-22A SIMULATOR MODEL

Deriv-ative	$V(\lambda)$						
	0(90)	30(65)	60(45)	80(30)	100(15)	120(0)	Kts(Deg)
X_u	-.15	-.17	-.18	-.19	-.19	-.19	1/sec
X_w	0.0	-.039	-.022	+.020	.087	.178	1/sec
Z_u	-.0044	-.141	-.216	-.251	-.270	-.270	1/sec
Z_w	-.12	-.418	-.572	-.637	-.660	-.640	1/sec
M_u	.015	-.0065	-.010	-.0084	-.0066	-.0060	rad/ft-sec
M_w	.0009	-.0080	-.017	-.0115	-.0050	-.0040	rad/ft-sec
M_q	.226	.047	-.141	-.308	-.498	-.710	1/sec
$X_{\delta_{es}}$	-.14	-.32	-.35	-.31	+.15	.20	ft/sec^2/in.
$X_{\delta_{cs}}$	0.0	.38	.68	.90	1.13	1.35	ft/sec^2/deg
$Z_{\delta_{es}}$	-.16	-.085	+.050	.25	.61	.70	ft/sec^2/in.
$Z_{\delta_{cs}}$	-1.50	-1.16	-.90	-.70	-.50	-.30	ft/sec^2/deg
$M_{\delta_{es}}$	.350	.333	.320	.310	.300	.290	rad/sec^2/in.
$M_{\delta_{cs}}$	.0003	.0136	.024	.037	.040	.048	rad/sec^2/deg

(a) Longitudinal

Deriv-ative	$V(\lambda)$						
	0(90)	30(65)	60(45)	80(30)	100(15)	120(0)	Kts(Deg)
Y_v	-.124	-.229	-.280	-.300	-.303	-.290	1/sec
L'_v	-.015	-.030	-.037	-.040	-.040	-.038	rad/ft-sec
L'_p	+.07	-.49	-.81	-0.97	-1.06	-1.09	1/sec
L'_r	.0009	0.84	1.36	1.65	1.85	1.98	1/sec
N'_v	.0011	.0011	+.0008	-.0002	-.0012	-.0013	rad/ft-sec
N'_p	.0001	-.073	-.121	-.152	-.178	-.199	1/sec
N'_r	-.170	-.208	-.205	-.165	-.100	-.080	1/sec
$L'_{\delta_{as}}$	.38	.38	.38	.38	.38	.38	rad/sec^2/in.
$L'_{\delta_{rp}}$	+.095	-.128	-.147	-.128	-.102	-.080	rad/sec^2/in.
$N'_{\delta_{as}}$	.043	.047	.054	.060	.068	.077	rad/sec^2/in.
$N'_{\delta_{rp}}$	.230	.184	.139	.100	.058	.055	rad/sec^2/in.

(b) Lateral-Directional

The performance of the revised digital computer program, analog computer, and VSS was evaluated by reproducing the final Task III evaluation task, angular augmentation control systems, and display logic on the simulator using the new equipment and then conducting piloted decelerating approaches in order to reveal any problem areas in the simulation.

The following subsection discusses the functions of the analog computer and VSS and their integration for the simulation of the AV-8A in transiti

5.2 AV-8A MODEL MECHANIZATION

The simulation of the AV-8A stability and control characteristics developed in Section IV was implemented on the ground simulator in a manner which was judged to be both logical from an experimental point of view and compatible with the actual aircraft experimental systems. Specifically, the simulator digital computer retains the function of calculating the basic X-22A equations of motion and the guidance parameters that will be supplied in the flight program by the microwave landing system (MLS). The VSS is used to the extent possible to provide the characteristics of the basic AV-8A model; the analog computer will be used to generate the models of the SCAS for the upcoming AV-8B simulation program and is currently programmed with a simplified model of the AV-8A SAS (documented in Appendix II). Although it is possible to mechanize many of the control system schemes directly on the VSS and thus free a good part of the analog computer capability for other uses, it was decided to differentiate the functions of the two experimental systems in the above manner in general to provide a more readily comprehensible approach to a complex problem and specifically to separate out the simulated AV-8A control input from the actual X-22A control input for the purpose of control usage measurements. This separation of functions between the VSS and analog computer is illustrated schematically in Figure 5-1.

The aerodynamic/propulsive force and moment characteristics of the AV-8A in transition were mechanized on the VSS in terms of perturbations from a reference transition rather than by applying the fixed operating point simulation technique which involves perturbations of the motion and control variables from initial trim conditions. The perturbation technique involves not only feedback gains and control gearings which vary as a function of flight condition (Section IV) but also motion feedback and control variables expressed in terms of perturbations from reference values which are also functions of flight condition. As applied to the AV-8A simulation problem, the technique ideally yields a valid simulation of the aircraft dynamics for "small" perturbations of the motion and control variables about their reference values at various fixed operating points along the reference transition as well as a faithful reproduction of the AV-8A trim changes with flight condition. For example, with the VSS engaged, the actual X-22A pitch control input (Δ_{es}) may be expressed as (see Figure 5-1):

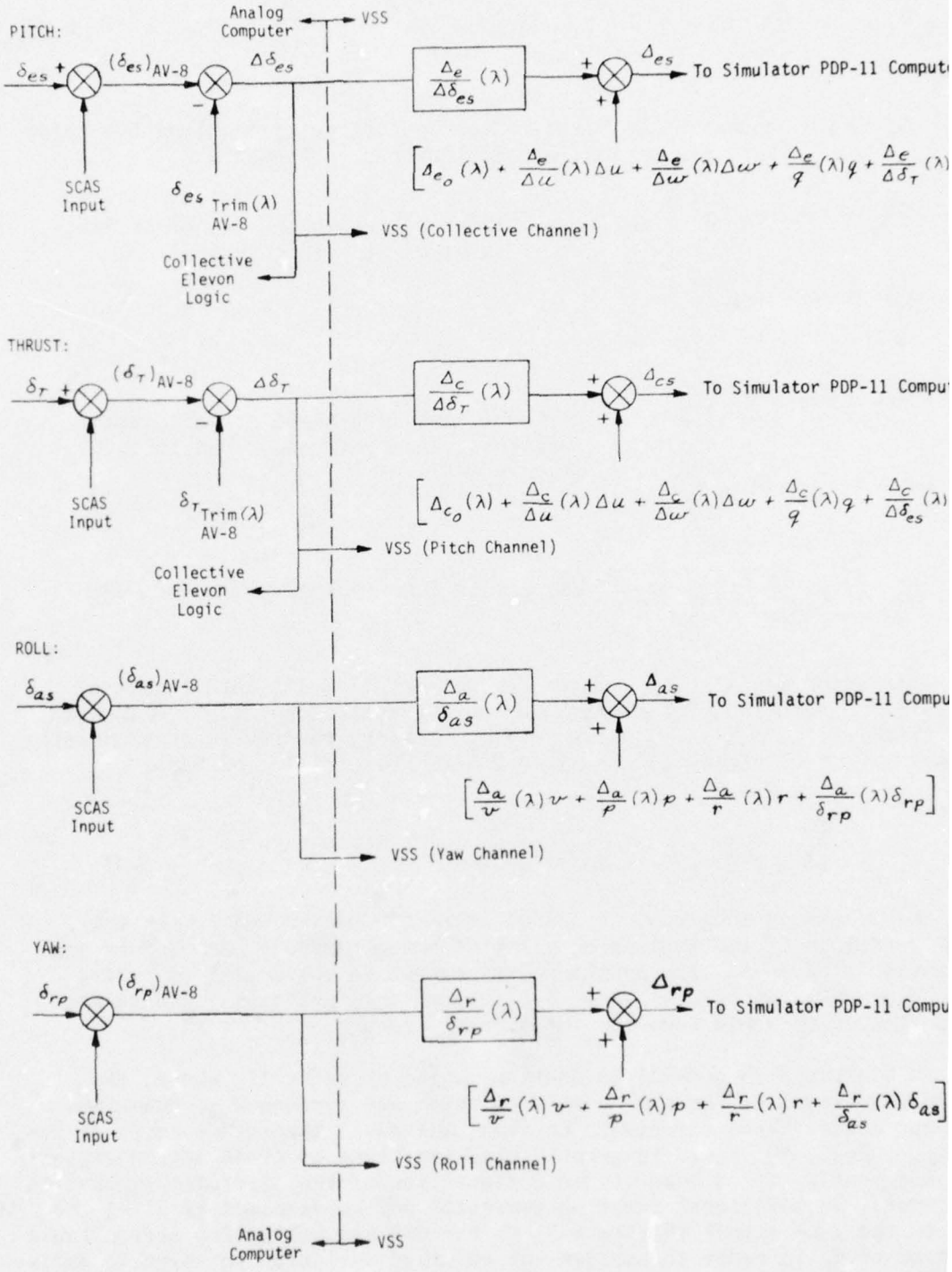


Figure 5-1 AV-8A MODEL MECHANIZATION

$$\Delta_{es} = \Delta_{e_o}(\lambda) + \frac{\Delta_e}{\Delta u}(\lambda)\Delta u + \frac{\Delta_e}{\Delta w}(\lambda)\Delta w + \frac{\Delta_e}{q}(\lambda)q + \frac{\Delta_e}{\Delta \delta_T}(\lambda)\Delta\delta_T + \frac{\Delta_e}{\Delta \delta_{es}}(\lambda)\Delta\delta_{es}$$

where $\Delta_{e_o}(\lambda)$ = actual X-22A "trim" pitch control position along the reference transition; a function of λ (Figure 5-2).

$$\left.\begin{aligned} \Delta u &= u - u_R(\lambda) \\ \Delta w &= w - w_R(\lambda) \end{aligned}\right\} \quad u_R, w_R: \text{ reference values of } u, w \text{ as functions of } \lambda \text{ . (Figure 5-3).}$$

$$\left.\begin{aligned} \Delta\delta_{es} &= \delta_{es} - \delta_{es_{\substack{TRIM \\ AV\text{-}8}}}(\lambda) \\ \Delta\delta_T &= \delta_T - \delta_{T_{\substack{TRIM \\ AV\text{-}8}}}(\lambda) \end{aligned}\right\} \quad \text{perturbations from AV-8A "trim" control positions along reference transition (Figure 5-4).}$$

$\frac{\Delta_e}{\Delta u}(\lambda)$, $\frac{\Delta_e}{\Delta w}(\lambda)$, $\cdots$ = VSS gains; functions of λ (Table 4-5b).

A similar expression may also be written for the actual X-22A thrust control input (Δ_{cs}). A solution of the pitch and thrust control equations with the X-22A in "trim" (i.e., $\Delta_{es} = \Delta_{e_o}$; $\Delta_{cs} = \Delta_{c_o}$) along the reference transition ($\Delta u = \Delta w = q = 0$) yields $\Delta\delta_{es} = \Delta\delta_T = 0$ with the restriction that:

$$\left(\frac{\Delta_e}{\Delta\delta_{es}}\right)\left(\frac{\Delta_c}{\Delta\delta_T}\right) \neq \left(\frac{\Delta_e}{\Delta\delta_T}\right)\left(\frac{\Delta_c}{\Delta\delta_{es}}\right) \quad \text{for any value of } \lambda$$

Hence for the values of longitudinal control gearings mechanized (Table 4-8), the "trim" positions of the evaluation pilot's control without SCAS inputs are always the simulated AV-8A trim positions programmed on the analog computer; the presence of SCAS inputs will alter the trim control positions in a manner similar to that which would occur on the actual aircraft.

As discussed in general in Section IV and specifically above, the gain schedulings required for the AV-8A simulation are performed as functions of X-22A duct angle, hence airspeed. However, the AV-8A throttle control derivatives (X_{δ_T} , Z_{δ_T} , M_{δ_T}) are in general also functions of AV-8A nozzle angle (θ_j); consequently, for a more accurate simulation of the aircraft response to throttle inputs, an additional function generator may be required to alter the magnitude of the $\Delta\delta_T$ signal (Figure 5-1) to the VSS and collective elevon logic as a function of θ_j in order to achieve the required variation in throttle derivatives with AV-8A configuration change.

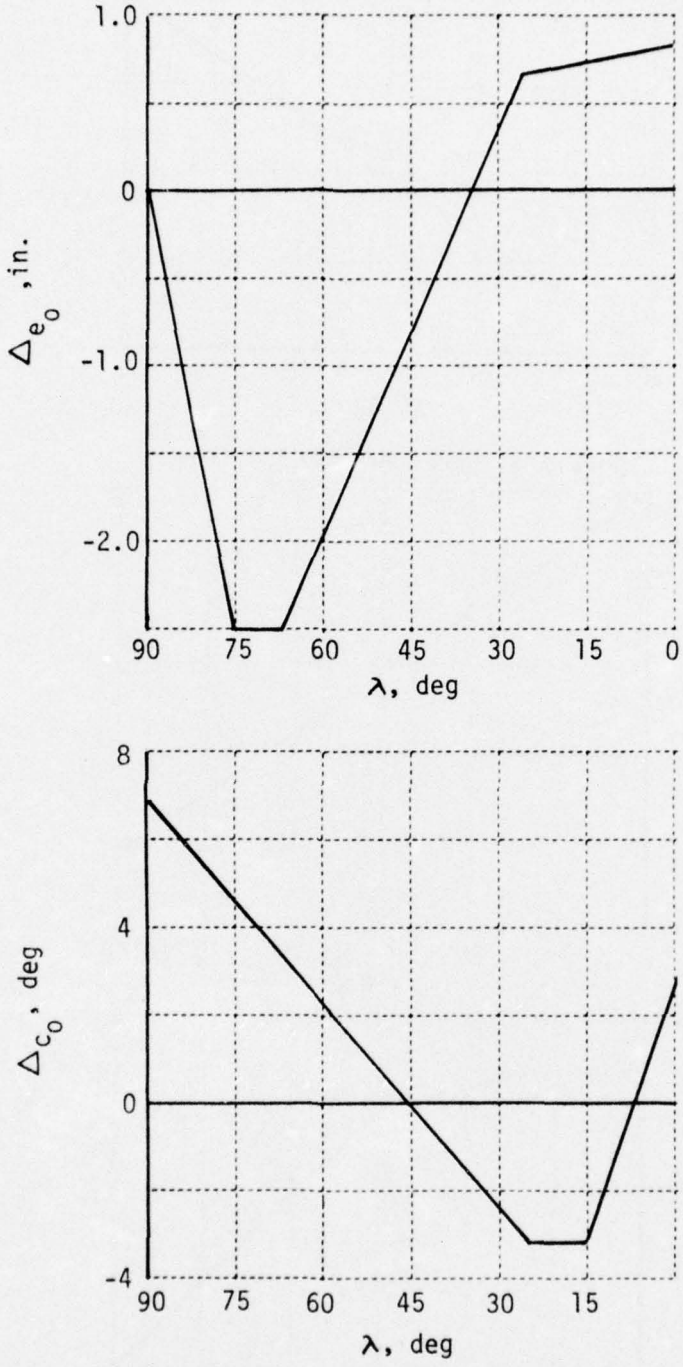


Figure 5-2 X-22A PITCH AND COLLECTIVE STICK TRIM POSITIONS

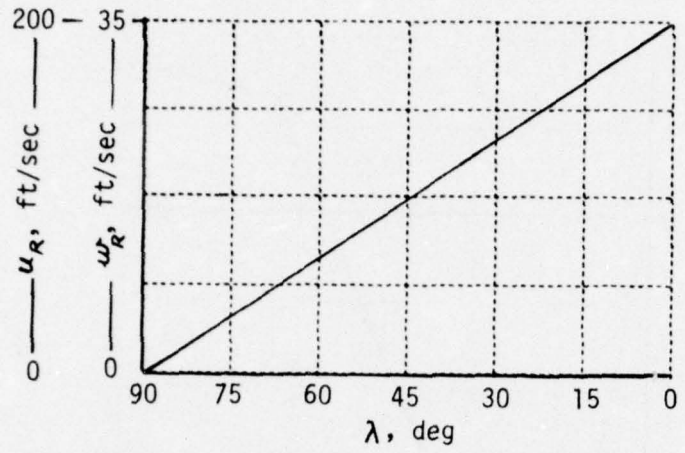


Figure 5-3 REFERENCE VELOCITIES

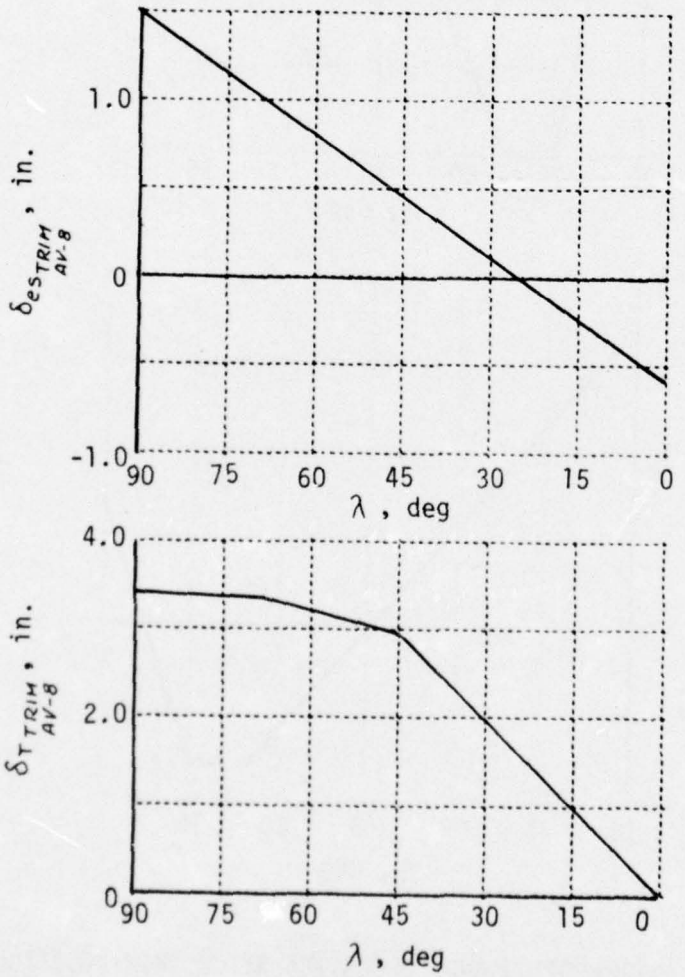


Figure 5-4 AV-8 LONGITUDINAL STICK AND THROTTLE TRIM POSITIONS

Section IV also discusses the requirement for a third controller in the longitudinal degrees of freedom. This controller, the collective use of the elevons, has been incorporated in the simulation facility by an addition to the simulator digital computer program to account for the effects of collective elevon deflection on the basic X-22A and the programming of the logic to drive the elevons in a collective fashion on the analog computer. The alteration of the digital computer program consists simply of the addition of a single term each to the expressions for the X and Z aerodynamic/propulsive forces: $X_{\Delta_{EL}}(\lambda)\Delta_{EL}$ and $Z_{\Delta_{EL}}(\lambda)\Delta_{EL}$ respectively; the pitching moment due to collective elevon deflections is assumed to be negligible. The values of the collective elevon effectiveness derivatives, estimates based upon X-22A wind tunnel data and geometry, are programmed in tabular form similar to that used for the other stability/control parameters; selected values of these derivatives are presented in Table 5-2.

TABLE 5-2

COLLECTIVE ELEVON EFFECTIVENESS DERIVATIVES

λ Deg	$X_{\Delta_{EL}}$ Ft/Sec^2/Deg	$Z_{\Delta_{EL}}$ Ft/Sec^2/Deg
0	0.0	-0.4
15	-0.1	-0.39
30	-0.2	-0.35
45	-0.28	-0.28
65	-0.36	-0.17
90	-0.40	0.0

NOTE: Δ_{EL} {Positive Down (λ = 0); Positive Forward (λ = 90)}

The logic to drive the elevons collectively is currently programmed on the analog computer as:

$$\Delta_{EL} = \frac{\Delta_{EL}}{\Delta\delta_{es}}(\lambda)\,\Delta\delta_{es} + \frac{\Delta_{EL}}{\Delta\delta_{T}}(\lambda)\,\Delta\delta_{T}$$

where $\Delta_{EL}/\Delta\delta_{es}$ and $\Delta_{EL}/\Delta\delta_{T}$ are functions of λ as presented in Section 4.2.4 and Δ_{EL} is the collective elevon input signal to the digital computer; currently limited to $\pm$4.5 deg.

5.3 SIMULATOR CHECKOUT

Both static and dynamic tests were conducted to ensure the proper operation of the various elements of the simulator facility when integrated as indicated in Figure 5-1 to provide a simulation of the AV-8A aircraft. The static tests consisted primarily of operational checks of the analog computer and VSS function generators by inserting known values of the state and control variables, measuring the appropriate output, and comparing this value to the desired value at each duct angle; the operation of the collective elevons was checked out using a similar input-output technique. Dynamic testing consisted of both fixed operating point time history comparisons and piloted decelerating approaches. Longitudinal and lateral-directional responses to control inputs at trimmed velocities of 0, 60, and 120 knots were recorded and compared to the time histories presented in Figures 4-1 and 4-4; the dynamic response characteristics of the simulator were judged to match the desired characteristics satisfactorily. The final test of the AV-8A simulation consisted of simulated decelerating approaches with the basic AV-8A plus SAS (Appendix II) along the Task III approach profile using the automatic duct rotation feature of the X-22A, the control director electronic display format (ED-3) with the RATE system director logic, and the throttle control of thrust magnitude (Reference 31); no obvious system-related problems were revealed.

Section 6

CONCLUSIONS AND RECOMMENDATIONS

The general conclusion from this study is that it is feasible to simulate in the X-22A aircraft an AV-8A class VTOL performing terminal area operations. As has been described in this report, most of the methodology for performing such a simulation has been developed and mechanized for further experimental investigation on the X-22A ground simulator; it has been demonstrated that excellent simulation fidelity below 60 kt. is possible and that the mechanization of the simulation can be performed with the X-22A equipment.

Specifically, the study objectives were achieved by the accomplishment of the following tasks:

- A generic model of the stability and control derivatives of the AV-8A was developed, primarily from the wind tunnel data given in Reference 2. The model was developed for an angle of attack of 8 degrees and glide slope angle of 5 degrees to be consistent with previous simulations (References 5, 6); values of the derivatives were computed for six trimmed velocities (V_0 = 0, 30, 60, 80, 100, 120 kt). The model is linear around a set of developed reference conditions which are a function of trim velocity only. Comparisons of the characteristic roots with available data in Reference 3 indicate excellent agreement at all six trim velocities.

- The variable stability gains for the lateral-directional simulation were computed using a Calspan-developed procedure which matches desired modal characteristics (Reference 28). Both feedback and feedforward (gearing) gains to the lateral stick and rudder pedals were calculated for all six flight conditions. Excellent matching of time history responses in sideslip, roll rate, roll attitude, and yaw rate to both aileron and rudder inputs was achieved at all flight conditions. The only discrepancy is the lateral acceleration response, which is significantly higher in the simulation than in the AV-8A model; this difference arises because of the larger Y_β in the X-22A which cannot be altered with the variable stability system. Flying qualities parameters of the AV-8A model and the simulation were computed for comparison with MIL-F-83300 (Reference 23); for all flight conditions, these parameters were either exactly the same or indicated equivalent levels of flying qualities.

- Several methods of computing the variable stability gains for the longitudinal simulation were examined. An extension of model-in-the-performance-index optimal control theory to allow computations with unstable models was developed and

selected as the most useful method for computing the feedback gains assuming two controllers (longitudinal stick and collective blade pitch). The major criterion in the iterative application of this procedure to compute feedback gains was that the characteristic roots of the simulation match those of the model; this criterion was met well at all six velocities. The gearing (feedforward) gains were computed using an equation-error least-squares technique that reproduces the model control matrix (and hence the initial accelerations to control inputs) exactly if three controllers are used. For these computations, it was necessary to assume the expansion of the variable stability system capability to include collective elevons, thereby providing a third controller. This expansion is necessary because of the markedly different thrust inclinations at a given speed between the X-22A and AV-8A model: to match initial responses to simulated thrust inputs at the higher speeds (V_o = 100, 120), which are low duct angles for the X-22A, the collective elevons are required to match the simulated thrust inclination. As a result of using three controllers for the gearing calculations, the simulated control matrix is an exact duplicate of the AV-8A model control matrix. Excellent matching of time history responses in longitudinal velocity, vertical velocity, pitch rate, and pitch attitude to both simulated pitch stick and throttle inputs was achieved for the three low-speed flight conditions (V_o = 0, 30, 60 kt). Good matching of the responses to pitch stick inputs is also obtained for the three higher speed conditions (V_o = 80, 100, 120 kt), but vertical velocity responses to simulated throttle inputs do not match. The discrepancy is attributable to significant differences between the simulated values and AV-8A model values of the stability derivatives Z_u and Z_w, which cannot be modified for high speeds (low duct angles) with the two controllers used for the feedbacks. Although the matching of the characteristic roots yields equivalent levels of flying qualities in terms of MIL-F-83300 requirements for the simulation and the AV-8A model at the higher speed conditions, it is recommended that additional studies be performed to improve the fidelity of the throttle responses for these conditions; the excellent matches to both stick and throttle inputs for the low speed cases imply good simulation.

- The X-22A ground simulator facility was updated and modified to reflect as closely as possible the aircraft characteristics and mechanization. The mathematical model of the basic X-22A, as programmed in the simulator's digital computer, was updated by incorporating values of stability and control derivatives that were identified from flight data during the Task III X-22A experiment (Reference 31). Incorporation of the airborne analog computer into the operation of the ground simulator was accomplished; this computer performs the guidance and control mechanization functions in flight, and its incorporation in the

simulator permits exact duplication of these functions. Finally, the ground simulator's variable stability system – an exact duplicate of that in the aircraft – was made operational, thereby allowing duplication of the function generation for the gains and reference conditions that will be required in flight.

- The simulation of the AV-8A model was mechanized on the ground simulator. The underlying philosophy of the mechanization is to perform the simulation of the basic AV-8A with the VSS as much as possible, and to use the airborne analog computer primarily to implement control system designs; although some of the control system functions could be performed on the VSS, the separation was selected to permit direct measurement of AV-8A control usage for the various control systems and to provide a rational method for dealing with a complex problem. Accordingly, the gain scheduling and state variable reference condition variations were programmed on function generator cards in the VSS as a function of duct angle (and hence trim velocity), and the operation of the VSS was modified to (1) permit reference values for longitudinal and vertical velocity to be introduced, and (2) permit longitudinal velocity, pitch rate, and pitch attitude feedbacks to the collective blade control. Reference or trim values of the simulated throttle and longitudinal stick are introduced at the interface between the analog computer and the VSS. The feel system is used to reproduce the force-displacement characteristics of the AV-8A cockpit controllers; a fore-and-aft controller simulates the throttle, and a smaller fore/aft controller will simulate the nozzle angle control. For checkout purposes, a simplified linear approximation to the AV-8A stability augmentation system is programmed on the analog computer. Checkouts of the simulation mechanization have been conducted with satisfactory results.

It is recommended that additional attention be given during the initial stages of the Task IV ground simulation experiment to the following problems discovered during this study:

- Responses to throttle inputs at the higher speeds. It may be necessary to (1) consider limited feedback to the collective elevons or (2) trade off initial acceleration responses against more closely matched velocity responses at a specified time.

- Trade off sideslip response matching, which is excellent with the current simulation, against lateral acceleration matching at the pilot's station.

- Initial deceleration for large nozzle angle changes. The current simulation can match the majority of the AV-8A deceleration profile for nozzle changes, which is essentially exponential, by duct angle changes. An exception is the initial deceleration, which may require washed-out collective blade pitch inputs as a function of nozzle change.

- Data deficiencies. Additional AV-8A/B data, particularly for reference conditions and throttle effectivenesses, are desirable.

REFERENCES

1. Key, D. L. and L. E. Reed: "VTOL Transition Dynamics and Equations of Motion with Application to the X-22A", Calspan Report No. TB-2312-F-1, June 1968.

2. Anon: "AV-8A Aerodynamic Characteristics", MCAIR Report No. MDC A1410, 31 January 1972.

3. Anon: "AV-8A Estimated Flying Qualities", MCAIR Report No. MDC A1411, 31 January 1972.

4. Anon: "Simulated Landings of a VTOL Aircraft on a Sea Control Ship", NR Report No. NR 72H-268, 15 September 1972.

5. Anon: "AV-8A Simulation of IFR Operations From Ship Decks", MCAIR Report No. MDC A3278, 25 January 1975.

6. Anon: "AV-8A Landing Aids Feasibility Investigation Final Report (Preliminary)", MCAIR Report No. A3618, 20 August 1975.

7. Anon: "AV-8A Automatic Flight Control System (AFCS) Control Laws", MCAIR Report No. A3580, 23 September 1975.

8. McGregor, D. M.: "A Flight Investigation of Various Stability Augmentation Systems for a Jet-Lift V/STOL Aircraft (Hawker-Siddeley P1127) Using An Airborne Simulator", National Research Council of Canada Aeronautical Report LR-500, February 1968.

9. Morello, S. A. et al.: "A Flight Evaluation of a Vectored-Thrust-Jet V/STOL Airplane During Simulated Instrument Approaches Using the Kestrel (XV-6A) Airplane", NASA TN D-6791, May 1972.

10. Mason, K. J. and C. R. Rosburg: "USAF Evaluation of the Harrier GR MK1", AFFTC TR No. 69-26, June 1969.

11. House, D. E. and G. A. Patterson: "Carrier Suitability Evaluation of the XV-6A (P.1127) Aircraft Final Report", NATC Report No. FT-98R-66, 17 October 1966.

12. McKinzie, G. A. and J. H. Ludwig: "P.1127 (XV-6A) VSTOL Handling Qualities Evaluation", AFFTC TR No. 68-10, August 1968.

13. Scheuren, W. J. and J. L. Dunn: "Final Report Flying Qualities Evaluation of the Harrier Airplane with V/STOL Sideslip Modifications", NATC Report No. FT-52R-71, 14 July 1971.

14. Branum, M. H. and J. M. Rebel: "Final Report Carrier and Advanced Airfield Aircraft Performance Trials of the Model AV-8A Airplane", NATC Report No. FT-59R-71, 23 July 1971.

15. Suit, W. T. and J. L. Williams: "Longitudinal Aerodynamic Parameters of the Kestrel Aircraft (XV-6A) Extracted From Flight Data", NASA TN D-7296, June 1973.

16. Margason, R. J. et al.: "Wind-Tunnel Investigation at Low Speeds of a Model of the Kestrel (XV-6A) Vectored-Thrust V/STOL Airplane", NASA TN D-6826, July 1972.

17. Anon: "AV-8A Primary and Auxiliary Flight Control System Analysis", MCAIR Report No. MDC A3091, 11 February 1975.

18. Rebel, J. M. et al.: "Final Report Shipboard Suitability Trials of Model AV-8A Aircraft with Pegasus 103 Engine and Quick-Release Holdback", NATC FT-72R-72, 6 November 1972.

19. Scheuren, W. J. et al.: "Final Report Single Phase Navy Preliminary Evaluation of the Harrier GR MK1 Airplane (U)", NATC FT-05R-69, 11 April 1969 (CONFIDENTIAL).

20. Scheuren, W. J. and J. L. Dunn: "Final Report Flying Qualities and Performance Trials of the Model AV-8A Airplane", NATC FT-27R-71, 28 April 1971.

21. Anon: "NATOPS Flight Manual Navy Model AV-8A Aircraft", NAVAIR 01-AV8A-1, February 1975.

22. Staples, J. J.: "Motion, Visual, and Aural Cues in Piloted Flight Simulation", AGARD Conference Proceedings No. 79 on Simulation, AGARD-CP-79-70, January 1971.

23. Chalk, C. R. et al.: "Background Information and User Guide for MIL-F-83300 – Military Specification – Flying Qualities of Piloted V/STOL Aircraft", AFFDL-TR-70-88, March 1971.

24. Chalk, C. R., R. C. Radford, and R. Wasserman: "Final Report on Program to Improve MIL-F-83300", AFFDL-TR-74-54, June 1974.

25. Newell, F. D.: "Criteria for Acceptable Representation of Airplane Dynamic Responses in Simulators Used for Pilot Training", Calspan Report No. BM-1642-F-1 (NAVTRADEVCEN 1146-1), 1 September 1962.

26. Streiff, H. G.: "Study, Survey of Helicopter and V/STOL Aircraft Simulator Trainer Dynamic Response", NAVTRADEVCEN 1753-1 and -2, August 1966 (Vol. I), May 1967 (Vol. II).

27. Aiken, E. W. and J. M. Schuler: "A Fixed-Base Ground Simulator Study of Control and Display Requirements for VTOL Instrument Landings with a Decelerating Approach to a Hover", Calspan Report No. AK-5113-F-2, February 1974.

28. Weingarten, N. C. and R. Wasserman: "An Analytical Method to Compute Cockpit and Nose Potentiometer Settings for Lateral-Directional Simulation in the Variable Stability T-33", Calspan Report No. BM-2821-F-1 (AFFDL-TR-70-73), August 1970.

29. Rynaski, E. G. and R. F. Whitbeck: "The Theory and Application of Linear Optimal Control", Calspan Report No. IH-1943-F-1, October 1965.

30. Tyler, J. S., Jr.: "Study of Models in Linear Optimal Control Theory and Application to Variable Stability Airplane Control Systems", Calspan Report No. IM-1836-F-1, November 1967.

31. Lebacqz, J. V. and E. W. Aiken: "A Flight Investigation of Control, Display, and Guidance Requirements for Decelerating Descending VTOL Instrument Transitions Using the X-22A Variable Stability Aircraft", Calspan Report No. AK-5336-F-1, September 1975.

GLOSSARY OF SYMBOLS

e	error term
F	characteristic matrix, open loop
F_c	characteristic matrix, closed loop
g	acceleration due to gravity, 32.2 ft/sec^2
G	control matrix
H	measurement matrix
I	identity matrix
$I_{(\ )}$	moment of inertia about body ( )-axis (ft-lb/sec^2)
I_{xz}	product of inertia in body axes (ft-lb/sec^2)
j	complex variable, $\sqrt{-1}$
J	gearing matrix
J	integrand (section 4.2.2)
$K,\ K'$	feedback matrix
L	aerodynamic moment about body X-axis (ft-lb)
$L'_{(\ )}$	dimensional rolling moment derivative $= \frac{1}{I_x}\left(1 - \frac{I_{xz}^2}{I_x I_z}\right)^{-1}\left[\frac{\partial L}{\partial(\ )} + \frac{I_{xz}}{I_z}\frac{\partial N}{\partial(\ )}\right]$ $\left(\frac{\text{rad/sec}^2}{(\ )}\right)$
M	aerodynamic moment about body Y-axis (ft-lb)
$M_{(\ )}$	dimensional pitching moment derivative $= \frac{1}{I_Y}\frac{\partial M}{\partial(\ )}$ $\frac{\text{rad/sec}^2}{(\ )}$
n	integer
n_x, n_Y, n_z	body axis accelerations (ft/sec^2)
N	aerodynamic moment about z-axis (ft-lb)
$N'_{(\ )}$	dimensional yawing moment derivative $= \frac{1}{I_z}\left(1 - \frac{I_{xz}^2}{I_x I_z}\right)^{-1}\left[\frac{\partial N}{\partial(\ )} + \frac{I_{xz}}{I_x}\frac{\partial L}{\partial(\ )}\right]$ $\left(\frac{\text{rad/sec}^2}{(\ )}\right)$
N_j^i	numerator of the $i/j(s)$ transfer function
p	body-axis roll rate (deg/sec, rad/sec)
P	steady-state augmented control gain matrix
q	body-axis pitch rate (deg/sec, rad/sec)
Q	state weighting matrix
r	body-axis yaw rate (deg/sec, rad/sec)

R	control weighting matrix
S	Laplace operator $\sigma \pm j\omega$
t	time (sec)
u	velocity along body X-axis (ft/sec)
u	control vector
v	velocity along body Y-axis (ft/sec)
V_o	velocity (kt, ft/sec)
w	velocity along body Z-axis (ft/sec)
X, Y, Z	aerodynamic force along body X, Y, Z axis, respectively (lb
$X_{(\ )}, Y_{(\ )}, Z_{(\ )}$	dimensional longitudinal, lateral, vertical force derivati $= \frac{1}{m} \frac{\partial X, Y, \text{ or } Z}{\partial (\ )} \left(\frac{\text{ft/sec}^2}{(\ )}\right)$
x	state vector
α	angle of attack (deg, rad)
β	angle of sideslip (deg, rad)
γ	flight path angle (deg)
$\delta_{(\ )}$	pilot's controller position
	e, E, es, ES longitudinal stick (in.), positive aft
	a, A, as, AS lateral stick (in.), positive right
	r, rp, RP rudder pedals (in.), positive right
	T, cs, CS throttle or collective stick (in.), positive increased thrust
$\Delta(\ )$	perturbation term $(\ ) - (\ )_o$, units of $(\ )$
$\Delta(s)$	characteristic equation
$\Delta_{(\ )}$	X-22A safety pilot's or VSS controller position
	e, E, es, ES longitudinal (in.), positive nose up
	a, A, as, AS lateral (in.), positive right wing down
	r, rp, RP directional (in.), positive nose right
	cs, CS thrust (in.), positive increased thrust
	el, EL collective elevons (deg), positive trailing e down and/or forward
ζ	damping ratio
ζ_d	damping ratio of dutch roll characteristic roots

ζ_ϕ	damping ratio of numerator roots in ϕ/δ_{as} transfer function
θ	pitch attitude (deg, rad)
θ_j	nozzle angle wrt engine axis (deg)
θ_j'	nozzle angle wrt fuselage reference line (deg)
λ	duct angle, measured from horizontal (deg)
λ	adjoint variable
$\Lambda_{(\ )}$	eigenvalue matrix of ( )
σ	real part of Laplace operator
τ	generalized time constant
τ_R	roll mode time constant (sec)
τ_S	spiral mode time constant (sec)
ϕ	Euler roll attitude (deg, rad)
$\lvert\phi/\beta\rvert_d$	magnitude of ratio ϕ/β for Dutch roll mode
ω	imaginary part of Laplace operator (rad/sec)
ω_d	undamped natural frequency of Dutch roll mode (rad/sec)
ω_n	undamped natural frequency (rad/sec)
ω_ϕ	undamped natural frequency of numerator roots in ϕ/δ_{as} transfer function (rad/sec)
∂_i/∂_j	partial derivative of i with respect to j
∇_u	gradient (vector) with respect to u

Subscripts

$(\ )_{LS}$	least-squares solution
$(\ )_m$	model
$(\ )_{OPT}$	optimal control solution
$(\ )_R$	reference trajectory value
$(\ )_{LID}$	lateral-directional
$(\ )_{LONG}$	longitudinal
$(\ )_p$	plant
$(\ )_o$	reference value (also trim)
$(\ )_{trim}$	trim value
$(\ )_D$	desired steady-state responses (section 4.2.4)

Superscripts

$(\dot{})$	derivative with respect to time
$(\ )^T$	matrix transpose
$(\ )^{-1}$	matrix inverse
$(\hat{})$	combined matrices
$(\ )'$	transformed problem (section 4.2.3)
$(\ )^\circ$	value of ( ) is degrees

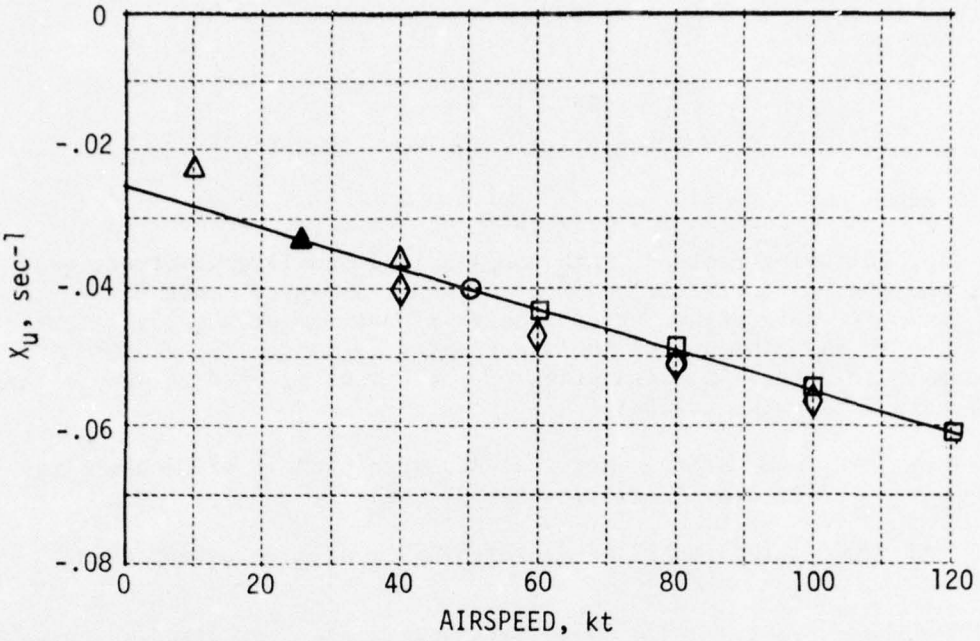
Appendix I

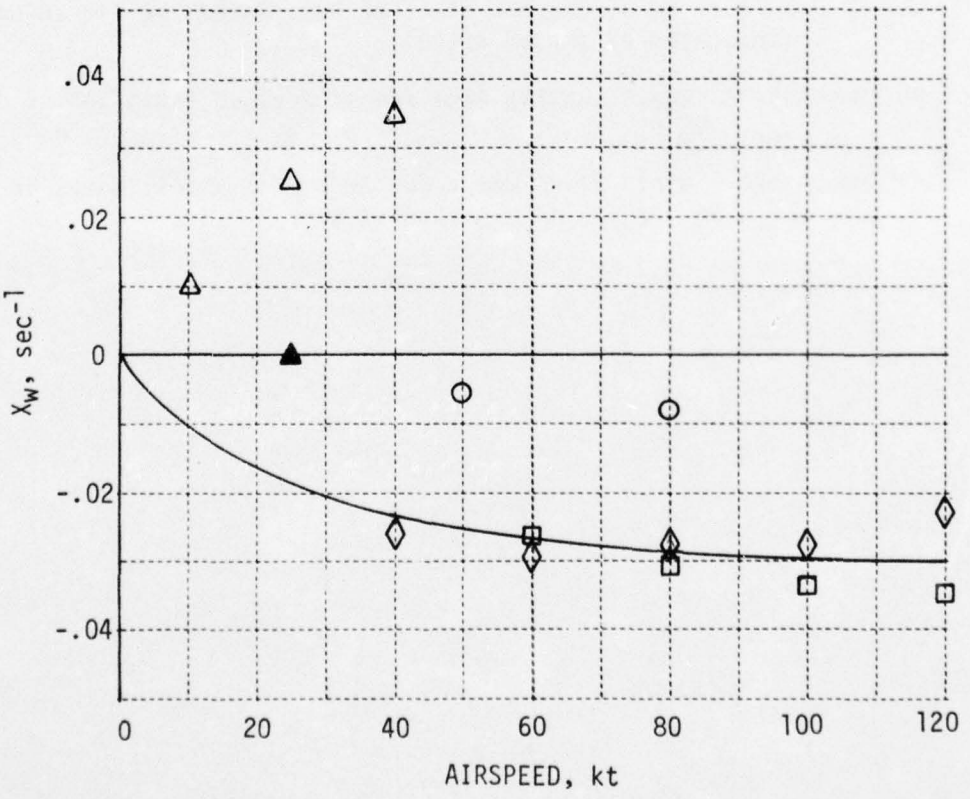
BASIC AV-8A MODEL STABILITY/CONTROL DERIVATIVES

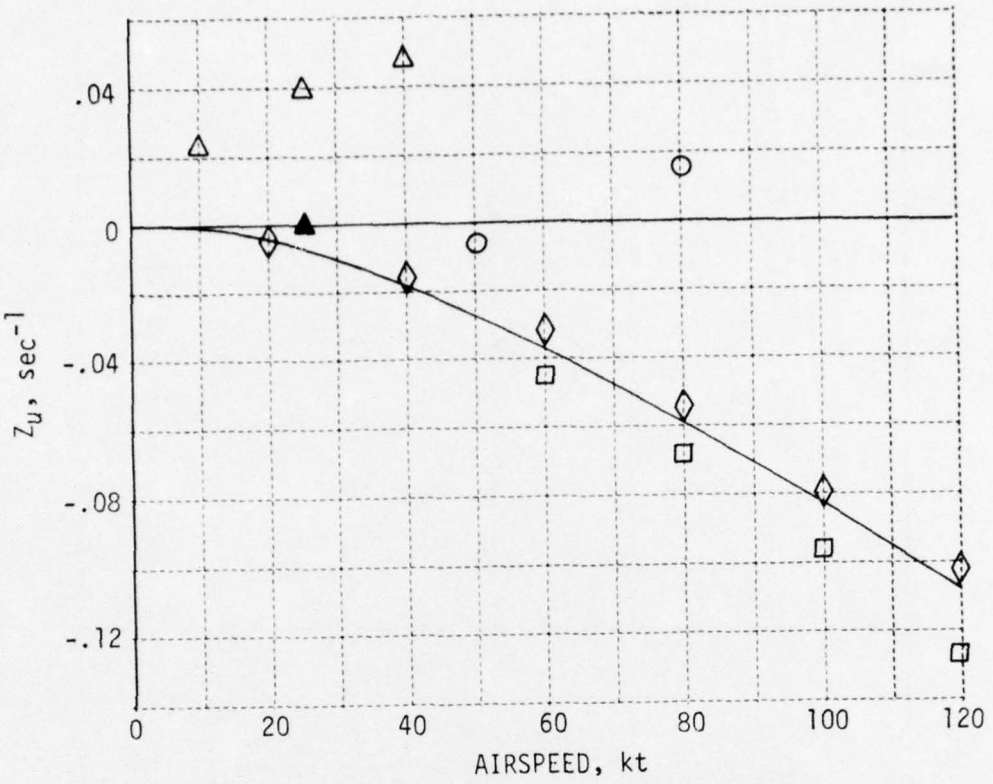
The following plots of both longitudinal and lateral-directional stability and control derivatives as functions of airspeed represent the results of the AV-8A data gathering and analysis portions of the preliminary program. The AV-8A mathematical model presented in Section 2 is based primarily upon these data. An explanation of the symbology used to denote the source of each data point follows:

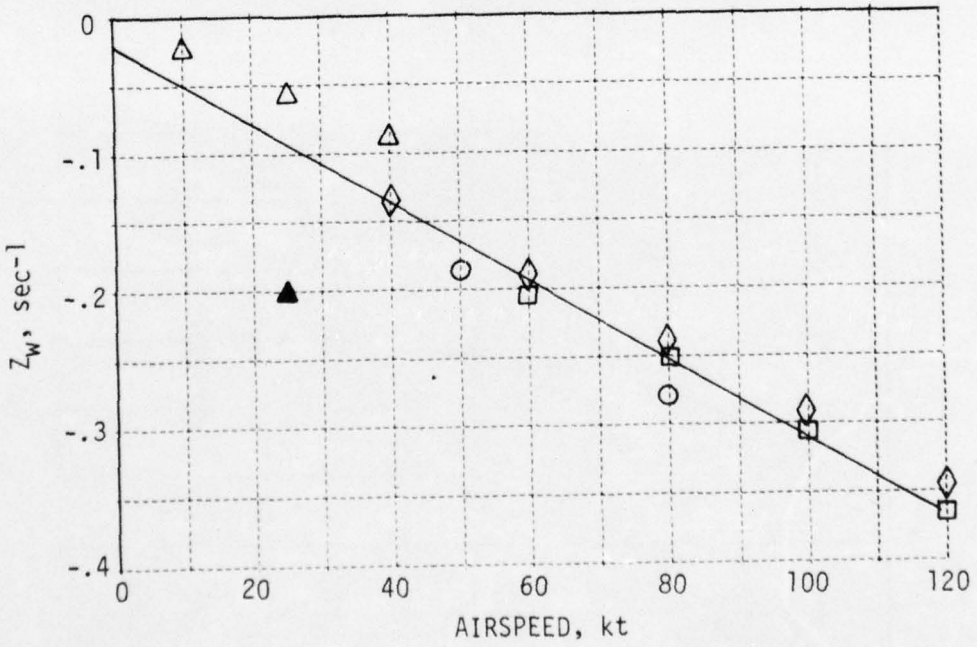
- ○ NRC, NAE LR-500: National Research Council of Canada simulation of P1127 (V = 50, 80 kts)
- □ MDC A1410: MCAIR AV-8A aerodynamic data, slow approach ($\theta_j = 70^o$)
- ◇ MDC A1410: MCAIR AV-8A aerodynamic data, decelerating transition ($\theta_j = 90^o$)
- △ NR 72H-268: NR simulation of AV-8A "validated" at V = 25 knots (indicated by shaded symbol)
- ⌓ MDC A3618: MCAIR Landing Aids study; revised estimates of L_β, N_β.
- ◇ MDC A3580: MCAIR AV-8A model for AFCS design; estimates of M_w, M_u, L'_v, N'_v presented here.

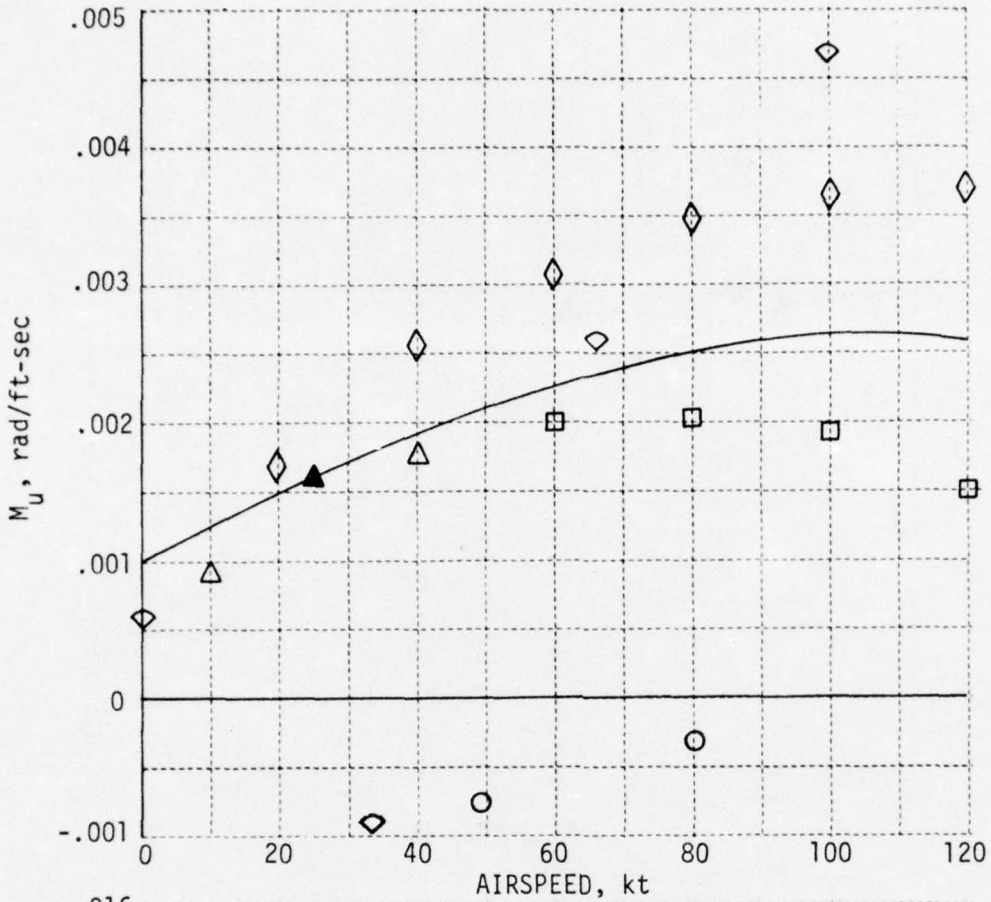
PRECEDING PAGE BLANK-NOT FILMED

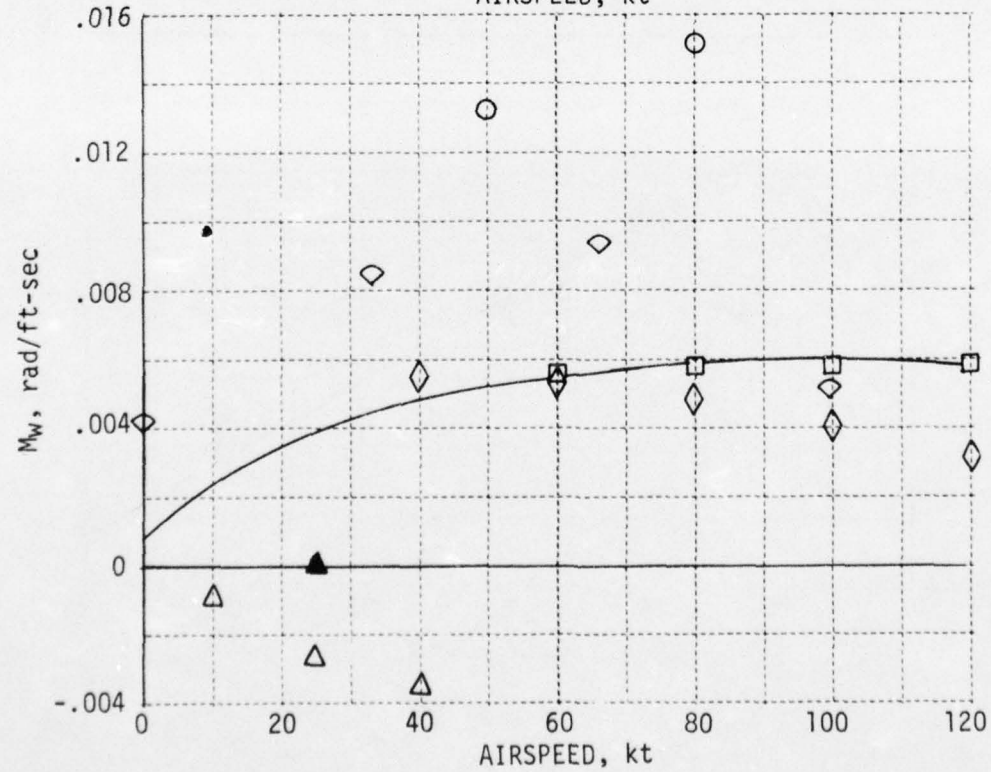

0
-.02
-.04
-.06
-.08
X_u, sec^{-1}
0
20
40
60
80
100
120
AIRSPEED, kt

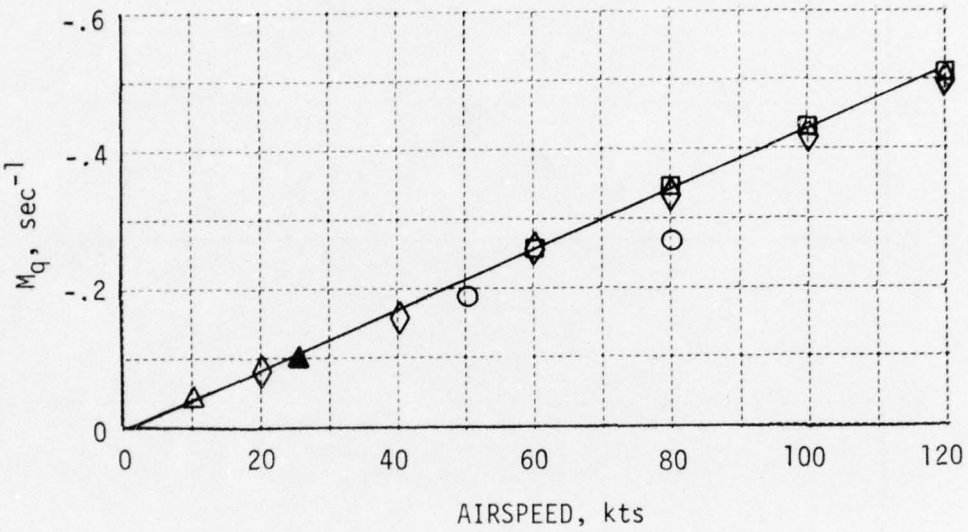

.04
.02
0
-.02
-.04
X_w, sec^{-1}
0
20
40
60
80
100
120
AIRSPEED, kt

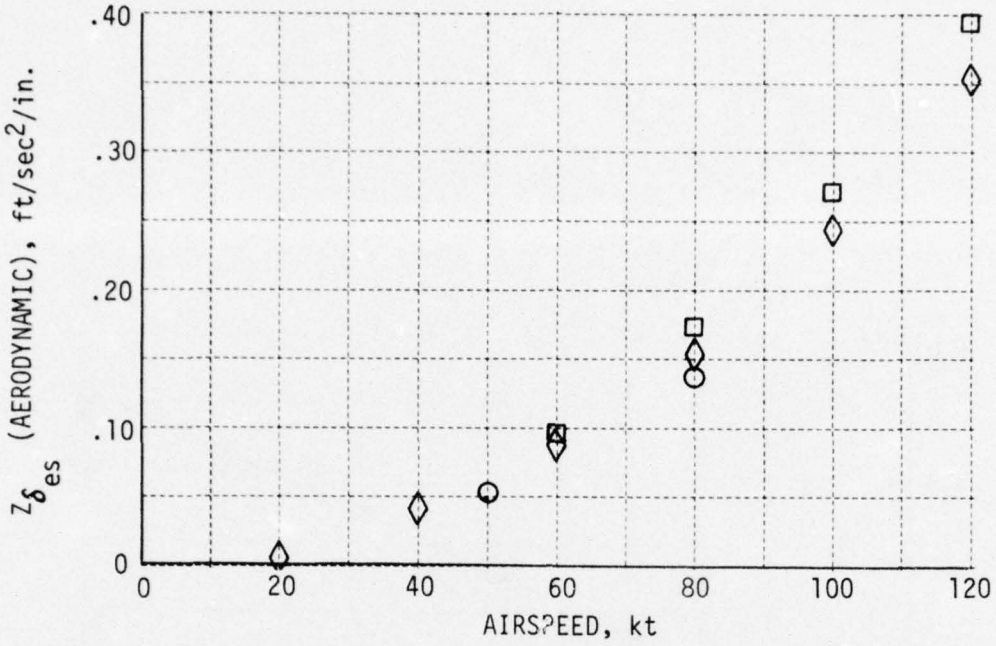

.04
0
-.04
-.08
-.12
Z_u, sec^{-1}
0
20
40
60
80
100
120
AIRSPEED, kt

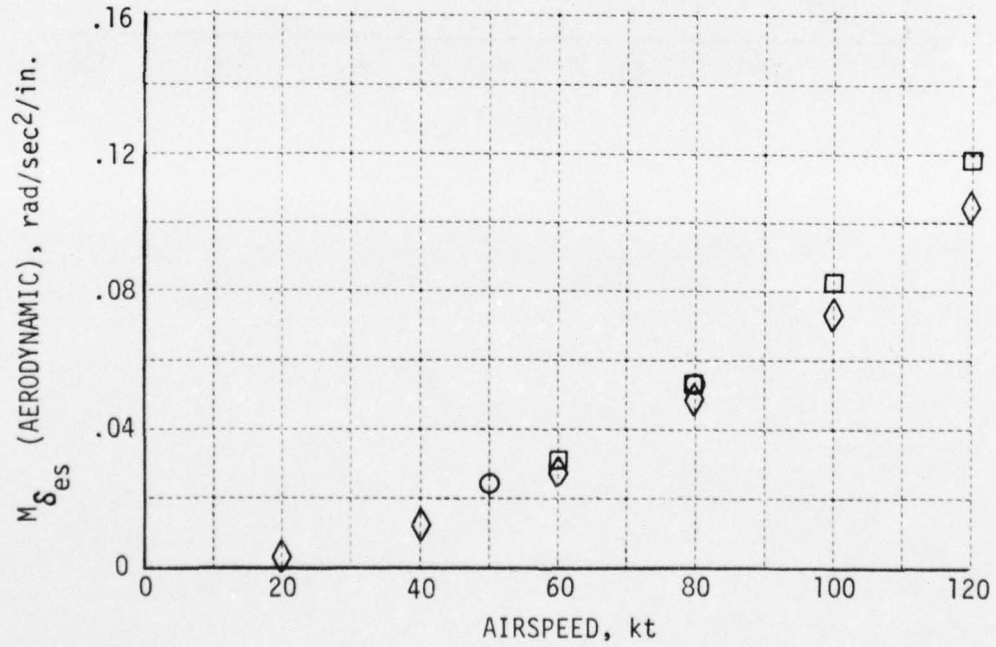

0
-.1
-.2
-.3
-.4
Z_w, sec^{-1}
0
20
40
60
80
100
120
AIRSPEED, kt

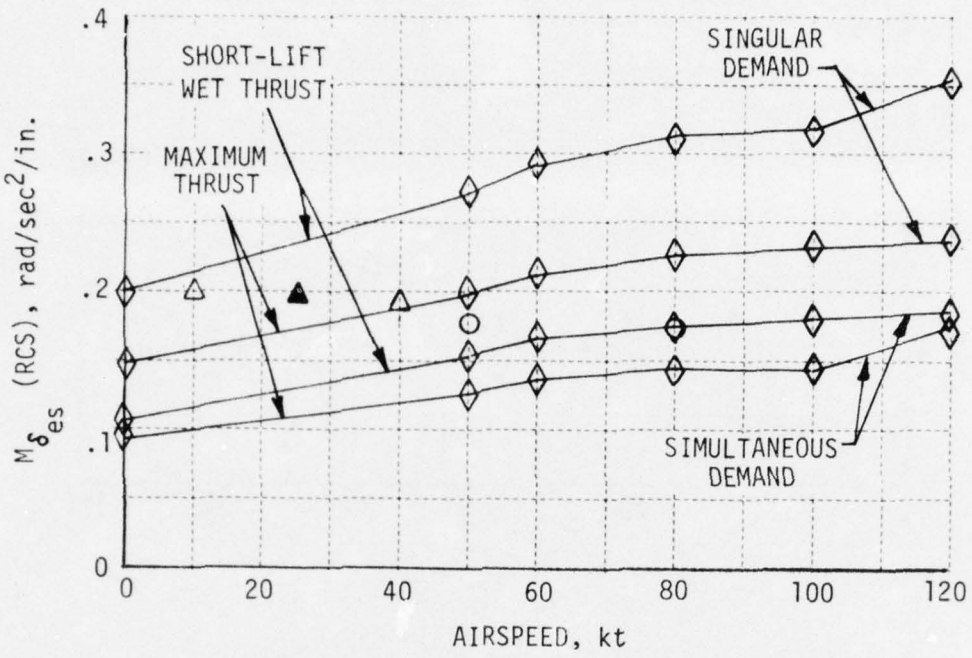

.005
.004
.003
.002
.001
0
-.001
M_u, rad/ft-sec
0
20
40
60
80
100
120
AIRSPEED, kt

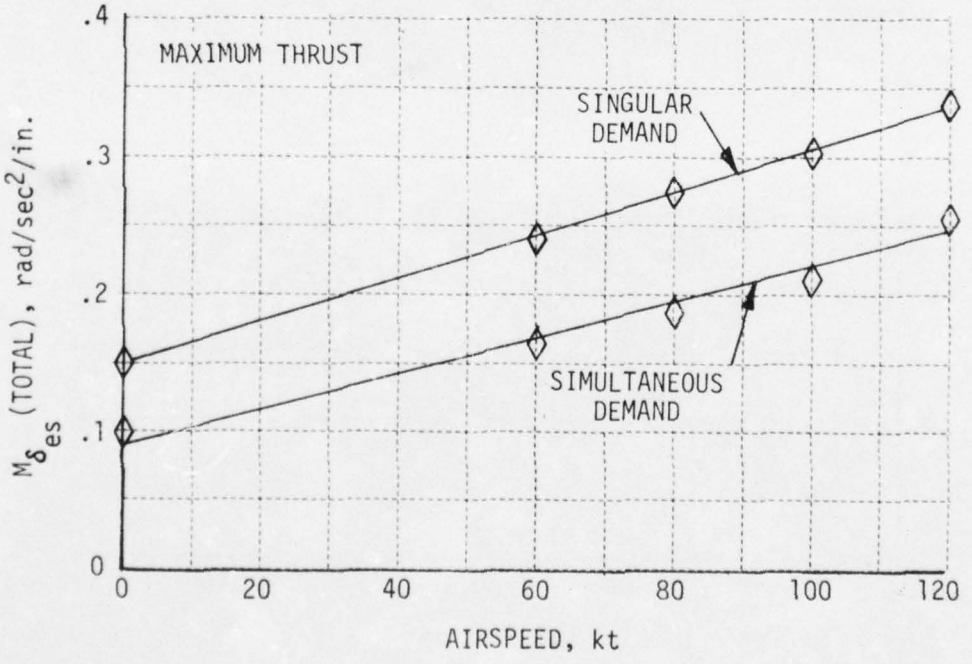

.016
.012
.008
.004
0
-.004
M_w, rad/ft-sec
0
20
40
60
80
100
120
AIRSPEED, kt

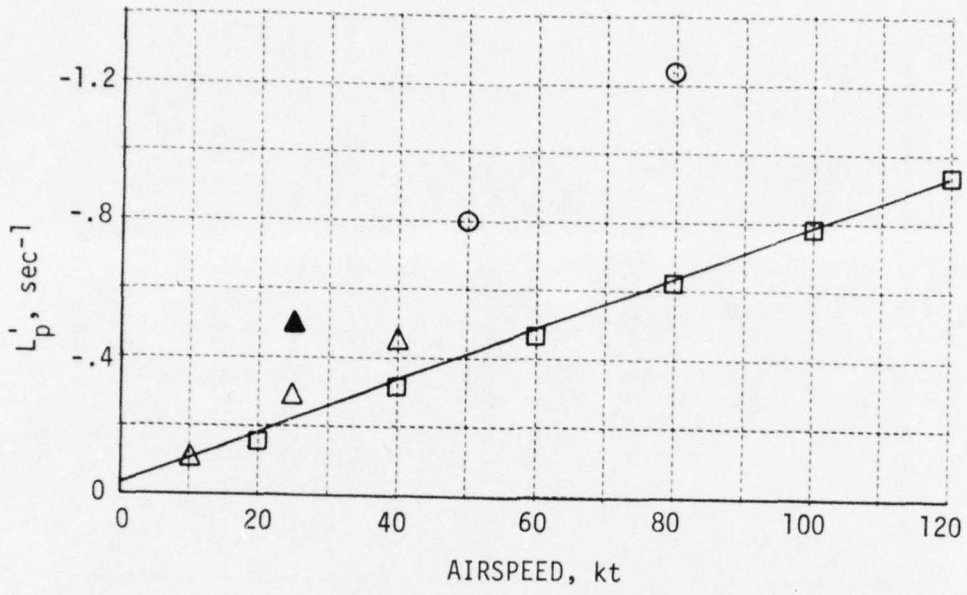

-.6
-.4
-.2
0
M_q, sec^{-1}
0
20
40
60
80
100
120
AIRSPEED, kts

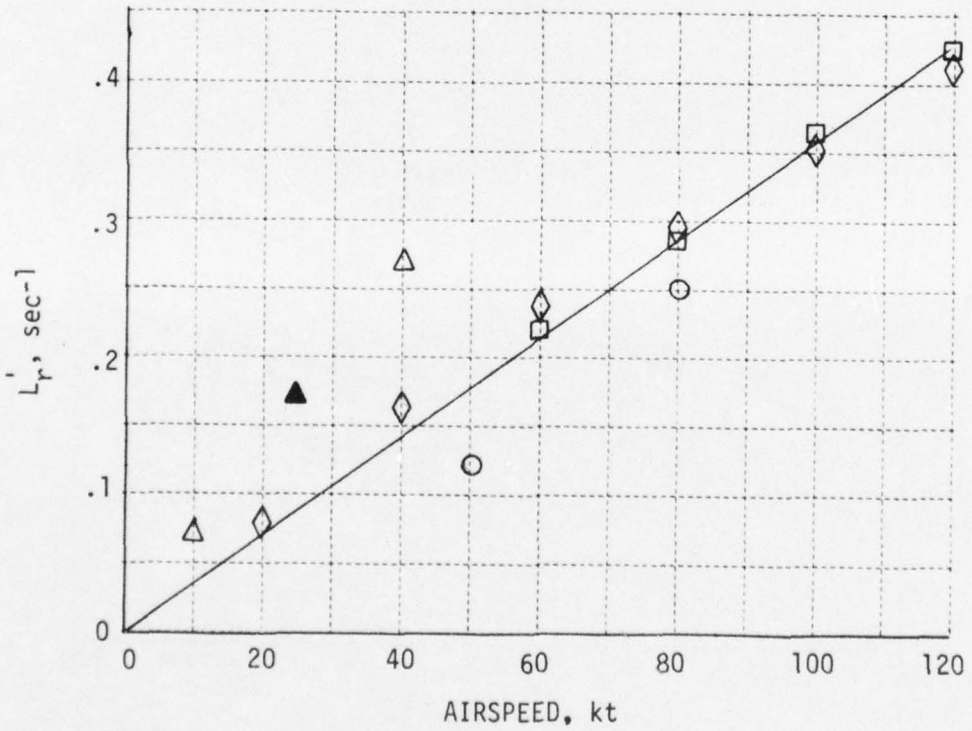

.40
.30
.20
.10
0
0
20
40
60
80
100
120
$Z_{\delta_{es}}$ (AERODYNAMIC), ft/sec^2/in.
AIRSPEED, kt

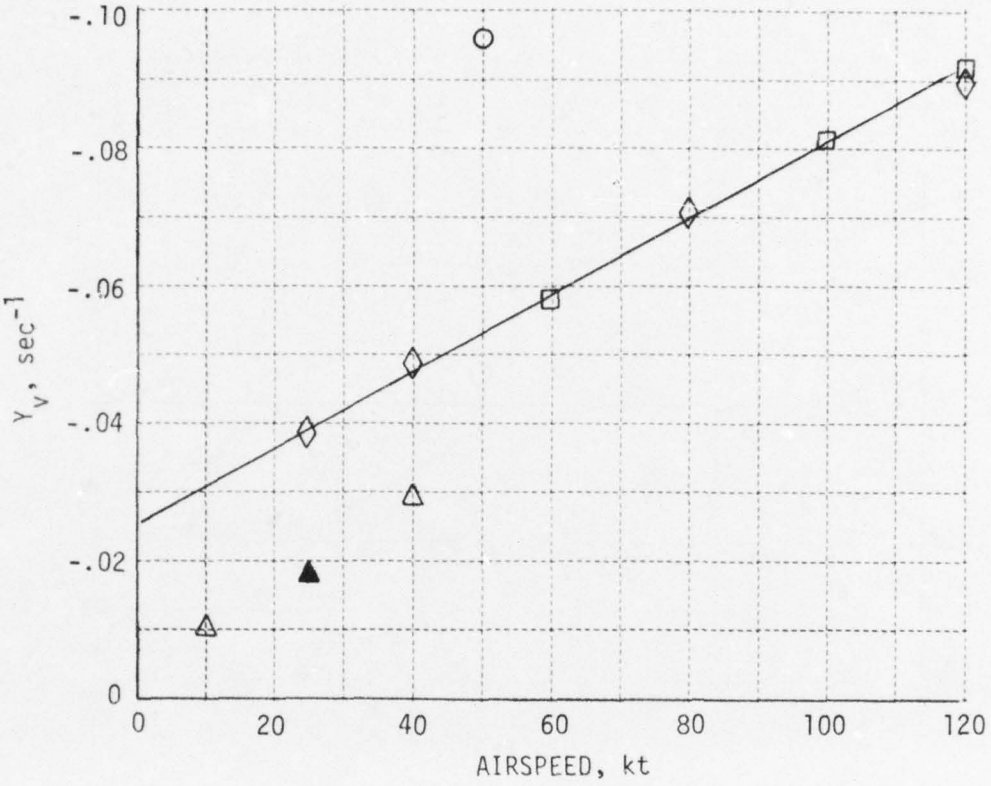

.16
.12
.08
.04
0
0
20
40
60
80
100
120
$M_{\delta_{es}}$ (AERODYNAMIC), rad/sec^2/in.
AIRSPEED, kt

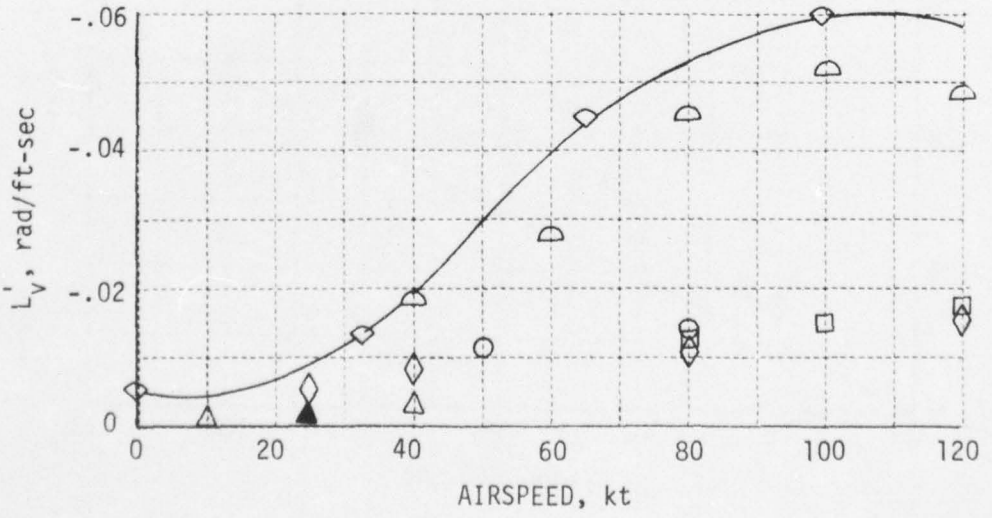

.4
.3
.2
.1
0
SHORT-LIFT
WET THRUST
MAXIMUM
THRUST
SINGULAR
DEMAND
SIMULTANEOUS
DEMAND
$M_{\delta_{es}}$ (RCS), rad/sec^2/in.
0
20
40
60
80
100
120
AIRSPEED, kt

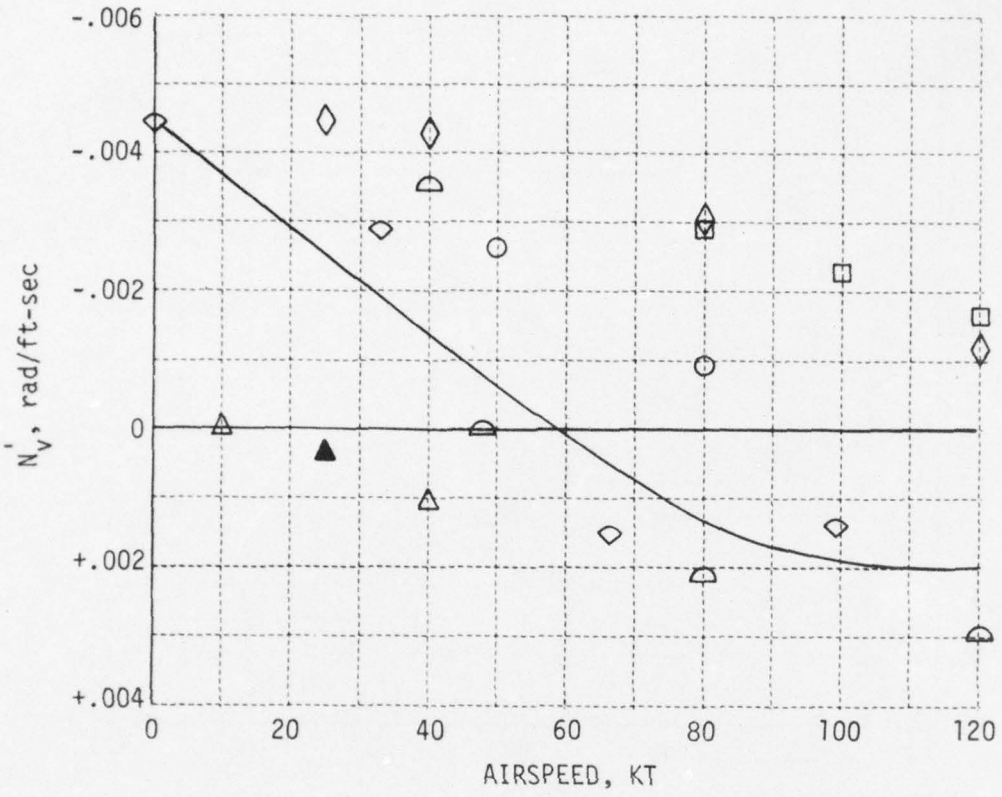

.4
.3
.2
.1
0
MAXIMUM THRUST
SINGULAR
DEMAND
SIMULTANEOUS
DEMAND
$M_{\delta_{es}}$ (TOTAL), rad/sec^2/in.
0
20
40
60
80
100
120
AIRSPEED, kt

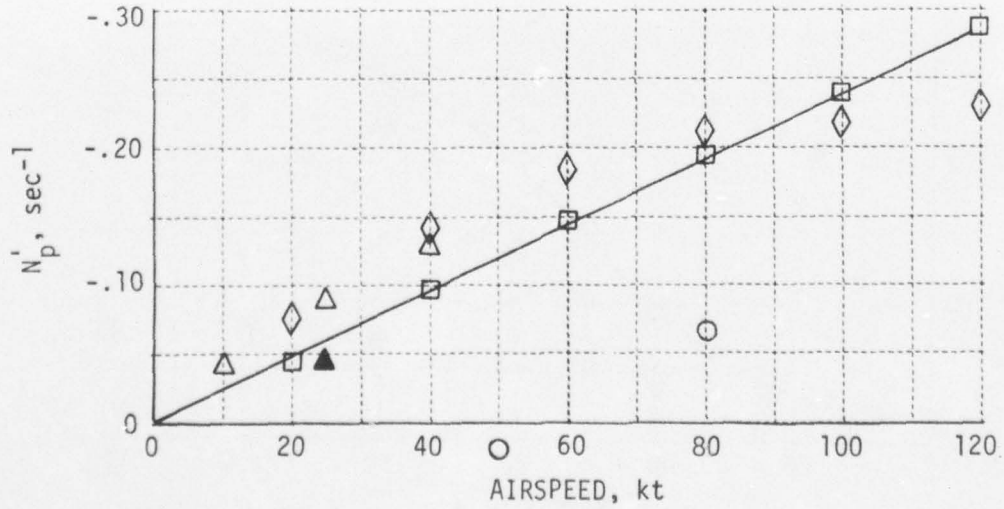

-1.2
-.8
-.4
0
L'_p, sec^{-1}
0
20
40
60
80
100
120
AIRSPEED, kt


.4
.3
.2
.1
0
L'_r, sec^{-1}
0
20
40
60
80
100
120
AIRSPEED, kt


-.10
-.08
-.06
-.04
-.02
0
Y_v, sec^{-1}
0
20
40
60
80
100
120
AIRSPEED, kt


-.06
-.04
-.02
0
L'_v, rad/ft-sec
0
20
40
60
80
100
120
AIRSPEED, kt


-.006
-.004
-.002
0
+.002
+.004
N_v', rad/ft-sec
0
20
40
60
80
100
120
AIRSPEED, KT

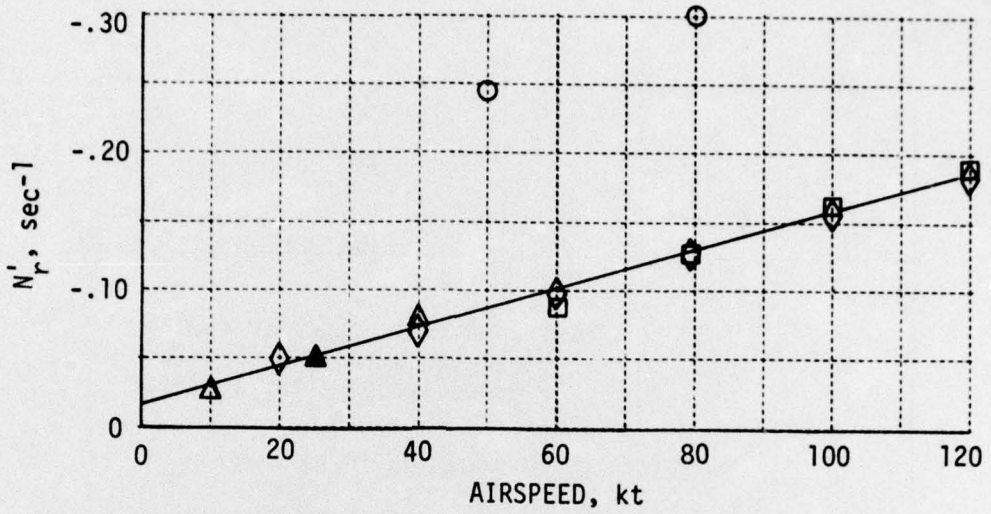

-.30
-.20
-.10
0
N_p', sec^{-1}
0
20
40
60
80
100
120
AIRSPEED, kt

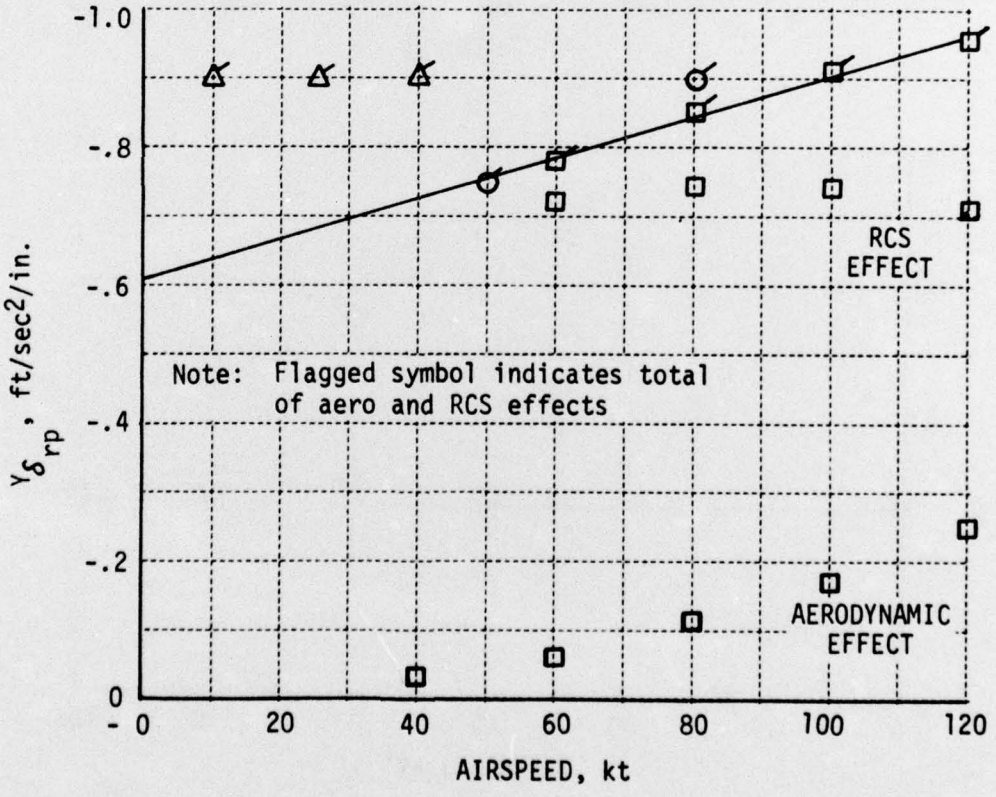
AD-A033 618 CALSPAN CORP BUFFALO N Y F/G 1/3
A STUDY TO DETERMINE THE FEASIBILITY OF SIMULATING THE AV-8A HA--ETC(U)
JUL 76 J V LEBACQZ, E W AIKEN N00019-76-C-0225
UNCLASSIFIED CALSPAN-AK-5876-F-1 NL

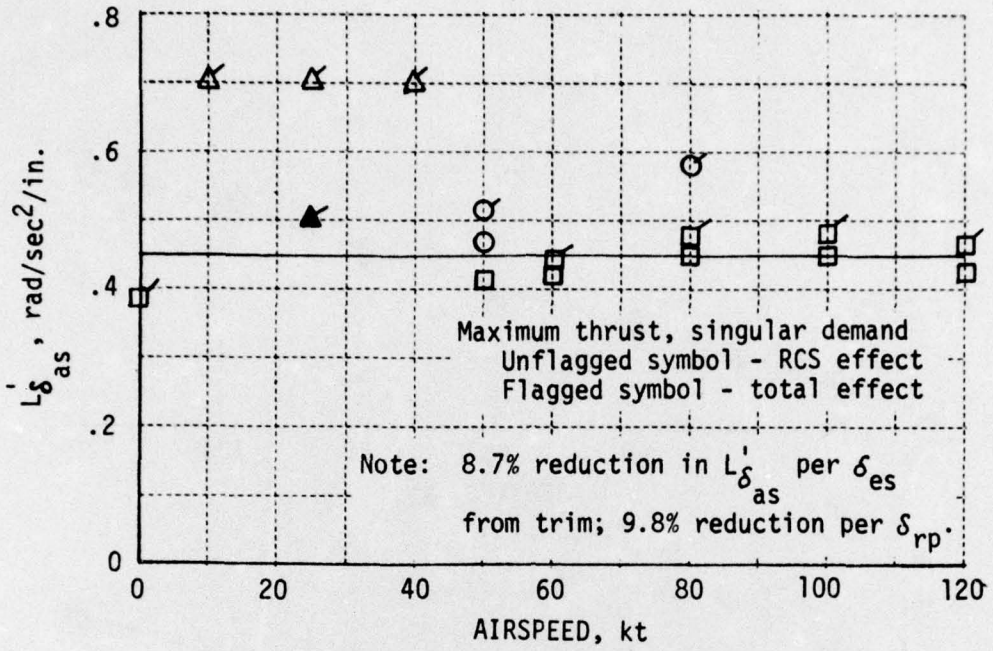
2 OF 2
AD
A033618

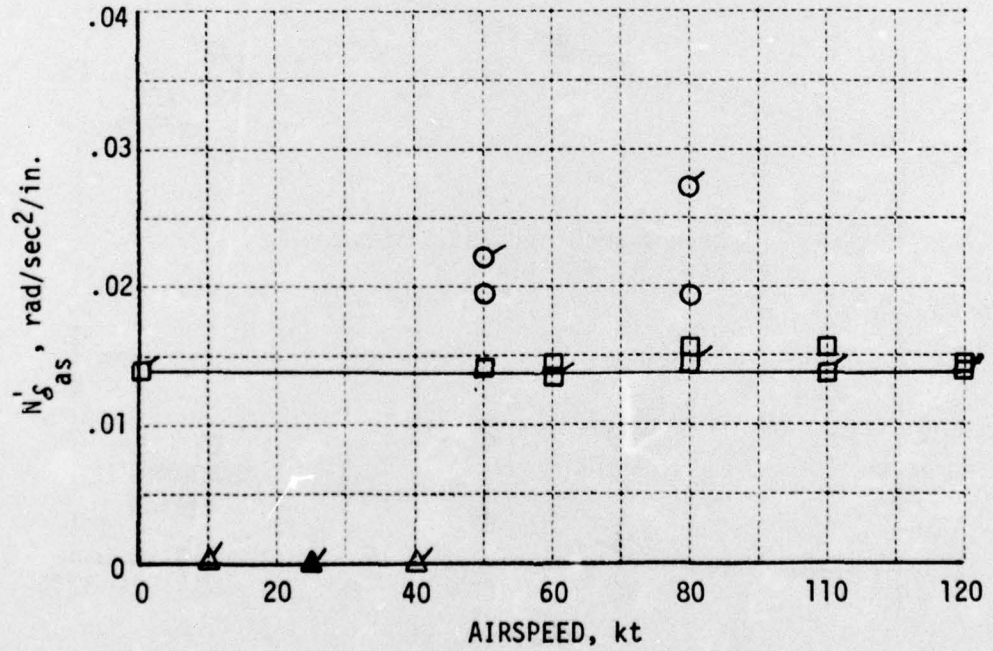


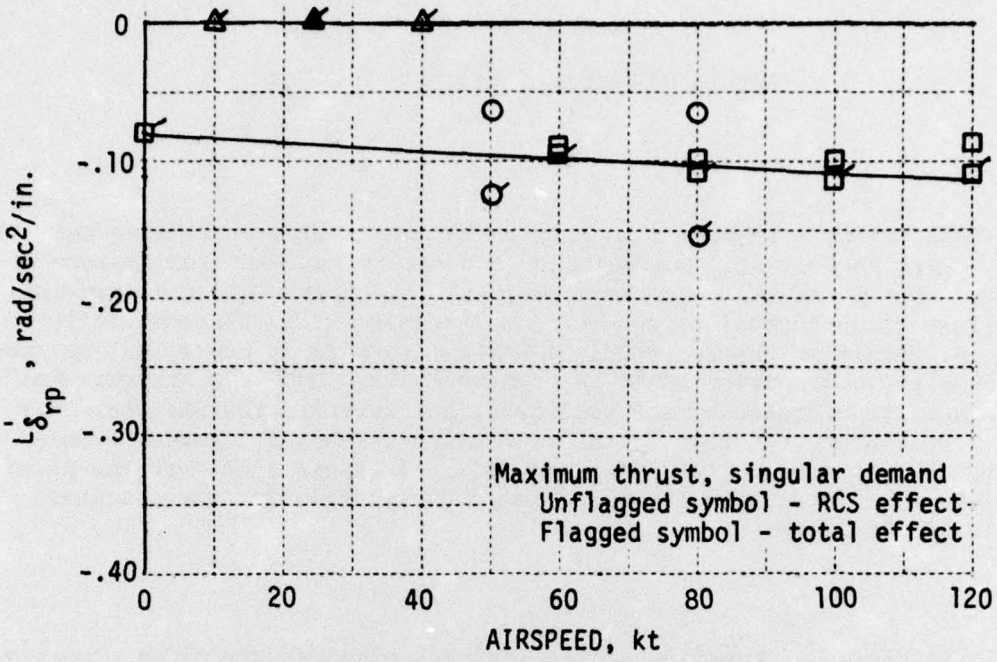
END
DATE
FILMED
2-77

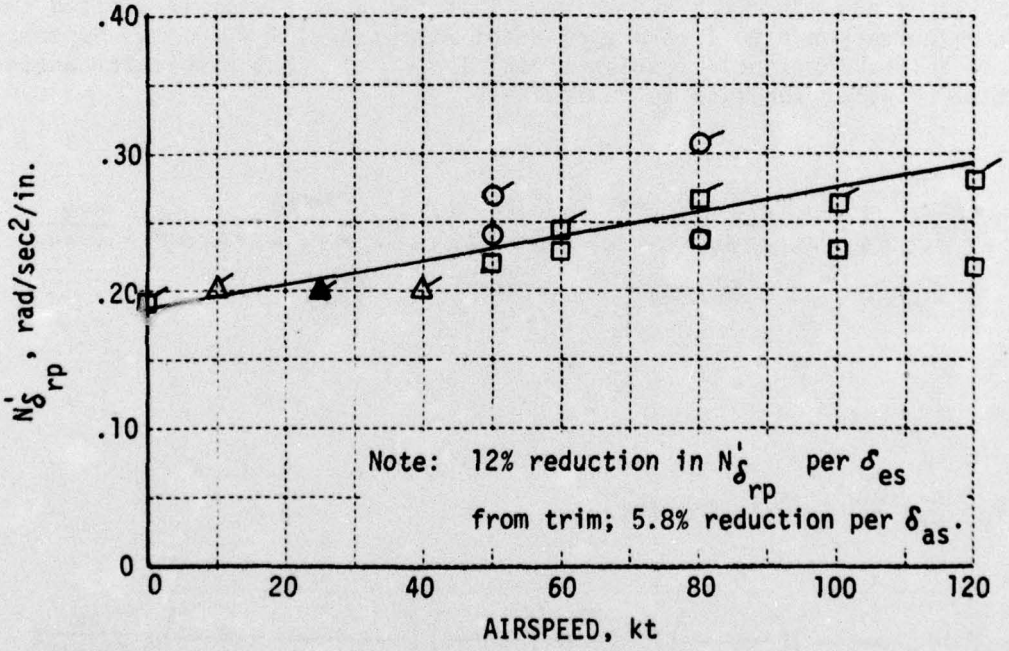

-.30
-.20
-.10
0
N'_r, sec^{-1}
0
20
40
60
80
100
120
AIRSPEED, kt


-1.0
-.8
-.6
-.4
-.2
0
$Y_{\delta_{rp}}$, $ft/sec^2/in.$
RCS
EFFECT
Note: Flagged symbol indicates total
of aero and RCS effects
AERODYNAMIC
EFFECT
0
20
40
60
80
100
120
AIRSPEED, kt


.8
.6
.4
.2
0
$L'_{\delta_{as}}$, rad/sec²/in.
Maximum thrust, singular demand
Unflagged symbol - RCS effect
Flagged symbol - total effect
Note: 8.7% reduction in $L'_{\delta_{as}}$ per δ_{es}
from trim; 9.8% reduction per δ_{rp}.
0
20
40
60
80
100
120
AIRSPEED, kt


.04
.03
.02
.01
0
$N'_{\delta_{as}}$, rad/sec²/in.
0
20
40
60
80
110
120
AIRSPEED, kt


0
-.10
-.20
-.30
-.40
$L'_{\delta_{rp}}$, rad/sec²/in.
Maximum thrust, singular demand
Unflagged symbol - RCS effect
Flagged symbol - total effect
0
20
40
60
80
100
120
AIRSPEED, kt


.40
.30
.20
.10
0
$N'_{\delta_{rp}}$, rad/sec²/in.
Note: 12% reduction in $N'_{\delta_{rp}}$ per δ_{es} from trim; 5.8% reduction per δ_{as}.
0
20
40
60
80
100
120
AIRSPEED, kt

Appendix II

AV-8A SAS CHARACTERISTICS

General

The AV-8A SAS is a limited authority three-axis system consisting basically of pitch and roll rate damping augmentation and a turn coordination feature in the yaw axis. The pitch SAS operates through the stabilator and the downward-blowing tail reaction control system (RCS) valve only; this characteristic introduces an anomaly in the longitudinal SAS-on dynamics in hover and low speed flight which will be discussed later in this appendix. Both the ailerons and the roll RCS valves are operated by the roll SAS; however, the yaw SAS uses only the dual yaw RCS valve at the tail, thus isolating the pilot's rudder pedals from SAS inputs. Apparently the pitch and roll SAS inputs also move the pilot's control stick. The details of the SAS dynamic characteristics are discussed in the following sections.

Pitch SAS

The AV-8A pitch SAS consists of the feedback of body-axis pitch rate (q) to the stabilator and aft pitch RCS valve. This feedback signal is limited to a value which corresponds to ±1.5 deg of stabilator travel (δ_H) or approximately ∓0.84 in. of longitudinal stick travel (δ_{ES}). The stabilator angle-to-pitch-rate transfer function is as follows:

$$\frac{\delta_H}{q}(s) = 7.22\left(\frac{s+5.3}{s+1.35}\right)\left(\frac{22.3}{s+22.3}\right)\left(\frac{45}{s+45}\right)\left(\frac{12}{s+12}\right)\left(\frac{17410}{s^2+132s+17410}\right), \frac{\text{deg}}{\text{rad/sec}}$$

CONTROL FILTER — STRUCTURAL FILTERS — ACTUATOR — RATE GYRO

Since $\delta_{es}/\delta_H \cong -0.56$ in./deg,

$$\frac{\delta_{es}}{q}(s) = -4.04\left(\frac{\quad}{\quad}\right)\left(\frac{\quad}{\quad}\right)\left(\frac{\quad}{\quad}\right)\left(\frac{\quad}{\quad}\right)\left(\frac{\quad}{\quad}\right), \frac{\text{in.}}{\text{rad/sec}}$$

During a decelerating transition or slow approach the dominant pitch control moment is supplied by the RCS. Since the pitch SAS operates through the stabilator which is linked directly to the aft pitch RCS valve, the stabilizing effect of the SAS inputs is significantly reduced when the stabilator setting is such that the valve is closed (Reference 21). Unfortunately this phenomenon occurs during the hover and low speed portion of the landing approach. Figure A-1 demonstrates that for airspeeds below ~ 55 knots the trim value of δ_H , hence δ_{es} , is such that the rear RCS valve is closed and the front RCS valve open. As the transition progresses, larger and larger error signals are required to open the rear valve; in fact, for airspeeds less than ~5 knots the maximum value of the limited error signal ($\pm$0.84 in.) will not open the valve at all without a pilot control input.

Therefore for airspeeds less than ~55 knots the pitch SAS provides little or no restoring moment in response to a nose-down pitch rate (stabilator effect only) and provides a significant restoring moment (stabilator plus RCS) only in response to nose-up pitch rates greater than some threshold value which increases with decreasing airspeed.

Roll SAS

The roll SAS consists of the feedback of body-axis roll rate (p) to the ailerons and roll RCS valves. This feedback signal is limited to a value which corresponds to ± 2 deg of aileron travel (δ_A) or approximately ±0.68 in. of lateral stick travel (δ_{as}). The aileron-to-roll-rate transfer function is as follows:

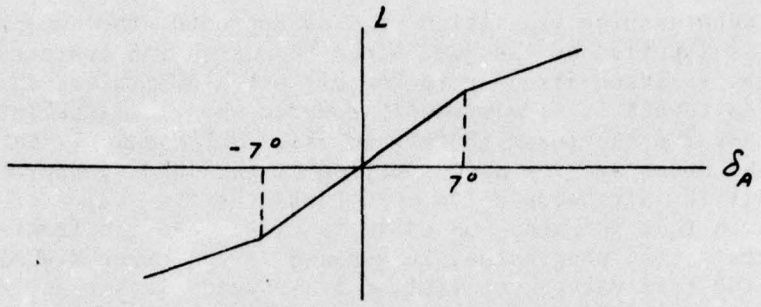
$$\frac{\delta_A}{p}(s) = -11.98\left(\frac{s+1.28}{s+0.774}\right)\left(\frac{25}{s+25}\right)\left(\frac{61}{s+61}\right)\left(\frac{17410}{s^2+132s+17410}\right), \frac{\text{deg}}{\text{rad/sec}}$$

CONTROL FILTER — ACTUATOR — STRUCTURAL FILTER — RATE GYRO

Since $\delta_{as}/\delta_A \cong$ 0.34 in./deg,

$$\frac{\delta_{as}}{p}(s) = -4.07\left(\quad\right)\left(\quad\right)\left(\quad\right)\left(\quad\right), \frac{\text{in.}}{\text{rad/sec}}$$

The roll RCS valves are linked to the ailerons so that at ~7 deg of aileron deflection the downward-blowing valve is fully open. During the remainder of the total aileron travel (± 12.0 deg) the upward-blowing valve on the opposite wing opens. The upward-blowing valve is less effective in providing a rolling moment; hence the functional relationship of rolling moment (L) and aileron deflection is "kinked" at $\delta_A = \pm 7^0$; i.e.,



Yaw SAS

The yaw SAS consists of the feedback of lateral acceleration as measured at the accelerometer (a_y) and washed-out yaw rate (r_{WO}), to the yaw RCS valve and an aileron-to-yaw RCS valve interconnect. The sum of the feedback and feedforward signals is limited to a value which corresponds to ±50% yaw RCS valve opening (±5 deg equivalent rudder (δ_{R_E})) or approximately ∓0.7 in rudder pedal travel (δ_{RP}). The equivalent rudder-to-lateral-acceleration transfer function is as follows:

$$\frac{\delta_{R_E}}{a_y}(s) = 0.86 \underbrace{\left(\frac{s+4}{s+8}\right)}_{\text{CONTROL FILTER}} \underbrace{\left(\frac{57}{s+57}\right)}_{\text{ACTUATOR}} \underbrace{\left(\frac{318}{s^2+19.45s+164}\right)}_{\text{ACCELEROMETER}}, \frac{\text{deg}}{\text{ft/sec}^2}$$

or

$$\frac{\delta_{rp}}{a_y}(s) = -0.12 \left(\quad\right)\left(\quad\right)\left(\quad\right), \frac{\text{in.}}{\text{ft/sec}^2}$$

since

$$\frac{\delta_{rp}}{\delta_{R_E}} \cong -0.14 \text{ in./deg}$$

where

$$a_y = a_{y_{cg}} + \dot{r}\ell_x - \dot{p}\ell_z + q(r\ell_z + p\ell_x)$$

and

$$\ell_x = -11 \text{ ft} \quad ; \quad \ell_z = -2.32 \text{ ft}$$

The equivalent-rudder-to-yaw-rate transfer function is:

$$\frac{\delta_{R_E}}{r}(s) = 12.3\left(\frac{s}{s+0.32}\right)\left(\frac{23}{s+23}\right)\left(\frac{57}{s+57}\right)\left(\begin{matrix}\text{RATE}\\ \text{GYRO}\end{matrix}\right), \quad \frac{\text{deg}}{\text{rad/sec}}$$

WASHOUT FILTER ACTUATOR

or

$$\frac{\delta_{rp}}{r}(s) = -1.73\left(\quad\right)\left(\quad\right)\left(\quad\right)\left(\quad\right), \quad \frac{\text{in.}}{\text{rad/sec}}$$

Finally, the equivalent-rudder-to-aileron transfer function is:

$$\frac{\delta_{R_E}}{\delta_A}(s) = -0.58\left(\frac{23}{s+23}\right)\left(\frac{57}{s+57}\right), \quad \frac{\text{deg}}{\text{deg}}$$

FILTER ACTUATOR

or

$$\frac{\delta_{rp}}{\delta_{as}}(s) = 0.24\left(\quad\right)\left(\quad\right), \quad \frac{\text{in.}}{\text{in.}}$$

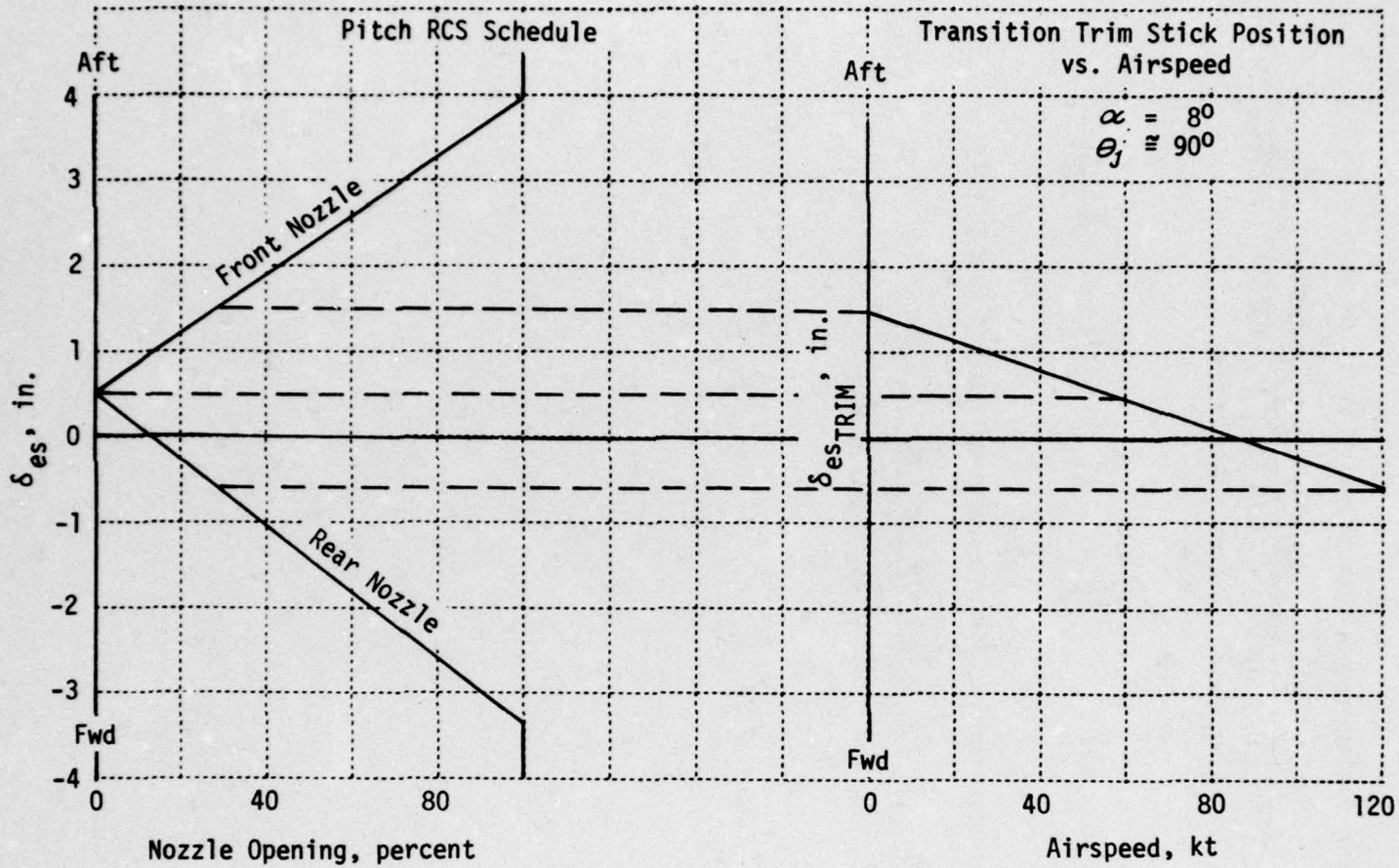


Figure A-1 AV-8A PITCH SAS CHARACTERISTICS

Unclassified

SECURITY CLASSIFICATION OF THIS PAGE (When Data Entered)

REPORT DOCUMENTATION PAGE

READ INSTRUCTIONS BEFORE COMPLETING FORM

1. REPORT NUMBER: Calspan [redacted] AK-5876-F-1	2. GOVT ACCESSION NO.
3. RECIPIENT'S CATALOG NUMBER	
4. TITLE (and Subtitle): A Study to Determine the Feasibility of Simulating the AV-8A Harrier with the X-22A Variable Stability Aircraft	5. TYPE OF REPORT & PERIOD COVERED: Final Report, November [redacted]75 - Jun[redacted]76
	6. PERFORMING ORG. REPORT NUMBER
7. AUTHOR(s): J. Victor Lebacqz [redacted] Edwin W. Aiken	8. CONTRACT OR GRANT NUMBER(s): N00019-76-C-0225 NEW
9. PERFORMING ORGANIZATION NAME AND ADDRESS: Calspan Corporation, Box 235, Buffalo, N. Y. 14221	10. PROGRAM ELEMENT, PROJECT, TASK AREA & WORK UNIT NUMBERS
11. CONTROLLING OFFICE NAME AND ADDRESS	12. REPORT DATE: Jul[redacted]76
	13. NUMBER OF PAGES: 96 (12. 107p.)
14. MONITORING AGENCY NAME & ADDRESS (if different from Controlling Office): Department of the Navy, Naval Air Systems Command, Washington D. C. 20361	15. SECURITY CLASS. (of this report): Unclassified
	15a. DECLASSIFICATION/DOWNGRADING SCHEDULE

16. DISTRIBUTION STATEMENT (of this Report)

Approval for Public Release: Distribution unlimited.

17. DISTRIBUTION STATEMENT (of the abstract entered in Block 20, if different from Report)

18. SUPPLEMENTARY NOTES

19. KEY WORDS (Continue on reverse side if necessary and identify by block number)

VTOL Flight Simulation
AV-8A Harrier Aircraft
X-22A Variable Stability Aircraft
VTOL Landing Approach
V/STOL Aircraft

20. ABSTRACT (Continue on reverse side if necessary and identify by block number)

A study program was undertaken to investigate the feasibility of conducting ground- and in-flight simulations of a jet-lift VTOL aircraft performing terminal area operations using the U.S. Navy X-22A V/STOL Research Facility. The objectives of the program were:

- to develop a generic mathematical model of the AV-8A aircraft during a decelerating approach to hover

DD FORM 1 JAN 73 1473 EDITION OF 1 NOV 65 IS OBSOLETE

Unclassified 407 727

SECURITY CLASSIFICATION OF THIS PAGE (When Data Entered)

- to develop the methodology for computing the variable stability gains required to simulate the AV-8A model with the X-22A
- to develop the procedures for implementing the simulation in the X-22A ground simulator

The general conclusion for this study is that it is feasible to simulate in the X-22A aircraft an AV-8A class VTOL aircraft during terminal area operations. The methodology for performing such a simulation is developed and the techniques for mechanization on the X-22A ground simulator for further experimental investigation are described. Excellent simulation fidelity is possible during low-speed flight ($\leq$60 kts). Areas which require further investigation include the discrepancies in response to throttle inputs at higher speed and the necessity for matching lateral acceleration responses at the pilot's station to control inputs.